ROUTING AND CONTROL MECHANISMS FOR DENSE MOBILE ADHOC NETWORKS

Sulochana Jayashamalee Sooriyaarachchi
(118025E)

Thesis submitted in partial fulfillment of the requirements for the degree Doctor of Philosophy

Department of Computer Science and Engineering
University of Moratuwa
Sri Lanka

September 19, 2016

DECLARATION

I declare that this is my own work and this thesis does not incorporate without acknowledgement any material previously submitted for a Degree or Diploma in any other University or institute of higher learning and to the best of my knowledge and belief it does not contain any material previously published or written by another person except where the acknowledgement is made in the text.

Also, I hereby grant to University of Moratuwa the non-exclusive right to reproduce and distribute my thesis/dissertation, in whole or in part in print, electronic or other medium. I retain the right to use this content in whole or part in future works (such as articles or books).

Signature: Date:

The above candidate has carried out research for the PhD thesis under my supervision.

Name of the supervisor:

Signature of the supervisor: Date:

Dedicated to my loving mother

ACKNOWLEDGEMENTS

I am blessed to be surrounded by many extraordinary people who made it possible for me to march forward in my life. Especially, I would rather express my sincere gratitude to my supervisor Dr. Chandana Gamage for his untiring effort in guiding me along the correct path in my research work while enhancing my research skills remarkably with constructive and invaluable criticisms. He also immensely supported me in publishing in reputed conferences. He not only encouraged me in participating in foreign hosted conferences such as IEEE WoWMoM in US and ACM MobiCom in France but also made it a reality by helping me find the funding which is a scarce resource in Sri Lankan universities.

I would also extend my sincere thanks to my co supervisor Dr. Anil Fernando in University of Surrey, UK who patiently helped me in obtaining a Commonwealth scholarship for a Split-Site research experience which ultimately did not get operationalized due to a hard personal circumstance. The vice chancellor, Prof. Ananda Jayawardane should also be mentioned here with gratitude in arranging this scholarship.

The contribution of the examiners Dr. Priyanka Undugodage, Dr. Upali Kohomban, Dr. Ravi Monaragala and especially Dr. Manodha Gamage and Dr. Himal Suraweera who spent their time and effort in giving insightful feedback for my work during progress reviews is commendable.

I would like to extend my special thanks to Prof. Gihan Dias and all the relevant staff in LK domain registry including Ms. Geethika for arranging the sponsorship for my US visit which was a valuable experience related to this research work. Dr. Shehan Perera as the research coordinator and all the colleagues including Ms. Vishaka Nanayakkara, Dr. Dilum Bandara, Mr. Sanjeewa Darshana, Mr. Thusitha Bandara and Ms. Akila Pemasiri helped me in various ways especially giving valuable inputs for preparing for conference participation abroad. I would like to thank Mr. Kishan Wimalawarne for helping me access research papers.

Furthermore, my grateful thanks are due to the Head of the Department of Computer Science and Engineering, Dr. Chathura de Silva and the former Dean of the Faculty of Engineering, Prof. Anuruddha Puswewala for their fatherly advises and help regarding the administrative process of my PhD. All the staff of the postgraduate division and the establishment division should also be mentioned for their friendly assistance in administrative procedures of the PhD and study leaves.

This thesis would not be a success without the help of my mother. I would extend my gratitude to my husband, all the extended family members and friends including Ms. Chathurika for the unconditional support and encouragement rendered to me.

ABSTRACT

It is not an exaggeration to mention that mobile devices have become ubiquitous and they are used for variety of purposes ranging from personal communication to disaster management and more. These devices are capable of establishing mobile ad hoc networks (MANETs) for multihop communication without the support of infrastructure. This enables more interesting and useful applications of mobile devices, for example for collaborative leaners in large classrooms, shoppers in crowded shopping malls, spectators in sports stadiums, online gamers and more.

MANETs have not sufficiently developed to a deployable level yet. Routing in MANETs is a major problem. It is challenging to devise routing protocols for MANETs due to dynamic topology resulting from mobility, limited battery life and impairments inherent in wireless links. Traditional routing approach is to tweak the existing routing protocols that are designed for wired networks. Therefore, it is common to appoint special nodes to perform routing controls and gather global state information such as routing tables. We identify this approach as the *fixed-stateful routing paradigm*. Fixed stateful routing does not scale with the density of MANETs because the routes will get obsolete quickly due to the dynamic topology causing frequent routing updates. The overhead for these frequent updates will be unacceptable when the MANETs become dense. For example, the control overhead of routing updates in most of the traditional routing protocols are of magnitude $O(N)$ or $O(N^2)$, where N is the number of nodes in the network.

We name the routing approach that does not require to maintain global network states and does not appoint key nodes for routing and control as *mobile-stateless routing paradigm*. We propose a novel concept called *endcast* that leverages message flooding for end to end communication in MANETs in mobile-stateless manner. However, flooding causes heavy amounts of redundant messages, contention and collisions resulting in a situation known as *broadcast storm problem*. When flooding is utilized for end to end communication, the messages will flood beyond the destination. We call this situation *broadcast flood problem*.

Repetitive rebroadcasting in simple flooding is analogous to biological cell division in the growth of human organs. *Chalone mechanism* is a regulatory system to control the growth of the organs. In this mechanism, each biological cell secretes a molecule called *chalone* and the concentration of chalones in the environment increases when the number of cells increases. When the chalone concentration exceeds a threshold the cells stop dividing themselves. *Counter based flooding* is one of the efficient flooding schemes, in which a node decides not to rebroadcast a received message if the message is subsequently heard multiple times exceeding a predefined threshold during a

random wait period. Inspired by the chalone mechanism in the growth of the organs we selected counter based flooding to unicast messages in a MANET. We proposed an *inhibition scheme* to stop the propagation of message beyond the destination to mitigate the broadcast flood problem. In this scheme, the destination transmits a smaller size control message that we call *inhibitor* that also propagates using counter based flooding but with a smaller random wait period than in the case of data message. Furthermore, inhibitors are limited to the region of the MANET covered by data flooding.

The proposed endcast scheme outperforms simple flooding in such a way that over 45% of redundant messages are saved in all the network configurations starting from 100-node network in ideal wireless conditions when the nodes were placed on a playground of $600m \times 400m$ and each node was configured to have $200m$ of transmission radius. Similarly, the protocol manages to save over 45% of redundant messages for all node densities ranging from 10 to 300 in realistic wireless conditions simulated by IEEE 802.11g standard wireless MAC implementation with power saving transmission radius of $40m$. This saving increases rapidly as networks grow by size in both the ideal and realistic wireless network conditions. The inhibition scheme of the protocol was also found to be effective, for example, redundant messages grow in number at a rate about 8 frames per every 25 nodes added to the network when there is inhibition in operation whereas the growth rate is about 170 frames per every 25 nodes when the protocol operates without inhibition in the simulated network scenario.

The major contribution of this research is the analytical model that we developed to design and evaluate endcast schemes. We developed a graph theoretic model to evaluate the propagation of messages in endcast, based on a preliminary model developed by Viswanath and Obraczka [2]. We modified the model by (i) improving its method of estimating the number of new nodes reached by each level of rebroadcast (ii) modeling the impact of node mobility and (iii) incorporating time domain representation to model the flooding schemes that involve random assessment delays (iii) enabling it to represent efficient flooding schemes such as counter based flooding. We present the process of estimating the area covered by the propagation of flooding messages using a geometric method. Time domain is represented by indesing the edges of the flooding graph by time. The counter value and the threshold in counter based flooding are converted into a rebroadcasting probability and estimated using a probability mass function that we constructed by considering the overlapping of radio range circles of the nodes.

CONTENTS

Declaration i

Dedication ii

Acknowledgements iii

Abstract iv

Contents vi

List of Figures x

List of Tables xiii

Declaration xvi

1 Introduction 1

1.1 Context and Motivation 4

1.2 Contributions 7

1.3 Organization 8

2 Literature survey 10

2.1 Introduction 10

2.2 Existing routing mechanisms in MANETs 10

2.2.1 Proactive routing protocols 12

2.2.2 Reactive routing protocols 14

2.2.3 Hybrid routing protocols 17

2.2.4 Cost of routing protocols 19
2.3 Flooding as a data forwarding scheme 20
2.3.1 Storm control 21
2.3.1.1 Ant colony heuristics 22
2.3.1.2 Foraging of honey bees 23
2.3.1.3 Swarm intelligence of termites 23
2.3.1.4 Multi-agent systems 23
2.3.1.5 Immune system 24
2.3.1.6 Bacterial activities 24
2.3.1.7 Diffusion-based systems 24
2.3.1.8 Epidemics 25
2.3.1.9 Cell proliferation 25
2.3.2 Flood control 25
2.3.2.1 TTL-based controlled flooding 26
2.3.2.2 Timer based control 26
2.3.2.3 Cell biological mechanisms 26
2.3.2.4 Negative feedback packets 27
2.4 Summary 27

3 Review of flooding schemes **28**
3.1 Introduction 28
3.2 Broadcast protocols in MANETs 29
3.2.1 Probabilistic flooding 32
3.2.2 Counter based flooding 34
3.3 Broadcast protocol evaluation 38
3.4 Simulation studies of flooding schemes in MANETs 44
3.5 MAC protocols enabling broadcasts 46
3.6 Mobility models 50
3.6.1 Selecting a mobility model 50
3.6.2 Impact of mobility on wireless links 53
3.7 Theoretical analysis of MANET flooding 57

3.7.1 Graph based representations of MANETs 57
3.7.2 Operational characteristics of MANETs 59
3.8 Summary 63

4 Research methodology **65**
4.1 Introduction 65
4.2 Unicast via simple flooding 65
4.3 Parameterizing a MANET that unicast via simple flooding 70
4.4 Graph based model for flooding schemes 73
4.4.1 Number of edges in flooding tree 76
4.4.2 Span of flooding tree 77
4.4.3 Nodes covered by the first level of rebroadcast 78
4.4.4 Nodes covered by next levels of rebroadcast 83
4.4.5 Effect of node mobility 84
4.5 Storm control 91
4.5.1 Graph based analysis of counter based flooding 91
4.5.2 Mathematical model for counter based flooding 95
4.6 Flood control 98
4.7 Summary 99

5 Proposed protocol **101**
5.1 Introduction 101
5.2 Controlling redundant rebroadcasts 103
5.2.1 Growth regulation in organs 104
5.2.1.1 Using growth as the inhibitor of growth 104
5.2.1.2 Terminal conditions of growth 104
5.2.1.3 Growth sensing mechanisms 104
5.2.2 Biological system to MANET mapping 105
5.2.3 Operational model of the bio-inspired system 107
5.3 Protocol architecture and design 108
5.4 Summary 117

6 Analytical model for the protocol 118

6.1 Introduction 118

6.2 Modeling of probabilistic flooding with Viswanath-Obraczka model . 119

6.2.1 Modeling node-to-node transmission on CSMA MAC 120

6.2.2 Modeling multihop transmission in flooding schemes 126

6.3 Proposed modifications to Viswanath-Obraczka model 129

6.3.1 Modeling the counter based flooding parameters 132

6.3.2 Modeling node mobility 142

6.4 Modeling the proposed protocol in a sample CSMA based network . . 143

6.5 Summary 149

7 Simulation results for the proposed protocol 151

7.1 Introduction 151

7.2 Experimental design 153

7.2.1 Experiments based on ideal wireless conditions 154

7.2.2 Experiments based on realistic wireless conditions 154

7.3 Simulation based experiments and results 158

7.3.1 Redundancy overhead 158

7.3.2 Reachability 163

7.3.3 Latency 166

7.4 Discussion 167

7.4.1 Effect of storm control 167

7.4.2 Effect of inhibition scheme 168

7.4.3 Effect of mobility 169

7.4.4 Effect of chalone threshold 172

7.5 Summary 172

8 Discussion and conclusions 175

Bibliography 190

LIST OF FIGURES

1.1 Research stages 7

3.1 Categorization of broadcast schemes in MANETs 31
3.2 Data propagation in simple flooding [2] 34
3.3 Total number of nodes reached by probabilistic flooding 35
3.4 Additional area covered by a rebroadcast 36
3.5 Expected additional coverage area by a node with rebroadcasts of neighbors 37
3.6 Motion of node N_k passing through the transmission region of node N_0 [95] 55
3.7 An example for time evolving graphs [102] 59

4.1 Problem of unicast via flooding 66
4.2 Geometric estimation of reached nodes at each rebroadcast level 67
4.3 Total number of frames in simple flooding with network density 68
4.4 Playground approximation by rectangular regions 69
4.5 Adjacency matrix of a sample network 71
4.6 Redundant rebroadcasting modeled as graph evolution 74
4.7 Redundant rebroadcasting modeled as graph evolution for sample network 75
4.8 Maximum hop count calculation 77
4.9 Geometric estimation of the area of regions that receive the frame at each rebroadcast level 78
4.10 Estimating the average area covered by rebroadcast level 1 79
4.11 Estimating average distance d_{av} between source and a neighbor 80
4.12 Probability mass function for nodes covered by rebroadcast levels 82
4.13 Redundant frames due to simple flooding in sample network 83

4.14 Problem of unicast via flooding in the presence of mobility 84
4.15 Network configurations at two time instances while the nodes are moving 85
4.16 Time evolving graph due to mobility 85
4.17 Flooding graphs for simple flooding in static and mobile networks 86
4.18 Motion of node N_k passing through the transmission region of node N_0 [95] 87
4.19 Probability of complete transmission with relative node speeds 90
4.20 Flooding graph for sample network with counter based flooding 93
4.21 Accumulation of frames for counter based flooding and simple flooding . 95
4.22 Geometric estimation of counter value by rebroadcast of neighbors 97
4.23 Broadcast flood in sample network with simple flooding 98

5.1 Chalone mechanism for cell proliferation control 105
5.2 Cell proliferation Vs message rebroadcasting 106
5.3 Event flow at a receipt of a data frame by a node 111
5.4 Log format 112
5.5 Abstract shape of threshold function proposed in [69] 112
5.6 State diagram for the protocol 115
5.7 Proposed protocol with respect to fixed-stateful and mobile-stateless routing approaches 116

6.1 Data propagation in probabilistic flooding 118
6.2 Illustration of hidden node problem [4] 120
6.3 Three state Markov chain model of a node 122
6.4 Two state Markov chain model of a channel 123
6.5 Second level retransmission 126
6.6 First two retransmissions of flooding 127
6.7 Estimating the average area covered by rebroadcasts 129
6.8 Geometric interpretation of counter based flooding 131
6.9 Librino algorithm for calculating area of intersecting circles 131
6.10 Trellis structure for sample five circles 133
6.11 Illustration of change in counter values of nodes in the presence of mobility 143

6.12 Variation of transmission probability 145
6.13 Illustration of hidden terminal problem for transmission from X to Y . . . 145
6.14 Successful transmission probability 146
6.15 Probability mass function of frame count from simulation data 147
6.16 Reachability with retransmission level in a MANET having density 100 . 148

7.1 Basic IEEE 802.11 DCF protocol [143] 156
7.2 Redundant frames by blind, SNCF and CA protocols 159
7.3 Example 15-node network 161
7.4 Number of rebroadcasts Vs distance between node pairs 162
7.5 Redundant frames until the end of events in SNCF and CA protocols . . . 163
7.6 Saved rebroadcasts (SRB) for CA and SNCF protocols for a 300-node network 163
7.7 Reachability of SNCF and CA protocols 165
7.8 Reachability (RE_{uf}) 166
7.9 Latency of CA protocol in terms of flooding completion time (FCT) in comparison with simple flooding 167
7.10 Redundant frames caused by CA protocol with and without inhibition scheme 169
7.11 Redundancy overhead and reachability of SNCF and CA protocols with mobility 170

8.1 Redundant rebroadcasting modeled as graph evolution for sample network 177
8.2 Geometric estimation of reached nodes at each rebroadcast level 178
8.3 Redundant rebroadcast frames with rebroadcast levels 179
8.4 Total number of frames due to propagation of simple flooding 180
8.5 Broadcast flood problem 180
8.6 Redundant rebroadcasting modeled as graph evolution for sample network 181

LIST OF TABLES

2.1 Complexity of proactive protocols [9] 12
2.2 Complexity of reactive protocols [9] 15
2.3 Complexity of hybrid protocols [9] 18
2.4 Complexity of constructing and maintaining virtual backbones [17] 20

3.1 Selecting flooding schemes for mobile-stateless endcast 33
3.2 Selecting performance metrics for mobile-stateless endcast 40
3.3 Selected performance metrics 42
3.4 Surveyed simulation parameters 46
3.5 Selecting a MAC protocol 50
3.6 Selecting a mobility model 51
3.7 Selecting values for RWP mobility model parameters 53
3.8 Comparson of algorithms for analyzing reachability of nodes in a given network topology 61
3.9 Selecting analytical models 62

4.1 Accumulation of frames in simple flooding 66
4.2 Accumulation of frames in simple flooding with network density 68
4.3 Metrics and definitions to describe graphs 74
4.4 Theoretical results for flooding propagation for 20-node sample network . 82

5.1 Comparison of cell proliferation with blind rebroadcasting 103
5.2 Mapping from biological system to MANET 106

6.1 Recursive calculation of intersection areas 140

6.2 Comparison of P_S in two definitions 146
6.3 Probabilities that the frame count is less than different threshold values . . 148
6.4 Parameter set for the reachability analysis of an example MANET 148

7.1 Simulation parameters for experiments in ideal wireless conditions 154
7.2 IEEE 802.11 parameters 156
7.3 Network densities of simulated topologies 157
7.4 Topologies with constant network density 158
7.5 Simulation parameters for experiments in realistic wireless conditions . . 158

LIST OF ACRONYMS

MANET	Mobile adhoc network
CSMA/CA	Carrier sense multiple access/ Collision avoidance
MAC	Medium access control
N_k	Node k
d_{av}	Average distance between a node and a neighbor
DCF	Distribution coordination function
SNCF	Sequence number controlled flooding
SRB	Saved rebroadcasts
RE	Reachability
CA	Cellular automata
RWP	Random waypoint
P_S	Probability of successful node to node transmission
RTS	Request to send
CTS	Clear to send
TTL	Time to live
N_{ix}	Node x at rebroadcast level i in flooding graph
N_T	Total number of nodes reached by flooding operation
β	Percentage additional area covered by propagation of flooding
P_b	Probability of successful reception at second level rebroadcast

EAC	Expected additional coverage
RAD	Random assessment delay
ROH	Redundancy overhead
FCT	Flooding completion time
n_i	Number of nodes reached at rebroadcast level i
E	Number of edges in flooding graph
P_{comp}	Probability of complete transmission
T_{RAD}	Random assessment delay time
C	Random variable counter in counter based flooding
K	Random variable threshold in counter based flooding
P_{tx}	Probability of rebroadcast of each node
T_{max}	Maximum value for random assessment delay
P_c	Critical probability

CHAPTER I

INTRODUCTION

The current trend in day-to-day communication of average people has dawned an era of the intensive use of mobile devices such as smart phones and slate type computers. The way the people interact via such devices has also dramatically changed and is heading towards a *network of everything* scenario. These potential networks involve not only mobile phones but also various sensing and actuating devices that monitor and alter the physical environment. These devices in general are capable of connecting with each other directly via communication technologies such as WiFi or Bluetooth. The abundance of such portable communication devices with wireless capabilities gives rise to potential ubiquitous computing experiences. The networking paradigm that best matches this scenario is the mobile ad-hoc network (MANET). The availability of a large number of networked mobile devices in a limited geographical area causes MANETs to be dense in nature.

In developing countries like Sri Lanka it is common that every single person owns at least a basic mobile phone though it will take a considerable time to make WiFi coverage available throughout the island. However, with the already available mobile devices with the public there is a plethora of useful and interesting applications that will enhance living standards of average people. For example, fleets of fishing boats in the sea, farmers protecting their crops in fields at night, a crowd gathered under a common shelter during disaster situations will be able to locate and communicate with relatives and friends using an on the fly MANET. Also animal tracking in situations

such as cattle management and wild elephant conservation is possible with low cost embedded signaling devices on animals when these devices are facilitated to form a MANET. Though MANET research has been in operation since late 1990s' and the ad-hoc mode of operation was included in IEEE 802.11 wireless LAN standards for decades MANETs have not developed in a caliber to support such practical applications especially in the context of dense MANETs. Conti and Giordano [3] criticize that MANETs in the context of large scale general purpose networks are at a high risk of failure due to the following reasons: (i) limited attention is devoted to the implementation and integration of protocols to the real systems, (ii) existing implementations are not stable and require high technical expertise to work with, (iii) lack of performance studies in real networks, (iv) performance problems in real implementation due to the gap between simulation studies and real systems and implementation deficiencies. Conti and Giordano [3] further suggest that MANET research should be targeted at specific applications as the best routing strategies for MANETs depend greatly on the application scenario.

Developed countries who lead the wireless networking research and deployment are already way ahead in installing wireless infrastructure such as WiFi hotspots and their current focus is more on wireless sensing, seamless handover among access points and interoperability and security in infrastructure mode wireless networks. However MANET protocols should still be developed to a deployable level to enable true potential of mobile devices and to support Internet of Things (IoT) with ubiquitous computing capability. If robust protocols are in place there will be a plethora of interesting applications that enhance the experience of collaborative learners in classrooms, shoppers in shopping malls, spectators in sports stadiums, online gamers and more.

MANETs are generally dynamic in terms of topology due to limited battery life and mobility added to the inherent impairments of wireless links such as interference and multipath loss. Wireless networks in general have other problems such as hidden terminal problem, exposed source problem and near-far problem. Devices are also limited in computing resources such as memory and processing power with respect to the increasing computing needs such as video streaming and real time gaming. Thus it

is challenging to implement an efficient routing mechanism in large scale general purpose MANETs. The nodes in a MANET should be able to communicate in multihop manner but there should not be dedicated infrastructure or special nodes performing routing and controlling to allow for dynamic nature of MANETs due to mobility and limited battery life. When the MANETs are dense, it is desirable that the nodes do not have to keep any states such as routing tables especially pertaining to global network.

Traditional routing approaches proposed and implemented in MANETs are based on existing routing protocols of wired networks. We consider these routing approaches that are based on fixed infrastructure and require to maintain routes as the *fixed-stateful approach*. However, the current trend in MANETs seeks a paradigm shift in approaching the problem of routing as various mobile devices emerge in large numbers and with powerful near-field wireless networking capabilities. In parallel to the technological advances, the concepts for ubiquitous computing and connectivity develop at a rapid phase. For example, IPv6 allows a large population of mobile devices to connect in a single network, while Bluetooth provides powerful near field communication. The opposite of the traditional routing paradigm is the *mobile-stateless approach*. Mobile-stateless approach should allow nodes in MANETs communicate in a stateless manner without special designated control nodes. The simplest mobile-stateless approach is blind rebroadcasting and a widely used better descendant of blind rebroadcasting is simple flooding. Flooding is currently used as an essential underlying process to enable traditional routing protocols, for example to disseminate route request messages in Ad-hoc On-demand Distance Vector (AODV) routing protocol.

However, flooding causes problems such as serious redundancy, heavy contention and collisions that are collectively referred to as *broadcast storm problem* [4]. There are a few variations of flooding that suppress redundant rebroadcasts [4, 5]. However, the suppression of redundant rebroadcasts will in turn result in low reliability and poor reachability. Various efficient flooding schemes will be critically evaluated in the context of mobile-stateless data forwarding and their performances will also be compared in terms of broadcast storm problem, reliability and reachability in Chapter 3.

Assume a disaster site where there is a large crowd gathered as in a relief camp.

There will be mobile devices available with the people. A relief team may be deployed to the site and the MAC addresses of the members will be registered and known to each other. There will be no infrastructure remaining in the arena due to the disaster so that the devices themselves should perform the routing functionality. In this type of situation there are many social interactions so that the network connectivity may exhibit the *betweenness centrality* property, which could be expoited for efficient unicast. The resulting networks could appear as long term stationary backbones. However this approach is in fixed-stateful paradigm whereas our approach is in mobile-stateless paradigm. Therefore, we do not further explore this idea in the context of this research.

Hence in this scenario a MANET should be formed and it will be a dense MANET. Since the devices are limited in battery life the power saving radio ranges are assumed. Therefore, the messages should be passed through the network in a multihop manner. For example a medical team member will have to send a message to the food store member in the relief team across the available devices in the vicinity including unregistered devices. The transmission model for the target solution is as follows:

- Our protocol should operate at the link layer so that we refer to the data units as frames
- Upper layers are assumed to give a list of destination MAC addresses for the known devices
- Physical layer is assumed to provide broadcast links and handle the collisions and multiple access

1.1 Context and Motivation

In general, the problem addressed by this research is message routing in MANETs. The specific type of MANETs we consider are dense and MANET density is defined in Section 3.4. We approach the problem from mobile-stateless paradigm and thus the particular problem that we consider in dense MANETs has the following features:

- No routing infrastructure such as special beaconing nodes

- Potentially large number of transmitting nodes
- Minimum amount of state information held by each node
- Stored state information is only locally relevant and subject to rapid change and frequently become invalid

According to the broad survey of existing MANET routing solutions that will be given in Chapter 2, traditional fixed-stateful approach of routing causes costs of discovering and maintaining routes. These routes quickly become obsolete due to the dynamic nature of MANET topology resulting in the need for frequent route updates. Therefore, we start with blind rebroadcasting as a mechanism to carry data from a source to a destination in a MANET. Blind rebroadcasting is the simplest stateless mechanism of spreading a message across a MANET to the destination to leave the nodes to be stateless and to allow for the dynamics of the network.

There are several types of networked communication, namely unicast, anycast, multicast and broadcast. Unicast is the communication between a single sender and a single receiver, which usually is along a one to one connection. Anycast is the communication from a single sender to any one of a group of receivers. Multicast is the communication from a single sender to a group of receivers. Broadcast is the communication from a single sender to all the members of the network.

None of the above terms reflect the type of communication that we achieve in this research where the data is flooded until it reaches the destination. Therefore, we coined the term *endcast* to give the essence of the idea. In endcast the data may propagate beyond the destination until the flooding is inhibited. The data does not take a preset route as in unicast but is propagated via multihop broadcast links.

In this research we investigate the routing approach that we call *endcast* in detail with a particular emphasis on building a theoretical basis for analyzing endcast schemes. When leveraged for endcast in MANETs, blind rebroadcasting and its variants such as simple flooding causes two main issues in delivering a message from a source to a destination across a MANET:

1. Broadcast storm: ideally only one message should propagate from the source to the destination though blind rebroadcasting causes excessive number of messages propagating all over the network.

2. Broadcast flood: even after reaching the destination the messages continue to propagate and get accumulated in the network unless an explicit mechanisms are implemented to stop the message propagation and remove the message

Furthermore, use of broadcast as the underlying link layer communication mode is disadvantageous in the context of energy efficiency. However, as all wireless network nodes operate through local broadcast, this lack of energy management is not a scenario that is specific to our research on dense MANETs. In fact, the development of an efficient set of protocols such as endcast schemes that control storm and flood problems, is a significant positive contribution towards conserving enegy in MANET nodes.

There are a number of examples where satisfactory solutions are proposed inspired by natural systems such as biological systems, especially in communication networks. After exploring the natural systems that mimic similar characteristics of blindly rebroadcasting MANETs we identified regulatory mechanisms that inspired us in controlling broadcast storms. A solution for broadcast flood was chosen among surveyed mechanisms. Ultimately a protocol was proposed that consists of a storm control mechanism inspired by the chalone mechanism of growth control in biological organs and a flood control mechanism that utilizes a negative acknowledgement mechanism.

The overall research experience was of the form in Figure 1.1. We hypothesized that flooding is an alternative unicast mechanism that will avoid costs of traditional MANET routing that require to discover and maintain routes. We then analyzed the problem of MANET routing in general and unicast in MANET via flooding in particular using theoretical bases. We developed a protocol based on flooding and analyzed it using both a theoretical model and a simulation model.

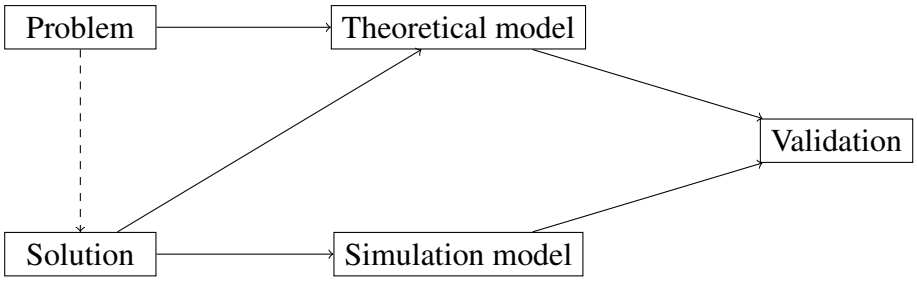

Figure 1.1: Research stages

1.2 Contributions

1. Proposed flooding as a unicast mechanism which we term *endcast* as opposed to the conventional use of flooding as a mechanism for network wide message broadcast

2. Built a theoretical model to analyze flooding with an emphasis on its performace when used as a unicast mechanism

3. Proposed a biologically inspired endcast scheme and developed an operational model for the proposed protocol based on cellular automata

4. Theoretically analyzed endcast and developed a analytical model for the proposed protocol

5. Implemented a simulation set up to evaluate the protocol efficiency

6. Publications

   Journal papers

   - S. J. Sooriyaarachchi, W. A. C. Fernando, C. D. Gamage, "A Cell Biology Inspired Model for Managing Packet Broadcasts in Mobile Ad-hoc Networks", *ICACT-TACT Journal - Transactions on Advanced Communications Technology*, vol. 4, no. 5, pp. 664-672, Sep. 2015.

   Conference papers

- S. Sooriyaarachchi, "A Cell Biology Inspired Data Packet Forwarding Scheme in Mobile Ad-hoc Networks", in *IEEE 16th International Symposium on a World of Wireless, Mobile and Multimedia Networks (WoWMoM 2015)*, Boston, MA, USA, 14-17 Jun. 2015.
- S. J. Sooriyaarachchi and C. D. Gamage, "A Cell Biology Inspired Model for Managing Packet Broadcasts in Mobile Ad-hoc Networks", in *The 17th International Conference on Advanced Communications Technology (ICACT 2015)*, Pyeong Chang, Korea, 1-3 Jul. 2015, pp. 693-698.
- S. J. Sooriyaarachchi, W. A. C. Fernando, C. D. Gamage, "Evaluation of Scalability of Hybrid Wireless Mesh Protocol in IEEE 802.11", in *International Conference on Advances in ICT for Emerging Regions (ICTer 2015)*, Colombo, Sri Lanka, 24-26 Aug. 2015, pp. 152-159.
- S. J. Sooriyaarachchi, "Poster: A Cell Biology Inspired Model for Controlling Redundant Rebroadcasts in Mobile Ad-hoc Networks", in *ACM 2015 Workshop on Wireless of the Students, by the Students and for the Students (S3'15)*, Paris, France, 11 Sep. 2015, p. 10.

1.3 Organization

This thesis is organized as follows: Chapter 2 surveys the existing MANET routing mechanisms with an emphasis on costs and consequently we identify that flooding is a candidate unicast mechanism (endcast). We also set the background for endcast by identifying *broadcast storm problem* and *broadcast flood problem* as the major problems. Further, we survey the candidate solutions for these problems in Chapter 2. Chapter 3 evaluates the already available efficient flooding mechanisms with respect to their applicability as a endcast scheme conforming to mobile-stateless routing paradigm. Research methodology is explained in Chapter 4 in which we build a theoretical basis with the help of a variety of models that capture aspects of endcast including graph theoretic representation of MANETs, probabilistic analysis of flood-

ing schemes, and time domain analysis of graphs to capture node mobility and delays in flooding mechanisms. We propose a endcast scheme in Chapter 5 that mitigates broadcast storm problem using a biological inspiration and reduces broadcast flood problem utilizing a negative acknowledgement mechanism. Moreover, we develop an operational model for the proposed protocol based on cellular automata. Chapter 6 analyzes the protocol efficiency using the developed analytical model in Chapter 4. We extend the analysis to capture realistic network conditions such as collisions and related problems in multihop communication. Simulation based performance evaluation of the protocol is described in Chapter 7. Chapter 8 discusses the results and concludes the thesis.

CHAPTER II

LITERATURE SURVEY

2.1 Introduction

In this chapter we set the theoretical background to approach the solution for the problem of finding a data forwarding mechanism in a dense MANET. Firstly, we survey the existing routing mechanisms ranging from the extreme of static routing with beaconing nodes to the extreme of blind rebroadcasting. We also highlight that flooding is an alternative mechanism to perform unicast data forwarding when equipped with methods to address the performance problems inherent in flooding. Consequently, this chapter brings up the performance issues in flooding and the major issues that we focus on during this research. Finally, we analyze each issue and explain the approach we have adopted to find a solution for each issue.

2.2 Existing routing mechanisms in MANETs

We considered a broad spectrum of existing solutions with an emphasis on the cost of keeping global states and assigning special nodes to perform routing and controls. Traditional routing approaches proposed and implemented in MANETs are based on existing routing protocols of wired networks. Data communication networks originated with the intention of connecting fixed wired terminals. The need for routing mechanisms arose as a result of the growth of the networks by size and geographical

spread. The networks started to support wireless nodes with the intention of using existing networked communication resources [6]. Hence, the wireless nodes always had the support of some kind of fixed infrastructure so that the wired routing protocols were tweaked and customized to support a few number of wireless nodes. Dedicated fixed infrastructure such as base stations in cellular networks and wireless access points in local area networks were established when the mobile nodes increased in number [7]. However, the concepts behind almost all routing protocols used in MANETs are hooked to fixed infrastructure at least by assuming few key nodes in the network to act as fixed and routing nodes. The most recent work in the area of MANETs is task group "s" amendment to the IEEE 802.11 as at year 2012, which defines Wireless Mesh Networks (WMN). WMNs show similar characteristics as MANETs, especially with its multihop communication. Mesh Stations even in IEEE 802.11 standard act as access points in infrastructure mode wireless networks thus managing routing and control [8].

According to IETF MANET Working Group, routing protocols are classified into proactive and reactive protocols depending on the type of routing information exchanged, and how and when the information is exchanged. Proactive routing protocols are the extensions of wired routing and the nodes are required to maintain one or more tables that contain latest routing information to any node in the network. These protocols are usually based on link state and distance-vector algorithms. In contrast, reactive protocols establish routes only when needed and the route is valid only until the destination is inaccessible or the route is no longer used [3]. There is another type of routing known as hybrid protocols that combine proactive and reactive schemes. Conti and Giordano [3] give a comprehensive list of MANET routing protocols and Abolhasan et al. [9] compare the complexities of a number of proactive, reactive and hybrid routing protocols. Accordingly, followings are the brief explanations for some of the protocols:

Table 2.1: Complexity of proactive protocols [9]

Protocol	**Convergence time**	**Memory overhead**	**Control overhead**
DSDV	$O(D{\cdot}I)$	$O(N)$	$O(N)$
WRP	$O(h)$	$O(N^2)$	$O(N)$
GSR	$O(D{\cdot}I)$	$O(N^2)$	$O(N)$
FSR	$O(D{\cdot}I)$	$O(N^2)$	$O(N)$
STAR	$O(D)$	$O(N^2)$	$O(N)$
DREAM	$O(N{\cdot}I)$	$O(N)$	$O(N)$
MMWN	$O(2D)$	$O(N)$	$O(X+E)$
CGSR	$O(D)$	$O(2N)$	$O(N)$
HSR	$O(D)$	$O(N^2{\cdot}L) + O(S) + O(\frac{N}{S}) + O(\frac{N}{n})$	$O\frac{(n{\cdot}L)}{I} + \frac{O(1)}{J}$
OLSR	$O(D{\cdot}I)$	(N^2)	$O(N^2)$
TBRPF	$O(D)$ or $D+2$ for link failure	$O(N^2) + O(N) + O(N+V)$	$O(N^2)$

D=diameter of the network, N=number of nodes in the network, I=average update interval, h=height of the routing tree, L=number of hierarchical levels, S=number of virtual IP subnets, n=average number of logical nodes in the cluster, V=number of neighboring nodes, E=edges in the routing tree, X=number of clusters (each cluster has one clusterhead)

2.2.1 Proactive routing protocols

- Destination-sequenced distance vector (DSDV): DSDV provides a single path using distance vector shortest path algorithm. Two types of update packets are used, namely full dump and incremental packets. Full dump packets contain all available routing information whereas the incremental packets contain only the information changed since last full dump. Routing overhead due to these packets grows according to $O(N^2)$ where N is the number of nodes in the network.

- Wireless routing protocol (WRP): WRP maintains four tables and stores prede-

cessor information. It also exchanges hello packets with neighbors if there is no record of a recent communication. WRP is not efficient in terms of memory and power consumption.

- Global state routing (GSR): GSR is based on traditional link state algorithm but the update messages are exchanged between intermediate neighbors only. However the size of the message grows with the number of nodes so that bandwidth consumption of update packets becomes larger with larger networks.

- Fisheye state routing (FSR): FSR is an improvement of GSR where the bandwidth consumption of update messages is reduced by updating the nearby neighbors at a higher frequency and updating neighbors outside the fisheye scope at a lower frequency.

- Source-tree adaptive routing (STAR): STAR is also based on the link state algorithm and each node maintains a source tree which is a set of links that forms the path to the preferred destinations. STAR supports Least Overhead Routing Approach (LORA) and Optimum Routing Approach (ORA) which together disseminate update messages conditionally when certain events occur.

- Distance routing effect algorithm for mobility (DREAM): In DREAM each node knows its own geographical coordinates through GPS and these coordinates are periodically exchanged between nodes and are stored in a structure called location table.

- Multimedia support in mobile wireless networks (MMWN): MMWN maintains the network as a clustering hierarchy. A cluster contains switches, endpoints and a location manager (LM). Only the LMs perform location finding and updating.

- Cluster-head gateway switch routing (CGSR): In CGSR also the nodes are clustered but the addressing scheme is simpler than MMWN. A mobile node is elected as a cluster head to manage all the other nodes in the cluster. Each node has to maintain a cluster member table, broadcast its information and update the table to maintain the clusters.

- Hierarchical state routing (HSR): HSR is also based on traditional link state algorithm but maintains hierarchical addressing and a topology map. Nodes in the close proximity are organized into clusters. A cluster contains a cluster head and internal nodes. Nodes that belong to more than one cluster are known as gateways.

- Optimized link state routing (OLSR): Based on traditional link state OLSR operates as a point-to-point routing protocol. It uses multi-point relay (MPR) approach to minimize number of rebroadcasts when updating the routing tables. For the MPR mechanism the nodes periodically broadcast their one hop neighbor information using hello messages. Thereby the nodes select a set of neighbors to act as relay nodes in such a way that all the two hop neighbors are covered.

- Topology broadcast reverse path forwarding (TBRPF): TBRPF is a hop by hop routing mechanism and it uses reverse path forwarding (RPF) to disseminate update messages. In this protocol each node builds a source tree that provides the paths to all reachable nodes. The source tree is built using a modified version of Dijkstra algorithm and topology tables that contain partial topological information. Since TBRPF reports only the changes of the source tree with the neighbors, it incurs minimum update message overhead compared to the protocols that exchange complete link state information.

2.2.2 Reactive routing protocols

These protocols maintain information pertaining to active routes only. The routes are discovered and maintained only when a packet needs to be forwarded to a destination. A route request packet is disseminated to discover a route and the destination will acknowledge it enabling the nodes to extract routing information. Reactive protocols are classified into two: source routing and hop-by-hop routing. In source routing on demand protocols, the packet carries the complete source and destination addresses whereas in hop-by-hop (also known as point to point) protocols the header carries the

Table 2.2: Complexity of reactive protocols [9]

Protocol	**Route discovery time complexity**	**Route maintenance time complexity**	**Route discovery communication complexity**	**Route maintenance communication complexity**
AODV	$O(2D)$	$O(2D)$	$O(2N)$	$O(2N)$
DSR	$O(2D)$	$O(2D)$	$O(2N)$	$O(2N)$
ROAM	$O(D)$	$O(A)$	$O(\|E\|)$	$O(6G_A)$
LMR	$O(2D)$	$O(2D)$	$O(2N)$	$O(2A)$
TORA	$O(2D)$	$O(2D)$	$O(2N)$	$O(2A)$
ABR	$O(D+P)$	$O(B+P)$	$O(N+R)$	$O(A+R)$
SSA	$O(D+P)$	$O(B+P)$	$O(N+R)$	$O(A+R)$
RDMAR	$O(2S)$	$O(2S)$	$O(2M)$	$O(2M)$
LAR	$O(2S)$	$O(2S)$	$O(2M)$	$O(2M)$
ARA	$O(D+P)$	$O(D+P)$	$O(N+R)$	$O(A+R)$
FORP	$O(D+P)$	$O(D+P)$	$O(N+R)$	$O(N+R)$
CBRP	$O(2D)$	$O(2B)$	$O(2X)$	$O(2A)$

D=diameter of the network, N=number of nodes in the network, A=number of affected nodes, B=diameter of the affected area, G=maximum degree of the router, S=diameter of the nodes in the localised region, M=number of nodes in the localised region, X=number of clusters (each cluster has one cluster-head), R=number of nodes forming the route reply path, $|E|$=number of edges in the network.

destination and the next hop address. However this requires periodic beaconing to gather neighborhood information.

- Dynamic source routing (DSR): In DSR protocol the packet needs to carry addresses of all hops on the route. Multiple routes can be saved in route cache of nodes so that the nodes will first check its cache before initiating a route discovery.

- Ad hoc on-demand distance vector (AODV): AODV is based on DSDV and DSR. However unlike DSR, AODV carries only the destination address and a sequence number. Sequence numbering is derived from DSDV.

- Routing on-demand acyclic multi-path (ROAM): ROAM uses internodal coordi-

nation along the directed acyclic (sub)graphs (DAG) and this operation is called diffusing computation. The subgraphs are derived using the distance of the nodes to the destination.

- Light-weight mobile routing (LMR): In LMR each node maintains routing information to their neighbors only and this will result in temporarily invalid routes and loops.

- Temporally ordered routing algorithm (TORA): TORA is based on LMR but the control messages are exchanged with the neighbors only.

- Associativity-based routing (ABR): ABR is also a source-initiated routing protocol and the routes are selected based on stability. Each node maintains an associativity tick for each neighbor. Higher associativity ticks imply that the relevant links are stable compared to those with lower ticks. However ABR requires periodic beaconing to assess associativity.

- Signal stability adaptive (SSA): SSA is derived from ABR but the routes are selected based on the signal strength and location stability rather than based on associativity ticks.

- Relative distance micro-discovery ad hoc routing (RDMAR): RDMAR calculates the distance between the source and the destination in terms of number of hops and limits the number of hops that the control messages should propagate. Distances are estimated from previous communications and messages are flooded if there are no previous records of communication for distance estimation.

- Location-aided routing (LAR): LAR also uses flooding for control messages but reduces the overhead using location information. Each node is assumed to know its location using GPS.

- Ant-colony-based routing algorithm (ARA): ARA reduces routing overhead by adopting food searching behavior of ants: ants leave trails called pheromone

while walking in search of food and the rest of the ants follow the path with highest pheromone concentration. In ARA protocol, route discovery begins when the source sends out forward ant (FANT) packets that calculate a pheromone value at each node depending on the number of hops it has taken to reach the node. At the destination a backward ant (BANT) packet is sent back to the source. When data packets are forwarded by the nodes their pheromone value increases otherwise the pheromone value decreases overtime and expires.

- Flow oriented routing protocol (FORP): FORP predicts route failure and uses alternate routes before failure. For route discovery Flow_REQ message is sent by the source and each node receiving it calculates a Link Expiration Time (LET) with previous node and appends that value to the Flow_REQ packet. At the destination a Route Expiration Time (RET) is calculated using the minimum LETs in the Flow_REQ packet and Flow_SETUP packet is sent back to the source. During data transmission the intermediate nodes append their LETs to the data packet so that the destination can predict the route expiration time. When the destination determines that a route is about to expire, the destination sends a Flow_HANDOFF message. When the source receives a Flow_HANDOFF an alternate route is selected by the source and then the source sends Flow_SETUP.

- Cluster-based routing protocol (CBRP): CBRP is a hierarchical protocol where nodes are grouped into clusters and a cluster head is appointed for each cluster. Only the cluster heads exchange routing information but cluster formation and maintenance introduce more overhead.

2.2.3 Hybrid routing protocols

These protocols include both reactive and proactive approaches combined. Mostly the routes to the nearby nodes are maintained proactively and the routes to the far away nodes are determined reactively.

- Zone routing protocol (ZRP): In ZRP zones are defined in terms of a certain number of hops as the range and proactive routes are maintained for nodes in the

Table 2.3: Complexity of hybrid protocols [9]

Protocol	**Scope**	**Route discovery time complexity**	**Route maintenance time complexity**	**Route discovery communication complexity**	**Route maintenance communication complexity**
ZRP	intra	$O(I)$	$O(I)$	$O(Z_N)$	$O(Z_N)$
	inter	$O(2D)$	$O(2D)$	$O(N+V)$	$O(N+V)$
ZHLS	intra	$O(I)$	$O(I)$	$O(\frac{N}{M})$	$O(\frac{N}{M})$
	inter	$O(D)$	$O(D)$	$O(N+V)$	$O(N+V)$
SLURP	intra	$O(2Z_D)$	$O(2Z_D)$	$O(\frac{2N}{M})$	$O(\frac{2N}{M})$
	inter	$O(2D)$	$O(2D)$	$O(2Y)$	$O(2Y)$
DST	intra	$O(Z_D)$	$O(Z_D)$	$O(Z_N)$	$O(Z_N)$
	inter	$O(D)$	$O(D)$	$O(N)$	$O(N)$
DDR	intra	$O(I)$	$O(I)$	$O(Z_N)$	$O(Z_N)$
	inter	$O(2D)$	$O(2D)$	$O(N+V)$	$O(N+V)$

I=periodic update interval, N=number of nodes in the network, M=number of zones or cluster in the network, D=diameter of the network, Z_N =number of nodes in a zone, cluster or tree, Z_D =diameter of a zone, cluster or tree, Y=number of nodes in the path to the home region, V=number of nodes on the route reply path

zone. Nodes that lie outside the zones are reached via reactive routing and the route discovery packets need to reach only a node at the boundary of a zone to determine the path.

- Zone-based hierarchical link state (ZHLS): ZHLS is a hierarchical protocol which assigns every node a node ID and a zone ID. Topology is made up of two levels: node level and zone level. No cluster heads or location manager nodes are assigned so less overhead for location management. However, a static zone map is required to route packets as the node ID and the zone ID of the destination are required.

- Scalable location update routing protocol (SLURP): In SLURP also nodes are assigned to non-overlapping zones but uses a mapping function for this assignment.

- Distributed spanning trees based routing protocol (DST): In DST the network is viewed as a set of trees where each tree consists of a root and internal nodes. A node may operate as a router, a merger or a configurer. Two routing strategies are available to discover routes: hybrid tree flooding (HTF) and distributed spanning tree (DST). In HTF the control packets are sent to all the neighbors and the adjoining bridges in the tree whereas in DST the packets go along the edges of the tree.

- Distributed dynamic routing (DDR): DDR is also a tree based protocol but does not require a root node for the protocol operation. Trees are formed using beaconing among neighbors and the trees in turn form a forest. Trees are connected using gateway nodes that belong to different trees but are in the range of each other. Each tree is also considered as a zone and assigned a zone ID using a zone naming algorithm.

2.2.4 Cost of routing protocols

According to Abolhasan et al. [9] asymptotic costs of the proactive, reactive and hybrid protocols listed in Section 2.2 are given in Tables 2.1, 2.2 and 2.3 respectively. According to Table 2.1 most of the proactive protocols have a memory overhead of magnitude $O(N^2)$ and control overhead of magnitude $O(N)$. However, MANETs are dynamic networks and the routes thus discovered will become obsolete quickly, even before the routes converge in a time of magnitude $O(D)$. Similarly, the reactive protocol overheads shown in Table 2.2 also become higher and wasteful because the routes will be invalid due to dynamic topology of the MANETs. Hybrid protocols require nodes to organize into zones and this also incurs costs apart from the costs of discovering and maintaining routes in Table 2.3.

Sholander et al. in [10] cite [11] that compares proactive, reactive and hybrid protocols by considering HSLS, DSR, and ZRP as examples respectively and that concludes the asymptotic routing overhead in terms of number of routing packets exchanged in the network is $O(N^{1.5})$, $O(N^2)$ and $O(N^{1.66})$ respectively in an N-node network. Most of the proactive protocols use clustering and appoint cluster heads to forward update

Table 2.4: Complexity of constructing and maintaining virtual backbones [17]

Backbone	[18][19][20]	[21]	[22]	[23][24]
Message complexity	$O(n^2)$	$\Theta(m)$	$O(n^2)$	$O(n \log n)$
Time complexity	$O(n^2)$	$O(\Delta^3)$	$\Omega(n)$	$O(n)$

n is the number of nodes, m is the number of edges, and Δ is the maximum nodal degree

messages. These hierarchical protocols do not scale with mobility and impose more overhead in managing mobility [9].

The operation of protocols that appoint special nodes such as cluster heads is equivalent to creating Connected Dominating Set (CDS) in graphs [12]. A dominating set is a subset D of vertices V in which all the vertices that are not in D are adjacent to at least one vertex in D. When vertices in D are connected the D is a CDS. MANETs are represented as a variety of graphs: most popular model of ad hoc networks is the Unit Disk Graph (UDG) which assumes fixed and common transmission range for all nodes normalized to one unit. A range of work is available that addresses the dominating set problem in unit disk graphs [13, 14, 15, 16]. Alzoubi et al. [17] summarize the message and time complexities of constructing and maintaining virtual backbones to perform routing tasks by analyzing seven different algorithms proposed in [18, 19, 20, 21, 22, 23, 24]. This analysis is based on connected dominating sets in unit disk graphs and the costs of analyzed algorithms are shown in Table 2.4.

2.3 Flooding as a data forwarding scheme

The above costs can be avoided if we use a simple mechanism such as blind rebroadcasting that does not require any state information or setting up of paths to send data across to the destination. Simple flooding is a slight improvement of blind rebroadcasting which is a popular mechanism of disseminating messages throughout a network. Simple flooding requires only the detection of duplicate packets. Conventionally, this is achieved by using a sequence number and storing the sequence number of packets received by each node during a certain period of time. This scheme is specifically

known as Sequence Number Controlled Flooding (SNCF) and popular by the name *simple flooding*. Ho et al. [25] argued that flooding is a possible alternative for reliable multicast in highly mobile ad hoc networks as traditional multicast solutions are not suitable. We propose that flooding is also an alternative for unicast so that the cost of discovering routes and maintaining them will be eliminated. Rahman et al. [26] also experimentally prove that flooding with tunable heuristics can be adopted as a reliable and efficient routing scheme in MANETs and these flooding based schemes are not inferior to sophisticated point-to-point forwarding schemes. When any kind of flooding is used for unicast data forwarding, it will be a waste of network resources due to:

- Broadcast storm: ideally only one message should propagate from the source to the destination though flooding causes excessive number of messages propagating all over the network. Tseng et al. [4] define this situation as *broadcast storm problem*.

- Broadcast flood: even after reaching the destination the messages continue to propagate and get accumulated in the network unless explicit mechanisms are implemented to stop the message propagation and remove the messages. We term this stuation as *broadcast flood problem*

2.3.1 Storm control

Broadcast storm problem is defined as the serious redundancy, contention and collision that occurs in flooding networks as explained below [4]:

- *Redundancy* occurs as the radio propagation is omni-directional and a single physical location may be covered by several nodes. By the time a node decides to rebroadcast a message, the neighbors may have already received the message.

- *Contention* becomes serious as many nodes that are close by each other try to rebroadcast almost simultaneously.

- *Collisions* are more likely to happen because broadcast in CSMA-like protocols provides no collision avoidance and do not implement RTS-CTS like handshake mechanisms.

The followings are the key characteristics of a blindly rebroadcasting MANET that causes storms: (i) each node has no state information about the topology or the neighborhood of the nodes, (ii) every node performs the same simple task of forwarding a received messages, (iii) total number of messages in the network grows exponentially and (iv) there is a large number of interacting nodes. We surveyed similar systems found in the nature in order to identify candidate regulatory mechanisms to control broadcast storms caused by flooding. Biological inspirations have given promising results in arriving at satisfactory solutions for difficult problems especially in communication networks. For instance, Wedde et al. [1] proposed an energy efficient routing algorithm known as BeeAdHoc for MANETs inspired by the foraging principles of honey bees to address the energy dilemma in MANETs. Gunes et.al [27] addresses the issue of packet overhead in routing and proposes Ant-Colony-Based Routing Algorithm (ARA) inspired by swarm intelligence in ant colonies. Similarly a number of studies base their solutions on ant colony optimizations [28, 29]. Moreover, Sarafijanovic and Boudec address the problem of node misbehavior in MANETs and gain inspirations from the human immune system for their solution [30]. Similarly, Kefalas et.al [31] bases their solution for the problem of modeling dynamic behavior of multi-agent systems on the evolution of human tissues.

The natural systems that we surveyed include ant colonies, foraging of honey bees, swarm intelligence of termites, multi-agent systems, immune system, bacteria quorum sensing, diffusion-based systems, epidemics and cell proliferation.

2.3.1.1 Ant colony heuristics

Ants lay trails known as pheromones while walking in search of food. They select a path at random at a junction and those who take the shortest path to the food will return fast on the same path thus increasing pheromone concentration quickly on that path. Other ants will follow the path with the highest pheromone concentration. This

behavior has inspired a number of routing protocols [27, 32, 28, 29]. However, these protocols are required to maintain routes and devised to discover and set paths. Though ants are a population of large number of autonomous entities each performing a simple set of similar tasks there is no exponential growth of items involved as in broadcast storms.

2.3.1.2 Foraging of honey bees

Bees are organized as several types of agents and two of them are key to foraging: foragers who collect water, nectar and pollen outside the hive, and scouts who discover new routes from hive to flowers and recruit foragers for discovered routes using metaphor of dance. The working principles of these agents have inspired a number of MANET routing protocols [1, 33, 34]. These protocols assign special nodes and use special control packets in order to find paths across the networks.

2.3.1.3 Swarm intelligence of termites

In order to build a formicary, termites also act in a similar manner to ants where a termite carries one pebble at a time and lays pheromone on the path. If it comes across another pebble on the path, it drops the pebble in hand on that spot. A termite that walks back without a pebble on seeing a pebble will pick it and walk along the increasing pheromone gradient. This behavior is based on stigmergy which is defined as the process of information dissemination using indirect mechanisms such as pheromones in the environment. A few examples for routing mechanisms for wireless networks inspired by stigmergy of termites are [35, 36, 37].

2.3.1.4 Multi-agent systems

Many biological systems such as ant colonies, termites, swarms of bees, flocks of birds are abstracted to multi agent systems due to the operational concepts such as differentiation of individual entities that can be considered as agents, interaction and communication among these entities, and evolution of entities according to a set of rules and actions. There are a few routing schemes proposed, based on multi-agent

concepts [38, 39, 40, 41]. However, these schemes also assign routing and control operations to special agents.

2.3.1.5 Immune system

Human immune system consists of cells that automatically detect infectious agents called pathogens. This system is able to recognize the invading pathogens, kill them and remember the invaders after resolving the situation. The coordination and communication mechanisms that take place in the immune system in performing these tasks have attracted computer scientists. Consequently there are several MANET routing schemes that are inspired by the immune system with an emphasis on security and detecting node misbehavior [30, 42, 43].

2.3.1.6 Bacterial activities

Bacterial foraging consists of four main steps: 1. guess a possible region with food, 2. decide whether to enter the region, 3. search the region and 4. decide whether to remain in the region or move to another region. Bacterial Foraging Optimization Algorithm (BFOA) used in a few routing schemes for wireless networks is inspired by the above foraging behavior [44, 45, 46, 47]. Another interesting bacterial activity is quorum sensing which is a system of stimuli and responses that depends on the population density. Ability to sense their own cell density and to behave as a population than individuals is the key property of quorum sensing. The signaling process in bacterial quorum sensing has inspired the clustering algorithm for sensor networks in [48]. Bacteria communicate with one another by using the variation of concentration of secreted molecules and this idea is known as molecular communication.

2.3.1.7 Diffusion-based systems

In an attempt to investigate molecular communication we came across diffusion based systems which may include regulatory mechanisms for growth scenarios such as broadcast storms. It is desirable that the messages are propagated in a manner similar to diffusion where more messages may be available close to the source but the packet

concentration decreases towards the destination. We tried to identify a model for diffusivity by referring to work such as [49, 50]. However, there was no suitable model that could fit the broadcast storm scenario with a candidate regulatory mechanism and we realized that the media such as air and liquid are taken for granted to behave according to laws of physics that result in diffusion of molecules.

2.3.1.8 Epidemics

The process of data packet dissemination from node to node in a MANET is perceived similar to the case of humans getting infected by the already infected humans as they come in contact during the time of epidemics [51, 52]. However, these epidemic models are suitable for performance evaluation of MANETs, for example to estimate the rate of propagation of packets. The epidemic models were unable to provide inspirations for growth regulation to control broadcast storms.

2.3.1.9 Cell proliferation

The process of growing in number due to the division of biological cells is known as *cell proliferation* [53]. Human organs grow by cell proliferation, however the organs do not grow infinitely. There should be some mechanism to regulate cell proliferation so that the organs end up growing into a particular shape and a size. Cell proliferation closely mimics message rebroadcasting because in both scenarios the numbers grow exponentially. After exploring this subject thoroughly we selected cell proliferation in the growth of the organs as a candidate system to inspire broadcast storm control in MANETs. Section 5.2 in Chapter 5 details the regulatory mechanisms in the growth of the organs and maps the MANET concepts to cell biological concepts.

2.3.2 Flood control

We define *broadcast flood* as the accumulation of messages in the network by propagating beyond the destination in the case of unicast via rebroadcasting. In order to avoid unnecessary message accumulation the conventional mechanisms in networking are to implement a counter like time-to-live (TTL) value or a timer. In TTL mech-

anism, the message carries a positive integer counter that decreases by one at each rebroadcasting. The message gets discarded when the TTL hits zero. When a timer is set, the message is discarded on the expiry of the timer, but this requires the nodes in the network to be time synchronized. Both of these schemes require the knowledge of global network topology, at least the network diameter, to assure that the message does not die before reaching the destination.

2.3.2.1 TTL-based controlled flooding

TTL based controlled flooding is used in [54] for searching in large networks, for example in searching the destination node in a MANET without a priori position information. TTL is also used as a mechanism to reduce the number of messages and beacons in mobile networks in [55]. However, TTL mechanism does not assure reliable data forwarding in unicast and this is apparent from the fact that the work in [54] uses several attempts to send a search query with increasing TTL values until an acknowledgement is received from the desired node.

2.3.2.2 Timer based control

Another packet control mechanism that is capable of reducing broadcast flood situation is to assign a time to kill each message as in [55]. The same concept is termed *discard timer* in a different context [56, 57, 58] where a timer is started to monitor the lifetime of a data unit to be discarded from the buffer. This idea can be extended to a MANET if nodes are time synchronized but it is impractical to time synchronize nodes in a dense MANET.

2.3.2.3 Cell biological mechanisms

Some types of biological cells are allowed to divide only a limited number of times. The number of divisions that a cell undergoes is measured by using some characteristics such as telomere shortening or DNA modification that occurs at each division [53]. These mechanisms are similar to TTL and timer based mechanisms for packet discarding in communication networks.

2.3.2.4 Negative feedback packets

Gao et al. [59] proposed *recall* protocol that terminates probe packets propagating in a sensor network. A special type of packets called *recall packets* is sent with a higher speed than probe packets to catch up and terminate the forwarding of probe packets. This concept does not require any topological information but there should be an efficient mechanism to disseminate the negative packets such as recall packets. Therefore, we ear-marked negative feedback packets as a better mechanism to control broadcast flood.

2.4 Summary

In order to find a solution to the dense MANET routing problem, we conducted a broad survey of existing routing schemes and found that it is too costly to discover routes and maintain states such as routing tables. It is not feasible and flexible to appoint special nodes as spines or backbone networks in a dense MANET. An alternative is to unicast data using simple flooding, but it causes broadcast storm and broadcast flood. After surveying different mechanisms available in different domains we chose biological cell proliferation in the growth of the organ to inspire a solution for storm problem and negative feedback messages to control broadcast flood. We propose the total solution in Chapter 5.

CHAPTER III

REVIEW OF FLOODING SCHEMES

3.1 Introduction

In Section 2.3 in the previous chapter we proposed that simple flooding is an alternative unicast mechanism. The endcast schemes avoid the cost of traditional MANET routing as explained in Chapter 2. Flooding is conventionally used for network-wide broadcasts. Traditional routing protocols also use simple flooding to disseminate control packets. However, simple flooding causes broadcast storm in general and broadcast flood situations when used in unicast, as explained in Section 2.3. There are various improvements proposed for simple flooding in the literature to address the broadcast storm problem by suppressing redundant rebroadcasts. These improved flooding schemes require only a subset of nodes in the network to forward the message and thus referred to as *efficient flooding* in [60]. In this chapter, we explore such efficient flooding schemes in terms of their characteristics, how they are modeled and evaluated, and also the underlying technologies that enable implementation of these schemes. In the following sections, the term *broadcast* refers to the network-wide reach of messages in multihop networks unless stated otherwise.

3.2 Broadcast protocols in MANETs

Tseng et al. [4] proposed five schemes to suppress redundant rebroadcasts in MANET flooding, namely probabilistic, counter-based, distance-based, location-based and cluster-based schemes. These efficient flooding schemes differ in how a mobile host estimates the redundancy and how it accumulates the knowledge to support the packet forwarding decision. In probabilistic flooding a received packet is rebroadcast with a certain probability. In counter based flooding a node counts the number of times the same frame is received and makes the rebroadcast decision based on this count. The relative distance between nodes is used to decide whether a node should rebroadcast a received packet in distance based schemes. When a packet is received from a close by node, the receiving node may gain only a small additional coverage area by rebroadcasting the packet. A node rebroadcasts a received packet depending on the location of the sender in location based flooding. In cluster based scheme, each node runs a cluster formation algorithm using periodic messages sent by the other nodes to advertise their presence and a cluster head is appointed for each formed cluster. According to these explanations, probabilistic flooding and counter based flooding use information that is totally local to the node without explicitly collecting topological information as in distance based, location based and cluster based schemes. Moreover, probabilistic and counter based schemes do not appoint special nodes such as cluster heads in cluster based scheme.

Williams and Camp [5] categorize flooding schemes into four families: simple flooding, probability based methods, area based methods and neighbor knowledge methods. Accordingly, probabilistic and counter-based methods in [4] are categorized under probability based methods while distance-based and location-based flooding schemes in [4] are listed under area-based methods as shown in Figure 3.1. According to this categorization, we are interested in probability based methods under which, both the probabilistic flooding and the counter based flooding are classified.

Flooding with self-pruning, scalable broadcast algorithm (SBA), dominant pruning, multipoint relaying (MPR), adhoc broadcast protocol (AHBP), connected dominating set (CDS) based algorithm, lightweight and efficient network-wide broadcast

(LENWB) protocol are examples of neighbor knowledge schemes according to the categorization of Williams and Camp [5]. Since neighbor knowledge schemes explicitly gather topological information rather than information totally local to the node, we do not consider them for mobile-stateless unicast.

Yassein et al. [61] categorized efficient flooding schemes in to two: probability-based broadcast schemes and deterministic broadcast schemes. Probability-based schemes include probability based, counter-based, location-based, distance-based and hybrid flooding schemes. Deterministic broadcast schemes include multipoint relaying, node-forwarding, neighbor elimination and clustering. Since deterministic broadcast schemes require topological information about the network they will not be suitable for mobile-stateless packet forwarding in MANETs. Yi and Gerla [60] classify flooding schemes into heuristic-based protocols, topology-based protocols and cluster-based protocols. They further categorize topology-based schemes into neighbor topology based and source tree based protocols. Cluster-based protocols are also subcategorized into active clustering and passive clustering. Figure 3.1 summarizes the classification of flooding schemes according to [5] and [62].

Another classification of broadcast storm control mechanisms are (i) imposing a partial routing overlay structure and (ii) selectively dropping messages [63]. Schemes in category (i) build a multicast or broadcast tree and require topological information while those in (ii) make nodes to independently decide whether to rebroadcast the packets using local information as in pure probabilistic flooding. According to Wu and Lou [64] broadcast protocols are categorized into global, quasi global, quasi local and local in terms of neighbor knowledge information. Flooding schemes are also classified as (i) 0-hop (no need of neighbor information), (ii) 1-hop neighbor information and (iii) 2 or more-hop neighbor information schemes [65, 66]

Some of these flooding schemes try to build a virtual backbone for ad hoc networks by selecting a subset of nodes as core to disseminate a message across the network. This core should consist of a connected dominating set (Section 3.7) that includes as fewer nodes as possible to reduce broadcast storm. Hence these schemes are often abstracted as finding a minimum connected dominating set in unit disk graphs [67].

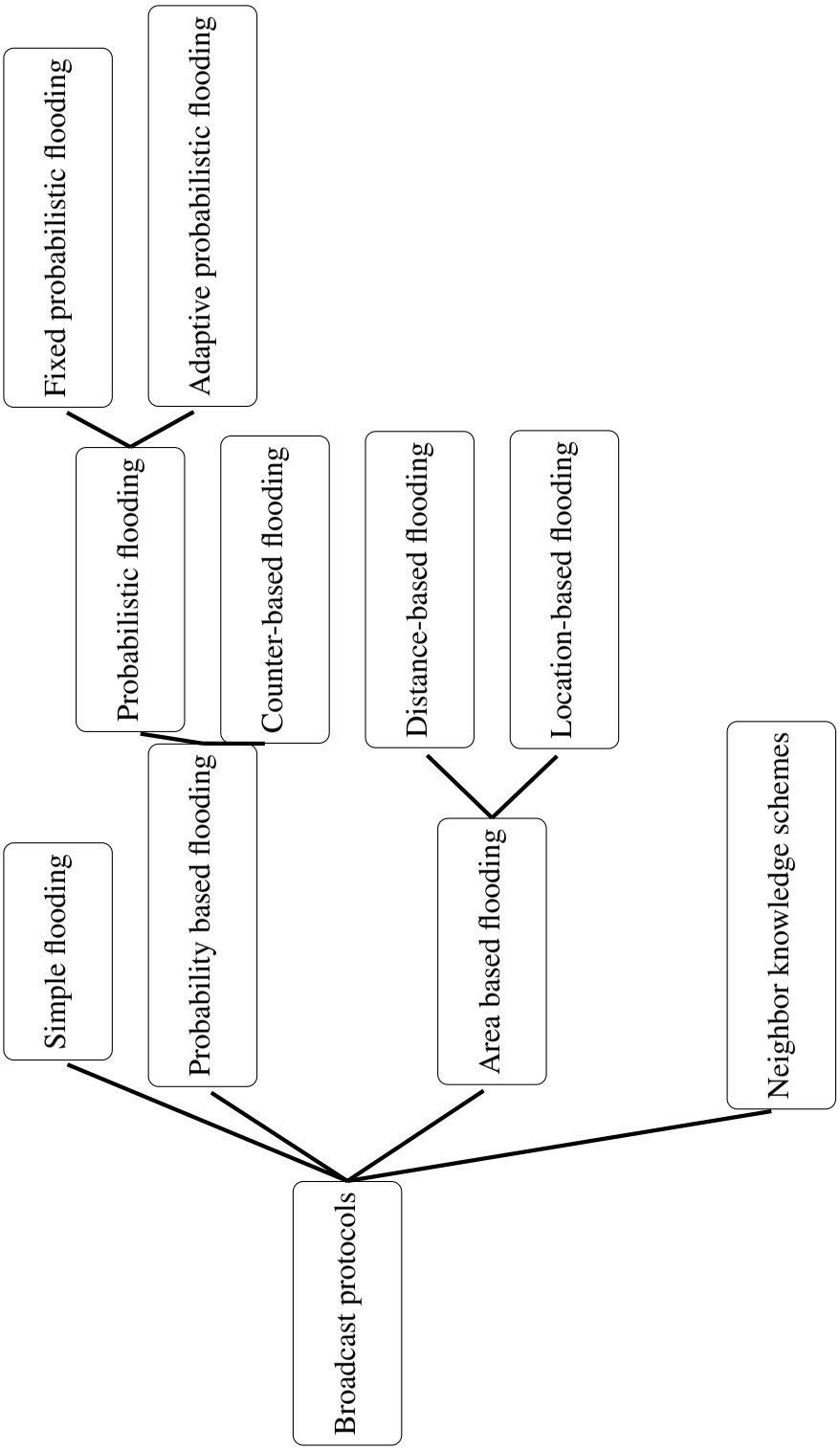

Figure 3.1: Categorization of broadcast schemes in MANETs

According to Williams and Camp [5] probability based and area based flooding schemes perform poor when node count increases. Schemes that use a random time delay suffer in congestive networks unless that delay is adapted to congestion level. Neighbor knowledge schemes that use two or more hop neighbor information do not adapt to highly mobile network conditions as the neighbor information get quickly outdated. They further suggest that probability based and area based schemes can be improved by adapting them to neighbor count and congestion level. However, the use of local beaconing to gather neighbor information and an adaptive delay mechanisms are discouraged as they negate the simplicity of the protocols.

Above analysis of existing flooding schemes, is to draw ideas for devising a flooding scheme for unicast in such a way that broadcast storms are minimized by suppressing redundant rebroadcast with the help of totally local state information and that suits dense MANETs. Table 3.1 summarizes the flooding schemes in terms of how they suit our expectation. Tseng et al. [4] claim that a simple counter based scheme can eliminate many redundant rebroadcasts compared to simple flooding when the node distribution is dense.

According to these explanations, we selected probabilistic flooding and counter based flooding for further investigation as they use information that is totally local to the node without explicitly collecting topological information as in area based schemes and neighbor knowledge schemes. Neighbor knowledge schemes appoint key nodes apart from gathering topological information so that they do not conform to mobile-stateless routing paradigm introduced in Chapter 1. Section 3.2.1 explains probabilistic flooding and Section 3.2.2 explains counter based flooding in detail.

3.2.1 Probabilistic flooding

In probabilistic flooding, a packet that a node receives for the first time will be rebroadcast with a probability P. To reduce the chances of collision and contention a random delay is used for rebroadcasting. We identify this scheme as a candidate scheme to base our mobile-stateless endcast.

Viswanath and Obraczka [2] model the propagation of the packet flooding using a

Table 3.1: Selecting flooding schemes for mobile-stateless endcast

category	**flooding scheme**	**state information**	**assign key nodes**	**select/reject for further study**
probability based	probabilistic flooding	0-hop	No	Select
	counter based flooding	0-hop	No	Select
neighbor knowledge based	flooding with self pruning	1-hop	No	Reject
	SBA	2-hop	No	Reject
	dominant pruning	2-hop	assign rebroadcasting nodes	Reject
	MPR	2-hop	assign multipoint relays	Reject
	AHBP	2-hop	assign broadcast relay gateways	Reject
	CDS based flooding	2-hop	assign broadcast relay gateways	Reject
	LENWB	2-hop	assign rebroadcasting priority	Reject
	cluster based	1-hop	assign cluster head	Reject
area based	distance based	1-hop relative distance	No	Reject
	location based	1-hop location	No	Reject

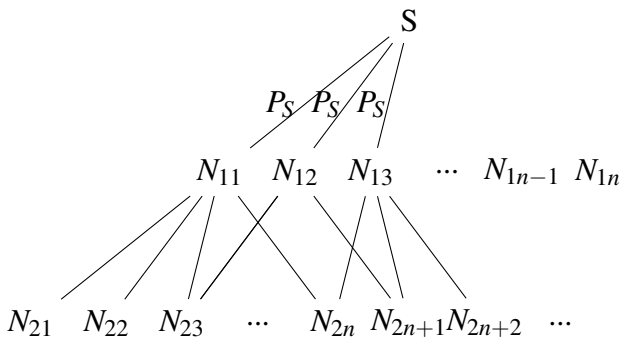

Figure 3.2: Data propagation in simple flooding [2]

tree as shown in Figure 3.2. Each level in the tree corresponds to the retransmission level, which implies the number of hops from S that the message has propagated. The total number of nodes reached by probabilistic flooding is estimated using Equation 3.1. Here, N_T is the total number of nodes that receive the transmission of S in Figure 3.2, l is the transmission level, N is the number of nodes within a transmission region, β is the expected increase in the coverage area achieved by the second level retransmission, P_S is the probability of successful transmission, P_b is the probability of successful reception and P is the probability of rebroadcasting in probabilistic flooding.

$$N_T = P_S N + P_S N \sum_{i=1}^{l-1} (\beta P P_b N)^i \tag{3.1}$$

Let, $N = 10$. Assume ideal wireless propagation, thus, $P_S = P_b = 1$. As Viswanath and Obraczka [2] also uses, $\beta = 41\%$ and this is a finding of Tseng et al. [4]. Then, the total number of nodes reached by the end of each retransmission level will give a plot as in Figure 3.3.

3.2.2 Counter based flooding

In counter-based flooding schemes a node counts the number of times the same message is heard during a random period of wait time. When this counter reaches a threshold a node decides not to rebroadcast the message.

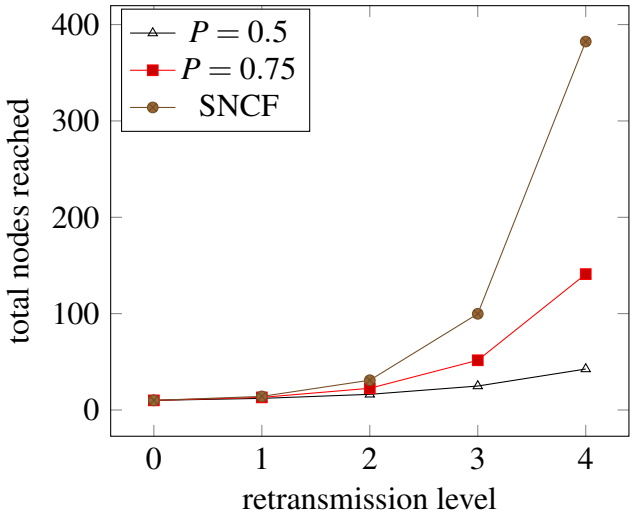

Figure 3.3: Total number of nodes reached by propagation of probabilistic flooding

Biological inspiration: Simple flooding is analogous to biological cell division in organ growth as already mentioned in Section 2.3. The number of cells accumulated in an organ is estimated via the concentration of a molecule called *chalone* in the medium by the *chalone mechanism* in the growth of the organs. Each cell is allowed to make an independent decision whether to divide, on the condition that chalone concentration does not exceed a threshold as explained in Section 2.3.1. This closely mimics counter based flooding scheme and thus we consider counter based flooding in detail here.

The threshold in counter based flooding should be set according to the expected coverage area obtained by rebroadcasting the message, which is referred to as Expected Additional Coverage (EAC) in [4].

Expected additional coverage (EAC): Consider a scenario in which a node A broadcasts a message and another node B that receives it decides to rebroadcast. Figure 3.4 represents this scenario and the shaded area will be the additional area that can benefit from the transmission of B. If S_A and S_B are the circular areas covered by A and B respectively, then S_{B-A} (the shaded area in Figure 3.4) is given by $S_{B-A} = S_B - S_{A \cap B} = \pi r^2 - INTC(d)$, where $INTC(d)$ given by Equation 3.2 is the intersection of S_A and S_B as derived in [4].

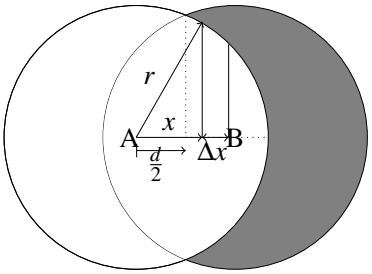

Figure 3.4: Additional area covered by a rebroadcast [4]

$$INTC(d) = 4\int_{\frac{d}{2}}^{r} \sqrt{r^2 - x^2}dx \tag{3.2}$$

For the case of two nodes placed d distance apart with transmission range of r has the minimum overlap of coverage when $d = r$ that is if B is at the boundary of the A's range in Figure 3.4. If node B decides to retransmit, the additional area that B covers is only 61%. Therefore, the additional coverage $\pi r^2 - INTC(x)$, varies from 0 to 61% when x varies from 0 to r. It is found in []broadcastStorm, if B is randomly located in the transmission region of A, the expected additional coverage (EAC) is given by Equation 3.3. By solving Equation 3.3 EAC is obtained as 41%.

$$EAC = \int_0^r \frac{2\pi x[\pi r^2 - INTC(x)]}{\pi r^2}dx \tag{3.3}$$

Tseng et al. [4] also define $EAC(k)$ as the expected additional coverage when a node rebroadcasts after hearing a message k times. They place k nodes randomly on the coverage area of node X and estimate the area covered by the transmission of node X excluding the area that is already covered by other k nodes using a simulation. The simulation results are shown in Figure 3.5. Accordingly, EAC drops rapidly when the counter value increases in counter based flooding. As per Figure 3.5, $k \geq 4$ gives only an EAC of less than 5%.

In order for the flooding schemes to be suitable in mobile-stateless routing paradigm in dense MANETs, the information collected by nodes to support its forwarding decision should be totally local to the node. Beaconing among neighbors, is also undesirable due to dense nature of the network. There should not be complex computations

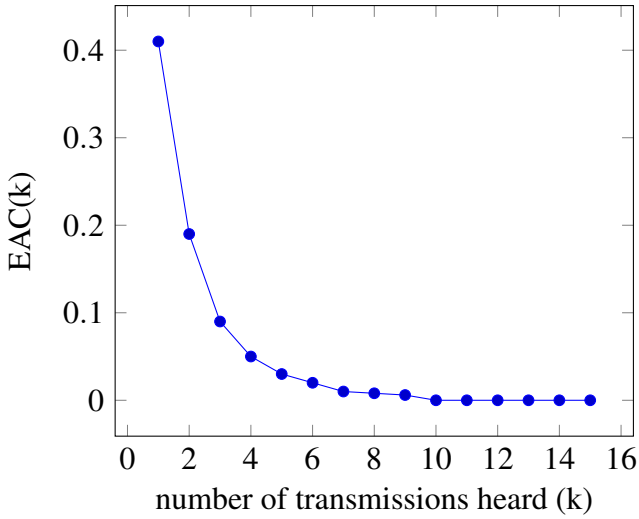

Figure 3.5: Simulation results for expected additional coverage (EAC(k)), achieved by a node when it hears from k neighbors [4]

in such dense networks for example in estimating internode distances using received signal strengths as in distance based flooding schemes.

Counter based flooding can be identified as a type of probability based, heuristic based mechanism that selectively drops packets to reduce broadcast storms. A number of counter-based flooding schemes are available in the literature such as Efficient Counter-based Scheme (ECS)[68] and dynamic counter based broadcast scheme [61]. An adaptive counter-based scheme is proposed in [69]. ECS in [68] combines the basic counter based and probabilistic flooding so that the forwarding decision is based both on the packet count threshold and the forwarding probability. If a node receives an unseen packet a counter is initiated to record the number of copies of the same message received during a random period of time and the packet will be rebroadcast with a certain probability if the counter is less than a threshold. Yassein et al. [61] propose a counter based flooding scheme which includes three thresholds namely C_{min}, C_{mid} and C_{max} and a threshold is dynamically selected depending on the number of neighbors.

A color based counter based broadcast scheme is proposed in [70]. In this scheme a broadcast message includes a color field and the nodes overhearing this message records the color. After a random period of time the number of colors is compared with a threshold η. If the number is less than η the message is rebroadcast with a

new color assigned to the color field. Another variation of counter based flooding is *DIS_RAD* proposed in [71] which gives the nodes closer to the border of the coverage area a higher probability of rebroadcasting to obtain a better additional coverage.

Random Assessment Delay (RAD) According to the explanations given at the beginning of this section, most of the flooding schemes require to keep track of some variable, for example the number of redundant messages received in counter-based flooding and the relative distance between the nodes in distance-based schemes. The nodes have to assess these variables to make a decision whether to forward a received message. This process requires a time interval such that the nodes are able to gather required information from the neighbors and to assess the information against a set of conditions. This time interval is termed Random Assessment Delay (RAD) in [5].

There is no such neighbor information gathering or assessment of any variable in simple flooding or SNCF except that the nodes have to look up the sequence numbers of messages to check for their redundancy. However, SNCF also requires a random delay in order to avoid collisions caused if all the neighbors of a transmitting node simultaneously rebroadcast the message.

The general method of setting the RAD that we denote here as T_{RAD} is to randomly select a value from a uniform distribution between 0 and T_{max} seconds, where T_{max} is the maximum possible delay [5]. RAD, not only allows nodes a sufficient time to receive required neighbor information and assess whether to rebroadcast, but also helps avoiding collisions.

3.3 Broadcast protocol evaluation

In general, routing protocols at the network layer in multihop wireless networks are evaluated using metrics such as number of hops, packet delivery fraction (PDF), end to end delay (E2E), routing overhead or normalized routing load (NRL), throughput and number of dropped packets (NDrp) [62]. **Packet delivery fraction (PDF)** or **packet delivery ratio (PDR)** is the ratio of the data packets delivered to the destination to those originated at the source [72, 73, 74, 75, 76]. **End to end delay (E2E)** captures all

possible delays such as queuing, buffering and propagation over the links from source to the destination and E2E is used in a number of publications [73, 77, 78, 75, 76]. **Routing overhead** which is also known as **normalized routing load (NRL)** is the number or size of routing control packets transmitted per data packet delivered at the destination [72, 74, 76]. **NDrp** counts the total number of dropped packets.

PDF and E2E are directly applied at the link layer in [72, 73, 74, 75, 76, 77, 78, 75] in the attempt to evaluate the Hybrid Wireless Mesh Protocol (HWMP), which is a link layer protocol proposed for wireless mesh networks (WMNs) in IEEE 802.11 standards. This is acceptable because HWMP sets paths by acting similar to AODV. However, at the link layer, the process of setting such multihop paths is termed *path selection* according to IEEE 802.11 standard. Similar to routing overhead used in network layer, *Path selection control overhead* is evaluated as a metric at the link layer [72, 74, 76].

PDF and NDrp are applicable when there is a risk that the packet is lost due to dropping by intermediate nodes in a single path. In contrast, in endcast, the packets multiply due to propagation. Therefore, we consider PDF and NDrp as not applicable.

Flooding schemes are used as an underlying process of network layer routing, for example to disseminate route request messages in AODV. Therefore, broadcast schemes are evaluated in two different contexts; (i) as a supporting scheme for end to end route discovery (ii) as a standalone message dissemination technique. In the former context, it is required to reach only the source-destination pair by the broadcast whereas in the latter case the objective is to reach as many nodes as possible.

Metrics that evaluate broadcast schemes when they are used to discover routes, are known as *discovery process metrics* in [62]. **Path found ratio (PFR)**, **route discovery delay (RDD)** and **bcast** are listed under discovery process metrics by Reina et al. [62]. PFR is the ratio of the number of paths found to the number of path requests and this metric is also known as discovery rate or connectivity success ratio. The time elapsed between the first broadcast of the route request and the first receipt of the route reply is termed as RDD. Average number of broadcast packets sent by a node per discovered path is given by bcast. Since, our aim is to unicast messages via a broadcast scheme,

Table 3.2: Selecting performance metrics for mobile-stateless endcast

context	**metric**	**property measured**	**unicast efficiency**	**broadcast efficiency**	**select/ reject**
routing metrics	PDF	number of packets	not applicable		
	E2E	time	yes	no	Select
	NRL	number or size of control packets	not applicable		
	NDrp	number of dropped packets	not applicable		
discovery process metrics	PFR	number of packets	not applicable		
	RDD	time	not applicable		
	Bcast	number of packets	not applicable		
broadcast efficiency metrics	SRB	number of nodes	no	yes	Select
	ROH	number of packets	no	yes	Select
	NR	number of broadcast actions	no	yes	Reject
	RE	number of nodes	no	yes	Select
	ARP	number of packets	yes	no	Reject
	Flooding completion time	time	no	yes	Select
	NPPR	packet rate	no	yes	Reject

this category of metrics is not applicable.

Reina et al. [62] identify metrics that evaluate broadcast schemes, when used as a standalone data dissemination technique, as *broadcast efficiency metrics*. Further, they classify these broadcast efficiency metrics into four categories according to what is measured: (i) redundancy metrics (ii) reachability metrics (iii) delay metrics and (iv) energy metrics. Broadcast schemes should be designed to reach as many nodes as possible with minimum redundant rebroadcasts while maintaining minimum delay and minimum energy consumption. Redundancy metrics include saved rebroadcasts (SRB), redundancy overhead (ROH) and number of retransmissions (NR). Reachability metrics include reachability (RE) and average reception percentage (ARP). Delay

metrics are normalized packet penetration rate (NPPR) and flooding completion time or broadcast end to end delay.

Saved Rebroadcasts (SRB) is given by $\frac{r-t}{r}$ where r is the number of nodes receiving the broadcast packet and t is the number of hosts actually rebroadcasting the packet [69]. **Redundancy overhead (ROH)** is defined in [62] as the sum of number of duplicate packets received at each node divided by the total number of nodes in the network. In ROH, the number of packets is divided by total number of nodes assuming that the flooding is reached by all nodes. In contrast we purposely limit the propagation of flooding. Therefore, we quantify redundancy in terms of total number of packets without dividing by number of nodes and we identify this definition by **Redundancy overhead for endcast** (ROH_{uf}). **Number of retransmissions (NR)** gives the total number of retransmissions. NR is also referred to as number of rebroadcasts [62]. All the flooding schemes that we have selected for further study, namely, simple flooding, probabilistic flooding and counter based flooding allow a node to rebroadcast a received frame only once. Therefore, number of rebroadcast actions equals the number of rebroadcasting nodes. SRB captures number of rebroadcasting nodes and as well as the number of receiving nodes. Therefore, we ignore NR. ROH is applicable to flooding when it is used as a technique to disseminate message to all nodes where as we use flooding for unicast communication.

REachability (RE) is given by $\frac{r}{e}$ where r is the number of nodes receiving the broadcast packet and e is the number of nodes that are reachable from the source at the time of broadcast according to the original definition by Tseng et al. [69]. This definition caters for the traditional use of flooding schemes where the objective is to reach all the nodes in the network. **Average reception percentage (ARP)** gives the percentage of messages originated at the source and received at the destination [62]. We are interested in how a single packet will propagate throughout the network, therefore, we do not select ARP.

Normalized packet penetration rate (NPPR) estimates how fast the broadcast packets travel across the network. Average latency is given by the interval between the time at which the broadcast is initiated and the time at which the last broadcast

Table 3.3: Selected performance metrics

Metric	Abbreviation	Definition
Reachability for endcast	RE_{uf}	ratio between the number of reached source-destination pairs to the number of reachable pairs
Reachability for flooding	RE	ratio between the number of reached nodes to the number of reachable nodes
Flooding completion time	FCT	time from initiation of flooding until the time at which the last action is done on the packet
Saved rebroadcasts	SRB	ratio between the number of nodes that do not rebroadcast and the number of nodes that receive the packet
Redundancy overhead for endcast	ROH_{uf}	total number of duplicated packets by the end of flooding propagation

happens or the last host decides not to rebroadcast [69]. This is also known as **flooding completion time (FCT)** or broadcast end to end delay [62]. Since we are interested in how a single data packet injected by the source into the network will propagate towards the destination in endcast we will not consider packet rates as in NPPR. However, it is essential to evaluate latency because the flooding schemes involve a random delay (RAD) as explained in Section 3.2.

SRB, RE and Average latency are introduced in [69] to evaluate performance of flooding mechanisms. A number of performance studies in the domain of broadcast protocols uses these metrics for their protocol evaluations [79, 80, 81, 22, 82, 83, 84, 85]. However, our protocol is aimed at endcast so that the performance metrics should capture both the *unicast efficiency* and *broadcast efficiency*. Unicast efficiency implies measures such as whether the protocol succeeds in delivering messages between all source destination pairs in an un-partitioned network and how long it takes to reach the destination. Broadcast efficiency metrics should measure how long it takes to finish the propagation of the flooding wave, the redundancy of rebroadcasts and accumulation of packets in the network due to flooding. According to Table 3.2 there are no metrics that cover both unicast and broadcast efficiencies simultaneously.

Therefore, we define metrics for endcast, which we denote by the subscript uf, by combining the concepts of routing metrics and broadcast efficiency metrics. The selected and rejected metrics are in Table 3.2. Accordingly, we define **Reachability for endcast** (RE_{uf}) as the ratio between the number of reached source-destination pairs to the reachable pairs. If the number of reached node pairs by the flooding scheme is r_{uf} and the number of all reachable pairs by topology is e_{uf} then $RE_{uf} = \frac{r_{uf}}{e_{uf}}$.

It is essential to evaluate redundant rebroadcasts as a measure of storm condition when any kind of flooding is used. Therefore, we select both SRB and ROH_{uf}. SRB gives redundancy in terms of number of rebroadcasting nodes, thus SRB can be considered as the redundancy from the transmitters' point of view. ROH_{uf} gives the number of packets received thus it can be considered as a measure of redundancy from the receivers' point of view.

Finally, we selected the set of metrics in Table 3.3 for the evaluation of proposed protocol. The protocol is evaluated by simulations in Chapter 7 using these metrics. Furthermore, redundancy and reachability should be analyzed together because in trying to reduce redundancy, reachability will be compromised as explained below;

Redundancy - Reachability tradeoff: In flooding mechanisms the number of redundant messages in the network can be reduced by allowing only a subset of nodes rebroadcast as done by efficient flooding. In doing that, there is a risk that the messages will not reach some parts of the network. A number of studies also highlight that the flooding mechanisms should be designed with the tradeoff between redundancy and reachability in mind [63, 4, 62]. Reachability quantifies number of reached nodes in comparison with number of reachable nodes. We defined reachability for unicast as reached source-destination pairs in comparison with reachable pairs as explained earlier in this section. Number of redundant messages and the number of nodes that rebroadcast are captured as redundancy metrics as explained before. We selected SRB and ROH_{uf} as redundancy metrics, and RE and RE_{uf} as reachability metrics as shown in Table 3.3. However, SRB or ROH alone cannot show that a flooding scheme performs good or bad. These redundancy measurements must accompany RE measurements to evaluate efficiency of the protocol.

3.4 Simulation studies of flooding schemes in MANETs

MANETs in general are extensively tested in simulations. Major aspects of MANET simulations are shape and size of the geometric area on which the network is placed, number of nodes, node placement or node distribution and mobility. Further, our protocol is targeted at the link layer, which takes the support of the underlying MAC layer and the physical layer for message dissemination. There are important parameters and assumptions related to the MAC and the physical layers in testing link layer protocols. In this section, we explore the simulation studies in the field of MANETs with an emphasis on experiments that evaluate flooding schemes. The aim of this section is to identify important simulation parameters and suitable values for testing our protocol.

Tseng et al. [69] develop a simulator in C++ with an event-driven simulation engine because the MANETs can be modeled as processes that communicate via signals. They simulate CSMA/CA using a simplified version of IEEE 802.11 MAC. Simulation parameters are; transmission radius is 500m, broadcast packet size is 280 Bytes, data rate is 1 Mbps, and IEEE 802.11 suggestions for DSSS physical layer timing (slot time, interframe specifications, and backoff window sizes). They use a geometric area that they call a *map* of sizes 1×1, 3×3, 5×5, 7×7, 9×9 and 11×11 units where a unit is 500m. Nodes are randomly placed and allowed to move randomly defined as a series of turns.

Williams and Camp [5] also place nodes randomly. They characterize the networks as sparse to dense in terms of average number of neighbors per node. Their NS-2 simulation is a $350m \times 300m$ network area. Each node has 100m transmission radius and data packet size is 64 Bytes. Number of nodes vary from 20 to 110 in such a way that the average neighborhood varies from 3.8 to 21.2. This neighborhood range is considered to cover the gamut of sparse to dense MANETs in [5]. The study uses NULL MAC and static nodes to isolate protocol efficiency from the effects of mobility and congestion.

The simulation study conducted by Yassein et al. [81] consists of networks having

25 to 100 nodes placed randomly on a $600m \times 600m$ area with each node having a transmission radius of 250m and a bandwidth of 2Mbps. They experiment on probabilistic flooding by varying the retransmission probabilities from 0.1 to 1.0 with 0.1 increments. Random waypoint mobility is used with maximum speeds of 1, 5, 10, 20 m/s and with no pause times.

Yi et al. [60] simulate 20 randomly generated node topologies using Global Mobile Simulation (GloMoSim) library to test MANET flooding. They place 100 nodes in terrains of size $x \times 1000m$ where x varies from 250m to 1500m in steps of 250m. Transmission radius is 250m and channel capacity is 2 Mbps. Random way point mobility is used with minimum speed of 2 m/s, maximum speed of 20 m/s and a pause time of 100 s. Packet size is 100 Bytes and packets are generated at a rate of 4 flood packets per second.

The simulation study undertaken by Pleisch et al. [63] using JiST/SWANS simulation environment placed 150 nodes uniformly distributed in a field of size $600m \times 600m$ with each node having a maximum transmission range of 88m. Flooding is tested on top of IEEE 802.11b standard MAC.

NS-2 simulation conducted by Liu et al. [65] uses IEEE 802.11 MAC. Data packet is 256 Bytes and channel capacity is 2 Mbps. Number of nodes vary from 200 to 1000 and each node has a transmission range of 250m. Nodes are placed randomly on an area of $1000m \times 1000m$. Network generates 10 flooding messages per second on average. Maximum frame size is 8192 bits or 1024 Bytes referred to in IEEE 802.11 specification. Broadcasts use basic bit rate of 2 Mbps as per this specification.

Table 3.4 summarizes the simulation parameters and values as described above. Network density is an important parameter and the definition and values were found in the literature as explained below. We focus on networks that consist of nodes having power saving radio ranges as opposed to ranges of few hundred meters. Therefore, we select a radio range much less than the minimum of 88 m in Table 3.4. A radio range of 30 to 50 meters will be selected in our analyzes.

Network density: Network density for MANETs and sensor networks is characterized by: (i) average number of neighbors per node [5], (ii) number of nodes per unit

Table 3.4: Surveyed simulation parameters

parameter	**values**	
playground size	minimum maximum	$250m \times 250m$ $5500m \times 5500m$
number of nodes	200 to 1000	
network density (neighbors per node)	4 to 20	
radio range (m)	88 to 500	
data rate (Mbps)	1 and 2	
packet size (Bytes)	64, 100, 256, 280, 1024	

area [86]. We focus on mobile-stateless mechanisms of unicast so that global network details are not used. The second definition of network density, which is in terms of nodes per unit area gives a global perspective of the network as one should know the total number of nodes and the area that the network covers. On the other hand, the first definition of network density, which is in terms of neighborhood gives a local view of the network from the perspective of each individual node. Therefore, we use this definition as it is in line with mobile-stateless paradigm. Sparse to dense network evaluation in [5] is for neighborhood range 4 to 20.

3.5 MAC protocols enabling broadcasts

MAC protocols are required for the purpose of avoiding transmission collisions. It is important to test protocols in the presence of a suitable MAC protocol. The aim of this section is to identify a MAC protocol on which the proposed protocol should be tested. Menouar et al. [87] survey the following MAC protocols used in MANETs:

ALOHA protocols: Word “ALOHA” means “hello” in Hawaiian. ALOHA protocol is based on random access. A node transmits data when it wants to transmit. If a collision occurs it waits for a random amount of time before retransmitting. Maximum throughput of the protocol is found to be 18.4% of the channel capacity for a fixed message length. Since the pure randomness causes throughput reduction the slotted version of ALOHA (S-ALOHA) was proposed. The nodes transmit only at the

beginning of a time slot. Another variation of ALOHA is Reservation ALOHA (R-ALOHA), in which slots are reserved by nodes that used the previous slot successfully [88].

Carrier Sense Multiple Access (CSMA): In this protocol a node must sense the channel before transmitting. If the channel is sensed idle then the node transmits otherwise the transmission if deferred by a random time period. Basic CSMA can be easily used in multihop networks and it outperforms ALOHA protocol according to [89]. Demirkol et al. [90] showed in a survey of MAC protocols used in sensor networks that CSMA based protocols are satisfactory in adapting to topology changes. CSMA has few access modes, namely 1-persistent, non-persistent and p-persistent CSMA. In 1-persistent CSMA, if the channel is sensed to be busy, a node keeps listening until the channel becomes idle. In non persistent CSMA, channel waits for a random period without listening to the channel if the channel is sensed to be busy. In p-persistent CSMA, if the channel is sensed to be idle a node transmits with a probability p. If the node transmitted and the channel is still sensed to be idle then the node transmits again with the same probability. If the node does not transmit, then it waits for the next available time slot and transmits with probability p. If the channel is sensed to be busy the node senses the channel until it becomes idle.

Multiple Access with Collision Avoidance (MACA): MACA avoids collision using handshake with the destination. The sender broadcasts a Request to Send (RTS) frame so that all its neighbors are informed of an upcoming transmission. The destination replies with a Clear to Send (CTS) broadcast frame so that all its neighbors also knows of this transmission. The sender transmits data after receiving the CTS without colliding as the neighbors of both the sender and the receiver refrain from transmitting during this transmission. However this protocol does not solve exposed source problem because nodes will proceed with transmission after receiving a RTS if a CTS is not heard.

MACA Wireless (MACAW): MACAW includes RTS-CTS mechanism added with Data Sending (DS) frame and an Acknowledgement (ACK) frame to solve the exposed source problem. Although a node trying to transmit in the neighborhood of a source

may not receive the CTS, it will receive DS sent by the source thus the node is informed of an on-going transmission.

Busy Tone Multiple Access (BTMA): BTMA splits the channel into two sub channels; one for data and the other for control. Control channel carries busy tone signal when a data transmission is on going. A node should sense the control channel before sending data. On sensing an idle control channel a source will send a busy tone signal followed by data on the data channel. All immediate neighbors who sense busy tone forwards it to its neighbors also so that the two hop neighbors are informed of an on-going transmission thereby avoiding hidden terminal and exposed source problems.

Time Division Multiple Access (TDMA): In TDMA, the channel is split into fixed frames in time and each frame is split into fixed time slots. In TDMA based MAC protocols, there are data frames and control frames. Control frames are often used for reserving the channel.

Frequency Division Multiple Access (FDMA): In FDMA, the medium is divided in frequency so several nodes can transmit simultaneously. Any MAC protocol can be applied in each channel as for example MCSMA, which uses CSMA on each frequency channel.

Code Division Multiple Access (CDMA): In CDMA, several orthogonal codes are used to encrypt messages before transmitting. For example Multicode MAC (MC-MAC) uses one common code for control messages. The code is sent by the sender via RTS message. If the code has no conflict with other codes the receiver responds with CTS. Otherwise the CTS carries usable codes. The sender has to send a new RTS with one of these codes and receive a CTS to continue data transmission.

Hidden terminal problem and exposed source problem are highlighted in almost all publications as the major problems in wireless transmission especially affecting MANET due to its multihop communication [87, 89, 90, 91, 92]. There are few MAC protocols proposed for ad hoc networks to address hidden terminal problem and exposed terminal problem but these protocols have not attracted considerable attention to develop into an implementation level. For example Borgonovo et al. [91] proposed a protocol named ADHOC MAC that uses Reliable R-ALOHA (RR-ALOHA) and Ye et

al. [93] proposed a scheme known as S-MAC for energy efficiency but such schemes are at research level.

Ye et al. [93] broadly categorize MAC protocols used in sensor networks into contention-based and reservation-and-scheduling-based protocols. Accordingly, ALOHA, MACA, MACAW, BTMA and CSMA are contention based protocols whereas TDMA, FDMA and CDMA are reservation and scheduling based protocols. Reservation and pre-scheduling schemes are not suitable for dynamic networks such as MANETs because the predetermined schedules will get obsolete quickly when links break and reconnect as nodes move. Therefore, we consider only the contention based MAC protocols to carry unicast data via flooding.

Flooding schemes use MAC layer to provide contention-free broadcast links to carry multihop flooding messages. The term *broadcast* here refers to communication over a single link where transmission of a node is received only by the nodes in the coverage area of that node. It is inefficient to use handshake mechanisms such as RTS-CTS for broadcast links due to control message overhead. Therefore, MACA and MACAW schemes are not considered for further analysis though they are contention based protocols. CSMA is better than ALOHA protocols because CSMA reduces collisions due to its carrier sensing behavior. Wu and Varshney [92] show in a performance study that BTMA performs better than CSMA in terms of throughput. However, IEEE 802.11 MAC is CSMA based and hence CSMA is the most widely implemented MAC scheme by wireless network card manufacturers. Therefore, we select CSMA over BTMA in our MANET scenario with the intention of testing the proposed protocol on already available commodity wireless hardware as a task outside the scope of this research. Table 3.5 summarizes how we selected CSMA as the underlying MAC protocol for the proposed endcast scheme.

IEEE 802.11 MAC: MAC protocol in IEEE 802.11 standard is known as Distributed Coordination Function (DCF). According to Reina et al. [62], IEEE 802.11 DCF is the standard MAC layer employed in majority of the proposed broadcast schemes found in the literature and this fact is also evident from the studies surveyed in this research such as [69, 63, 65]. IEEE 802.11 DCF is built on research protocol

Table 3.5: Selecting a MAC protocol

MAC protocol	**select/ reject**	**reason**
CSMA	select	no control messages or handshake, widely implemented
ALOHA	reject	throughput less than CSMA
BTMA	reject	not implemented in widely available hardware
MACA	reject	inefficient for broadcast due to handshake using RTS, CTS control messages
MACAW	reject	inefficient for broadcast due to RTS, CTS, ACK, DS control messages
TDMA	reject	inefficient for broadcast due to reservation frames
FDMA	reject	inefficient for broadcast due to reservation of sub channels
CDMA	reject	inefficient for broadcast due to reservation of orthogonal codes

MACAW according to Ye et al. [93]. However, it does not use its RTS-CTS mechanism for collision avoidance in broadcasting. Therefore, IEEE 802.11 DCF in its broadcast mode is basically the non persistent CSMA. The most critical problem in using CSMA for multihop communication is considered to be the hidden terminal problem [2, 92]. CSMA is explained in detail with the help of a theoretical model in Chapter 6.

IEEE 802.15 protocols such as Bluetooth may also be considered. However, Bluetooth allows only eight devices to communicate and may not be sufficient to handle dense neighborhood considered in this research.

3.6 Mobility models

The aim of this section is to identify a suitable mobility model to test the proposed endcast scheme.

3.6.1 Selecting a mobility model

According to the broad survey by Bettstetter [94], mobility models used in analyzing wireless network are classified in different ways as follows; mobility for analytical

Table 3.6: Selecting a mobility model

mobility model	**select/ reject**	**reason**
RWP	select	theoretically tractable, can be simulated in a scalable manner, widely used so can compare results, select destination points as MANET nodes usually do
RD	reject	MANET nodes move towards destination points rather than towards directions
Random walk models	reject	suitable for macroscopic mobility rather than our target microscopic mobility

models and mobility for simulation models in terms of where the models are applied, microscopic models and macroscopic models according to the level of details in the model, 1D, 2D and 3D in terms of the dimensions of the mobility, deterministic, random and hybrid mobility models in terms of the degree of randomness in the mobility. Macro mobility models capture aggregated movements such as fluid flow type mobility and microscopic mobility captures individual user movements. Deterministic models are those created using real mobility traces. In random models either the directions or the destination points are selected at random. In hybrid models, determinism is visible either in the space domain or in the time domain. For example, movement in a city has space domain determinism as the movement is bounded by the streets and buildings. Event triggered movement on the other hand is deterministic in time domain.

As explained in Chapter 1, we target our unicast via flooding scheme for an application scenario such as in a disaster relief camp spanning a geographical area that cannot be covered by a single radio range. It can be assumed that the determinism in movement of nodes in such a scenario is minimal. Therefore, we consider mobility on a 2D open area at individual node level or microscopic level and the movement is not considerably bounded by the environment or the movement is random. Therefore, the mobility models that can be classified under 2D, random and microscopic mobility models will be explored in order to select a mobility model for testing the effect of mobility on the proposed protocol.

Random waypoint mobility (RWP): In RWP, a node randomly chooses a destination point or a waypoint in the area and moves with constant speed. This speed is chosen randomly from the uniform distribution of speeds between a minimum speed and a maximum speed. Then it waits a certain pause time. Next, it chooses a new destination and moves to this destination, and so on [86]. In general, a node in a MANET such as a human carrying a mobile phone, usually walks aiming at a waypoint, for example to meet someone. Therefore, RWP is suitable for modeling node mobility in MANETs.

Random way point (RWP) mobility model is the de facto model in studying mobile networks in general and MANETs in particular, as evident from a plethora of studies including [81, 60]. According to Bettstetter [86], RWP does not result in a uniform node distribution because the nodes at the edges of the area are likely to move towards the middle.

Random direction mobility (RD): In RD, nodes select a direction rather than a destination point. The direction is uniformly distributed in $\psi = [0...2\pi]$. Since the nodes can cross the borders and bounce back or wrap around, RD results in a uniform node distribution [86]. However, naturally, a node in a MANET such as a human will walk towards a destination rather than to directions. Therefore, we perceive that RWP node movement is better than RD for modeling application scenarios such as a disaster site thus we omit selecting RD.

Random walk models: Brownian motion and Markovian mobility are examples of random walk models. Brownian motion is able to give the probability distribution of the physical location of a node at a given time if the location of the node at a previous time is known. Markovian model represents the node placement in a physical region rather than at a particular location. For example, the movement of a user of a cellular network from cell to cell can be modeled using this model. The model is usually defined by a state transition diagram in which a state denotes a cell [86]. According to the definition these models are suitable for macroscopic movements such as particle

Table 3.7: Selecting values for RWP mobility model parameters

Parameter	**[95]**	**[72]**	**[73]**	**[96]**	**[97]**
minimum speed (m/s)	0.5	1	0	1	0
maximum speed (m/s)	1	2	2	19	20
pause time (s)	0.1	50	3	0-60	0

movement by diffusion or fluid flows whereas we try to model microscopic behavior of individual nodes.

Constant velocity model (CV): This is a simplified mobility model, which can act as a basic building block of mobility models such as RWP. CV model introduced by Cho and Hayes [95] assumes that nodes are randomly placed on an infinitely large boundless plane with a finite node density ρ. Nodes move linearly at constant speed in random directions but do not change direction while they move. We select CV for simplifying the analysis of the effect of mobility on flooding schemes.

Human walking: According to our disaster site application scenario, we consider mobility models that mimic human walking. Common practice is to use RWP with human walking speeds such as 1 to 2 m/s as in [72, 73, 96]. RWP is criticized for abrupt direction changes. If the networks perform satisfactorily in such spontaneous mobility changes the performance at mobility with smooth transitions should be better. Therefore, we also select RWP with speeds 1 to 2 m/s. There is a pause time between movement epochs. RWP with widely used parameter values also enable us to compare our work against large pool of similar work. Table 3.7 shows values used for RWP parameters in similar performance studies that evaluate routing and flooding schemes in MANETs.

3.6.2 Impact of mobility on wireless links

The nodes will move away from some nodes resulting in link breaks and move towards some other nodes causing new links to emerge. Therefore, the impact of mobility on

wireless networks is generally quantified in terms of the change of link state from up to down and vice versa. The impact of mobility on routing protocol performance is related to mobility via connectivity graph characteristics in [98]. Bai et al. [98] characterize mobility in terms of protocol independent properties such as spatial and temporal dependence, and geographic restrictions and they further show that RWP has zero dependencies. Connectivity metrics used in [98] are, number of link changes, link duration, path duration and path availability. We do not consider path duration and path availability as flooding schemes do not extract end to end paths. However, link-related metrics are important for evaluating the impact of mobility on flooding schemes. For example, a metric known as *link change rate (LCR)* is used, which is defined as the sum of rate of link breakage and rate of link generation in [95].

Cho and Hayes [95] analyze LCR with the help of a simplified mobility model that they name *constant velocity (CV) mobility model*. In CV model the nodes move linearly at a constant speed in random direction but they do not change direction while moving.

Link change rate According to Cho and Hayes [95] the links are newly generated at a rate of $2\rho rv$ when a node having a transmission radius r moves with speed v across a static network in which ρ nodes reside per unit area. This can be interpreted as the number of nodes with which a node makes connections in an area swept by a circle of radius r when the circle moves v meters per second. If all nodes move with same speed but towards different directions, the velocity can be represented by $\overrightarrow{v_k} = v(\overrightarrow{i}\cos\theta + \overrightarrow{j}\sin\theta)$. The direction of node N_0 is $\theta_0 = 0$. The relative velocity of N_k with respect to N_0 is denoted by $\overrightarrow{v_{k|0}} = \overrightarrow{v_k} - \overrightarrow{v_0}$. The magnitude of $\overrightarrow{v_{k|0}}$ is $v_{k|0} = v\sqrt{2-2\cos\theta} = 2v\sin\frac{\theta}{2}$.

The rate of link generation λ_{gen} by node N_0 is given by Equation 3.4. The link change rate (LCR) is given by $\lambda_{gen} + \lambda_{brk}$ where λ_{brk} is the link breaking rate. At steady state, the link generating rate equals the link breaking rate. Therefore, $LCR = 2\lambda_{gen} = \frac{16}{\pi}\rho rv$.

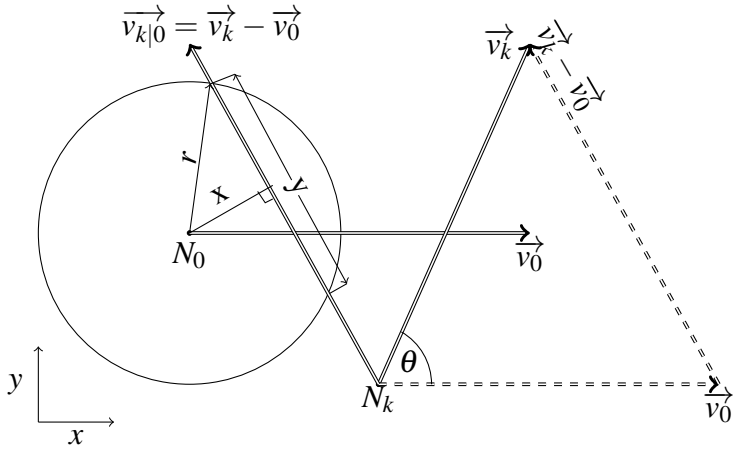

Figure 3.6: Motion of node N_k passing through the transmission region of node N_0 [95]

$$\lambda_{gen} = \int_0^{\pi} 2\rho r v_{k|0}(\theta)\frac{1}{\pi}d\theta = \frac{8}{\pi}\rho r v \tag{3.4}$$

Link duration Cho and Hayes [95] also derive the *link duration (T_{LD})*, which measures the lifespan of a node-to-node link from the time a node enters a transmitter's communication region to the time the node exits the region. This metric also represents the time from a link generation to link break. The event that the node N_k passes through the transmission region of node N_0, is described by the two parameters (X,Θ) shown in Figure 3.6.

Relative frequency of the event (X,Θ) is given by the joint probability density function $f_{X,\Theta}(x,\theta)$. According to Equation 3.4, the rate of link generation by node N_0 with passing by nodes is proportional to $v_{k|0}(\theta)$. Therefore, $f_{X,\Theta}(x,\theta)$ is proportional to $v_{k|0}(\theta)$. Consequently, $f_{X,\Theta}(x,\theta)$ is given by Equation 3.5.

$$f_{X,\Theta}(x,\theta) = \frac{v_{k|0}(\theta)}{\int_0^{\pi}\int_0^{r} 2v\sin\frac{\theta}{2}dxd\theta} \tag{3.5}$$

$$T_{LD}(x,\theta) = \frac{Y(x)}{v_{k|0}(\theta)} \tag{3.6}$$

In Equation 3.6, $Y(x) = 2\sqrt{r^2 - x^2}$. Average link duration $\overline{T}_{LD}$ is given by Equation 3.7.

$$\overline{T}_{LD} = \int_0^{\pi} \int_0^{r} T_{LD}(x,\theta) f_{X,\Theta}(x,\theta) dx d\theta = \frac{\pi^2}{8}(\frac{r}{v}) \tag{3.7}$$

Probability of complete transmission A node N_k that enters the communication region of node N_0 at time $t = 0$ will leave the region at time T_{LD}. For a message to completely get transmitted before N_k exit from the region with a message transmission time T_{comm}, the transmission must start at a time t, where $0 \leq t \leq T_{LD}(x,\theta) - T_{comm}$. Accordingly, conditional probability p_{comp} is given by Equation 3.8.

$$p_{comp}(T_{comm}|x,\theta) = \frac{max[T_{LD}(x,\theta) - T_{comm}, 0]}{T_{LD}(x,\theta)} \tag{3.8}$$

Total probability of complete transmission is given by Equation 3.9. Here, $g_{X,\Theta}(x,\theta)$ is the joint probability function of the event of transmitting a message by N_0 to N_k that crosses the communication region of N_0.

$$p_{comp}(T_{comm}) = \int_0^{\pi} \int_0^{r} p_{comp}(T_{comm}|x,\theta) g_{X,\Theta}(x,\theta) dx d\theta \tag{3.9}$$

Cho and Hayes [95] cite Little's theorem, which states that the average number of customers in a system is equal to the product of the arrival rate of the customers to the system and the average time that the customers spend in the system. By applying Little's theorem to single hop wireless communication in the presence of mobility, $g_{X,\Theta}(x,\theta)$ is found to be proportional to $v_{k|0}(\theta).T_{LD}(x,\theta) = Y(x)$. Therefore, $g_{X,\Theta}(x,\theta)$ is given by Equation 3.10.

$$g_{X,\Theta}(x,\theta) = \frac{Y}{\int_0^{\pi} \int_0^{r} Y dx d\theta} \tag{3.10}$$

We will be using this model to analyze the effect of mobility on multihop flooding in Chapter 4. The method requires to check whether the link duration is larger than message transmission time. The performance studies surveyed in section 3.4 have used radio ranges, data packet sizes and data rates in Table 3.4 and speeds of mobility in Table 3.7. For example, a node having 40 m radio range will require a node to cross the communication region by travelling a distance between 0 and 80 m, where 0 is when the node moves just touching the boundary whereas 80 m is when the node

moves along a diameter. If nodes move at a maximum speed of 2 m/s, the minimum link duration will be recorded when two nodes move in opposite directions resulting in a relative velocity with a magnitude of 4 m/s. On the other hand, a message length of 256 Bytes for example, will take only about 2 s to get transmitted via a 1 Mbps channel. Therefore, the message can be transmitted to a node that crosses the circular transmission region along a secant line with an intersecting distance that is not less than 8 m.

3.7 Theoretical analysis of MANET flooding

Theoretical models are a powerful tool to evaluate correctness and performance of protocols as well as to validate simulation results. There are a few attempts to model MANETs theoretically with the aim of analyzing variety of properties including reachability and connectivity. Among several abstractions of MANETs used for these theoretical analyses, main abstraction is the graphs. We survey theoretic models including graph realizations of MANETs in this section with the aim of modeling flooding schemes.

3.7.1 Graph based representations of MANETs

Unit disk graphs Unit disk graphs are a popular choice in which the MANET is assumed to have nodes with same transmission radius. In this representation, $G = (V,E)$ where V contains all the nodes and E contains all the edges. There exists an edge in the graph between nodes u and v if the distance between u and v is at most 1 where transmission radii of all nodes are identical at unit [99]. However, in real world MANETs links may not exist even though distance between u and v are in the range of each other due to hidden terminal or exposed source problem [67]. Another variation of unit disk graph is *quasi unit disk graph*. In this model, two nodes are connected by an edge if the distance between a pair of nodes is less than or equal to d which is a parameter between 0 and 1. If the distance between two nodes is greater than 1 there is no edge between them whereas the existence of an edge is not specified in the range

between d and 1 [99].

Transmission graph This is a graph $G = (V, E)$ in Euclidean space where the set V represent all the nodes and set E contains an edge from node u to v if u can directly transmit to v. The ability to transmit is determined by the path loss equation and signal-to-noise ratio formula [100].

Connectivity graph A graph $G(V, E)$ is a connectivity graph if a link $(i, j) \in E$ iff $D_{i,j}(t) \leq R$ at time t and $|V| = N$. Here $D_{i,j}(t)$ is the Euclidean distance between node i and j at time t, N is the number of mobile nodes and R is the transmission range of a node.

Evolving graphs Combinatorial models like evolving graphs capture dynamic nature over time [101, 102]. Combinatorial structures are systems that consist of many locally interacting components [103]. An evolving graph is an indexed sequence of subgraphs in which the journeys are the paths over time. Edges with non-decreasing time order is a journey. For example, consider the time evolving graph in Figure 3.7. The edge (A,B) exists from time slot 1 through 3, and edges (A,C) and (A,D) exists only at slot 4. The time indices on the other edges can be interpreted the same way. A message originated by node A at time slot 1 destined to F should be able to traverse through B and E if B manages to forward the message at time slot 2 and E manages to forward at slot 4. The path formed by (A,B), (B,E) and (E,F) is a journey because the indices on these edges can form the non-decreasing time order 1,2,4. Dynamic topologies of MANETs also result in connecting and disconnecting of wireless links over the time. If the wireless links are denoted by edges of a graph, then these dynamics can be modeled by time indexing the edges to form an evolving graph.

Random graphs Random graph models are analyzed using percolation theory in [104]. A trust computation system in a MANET based on local interactions and node cooperation is analyzed for the availability of a secure path, using phase transition phenomena in random graphs in [103]. *Random graphs* is a branch of study pioneered

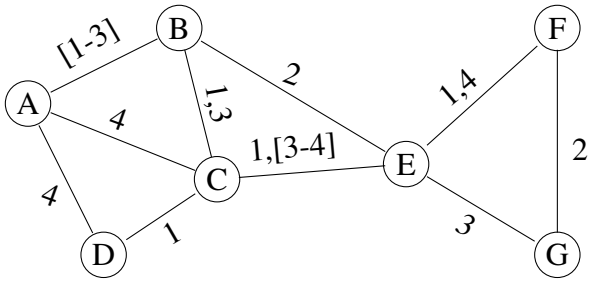

Figure 3.7: An example for time evolving graphs [102]

by Erdos and Renyi [105] and a type of random graph named Erdos-Renyi graph, $G(n,p)$ is defined as graph constructed starting with only n vertices and edges are added with a probability p. A random geometric graph, $G(n,r)$ is constructed by placing n vertices uniformly at random in $[0,1]^2$ and connecting any two points that are at most r distance apart [106].

3.7.2 Operational characteristics of MANETs

Extracting optimum set of nodes for MANET connectivity The aim of efficient flooding is to select the best sub set of nodes in such a way that every node can be reached via that set of nodes. Hence, efficient flooding boils down to the graph theoretic problem of finding a *connected dominating set (CDS)* and the protocols that create virtual backbones (Section 2.2.4) are specifically designed to extract a minimum CDS. A dominating set is a subset D of vertices V in which all the vertices that are not in D are adjacent to at least one vertex in D. A connected dominating set (CDS) is when the subgraph induced by D is connected. Finding such minimum D is proved to be an NP-complete problem [12].

Reachability in MANETs We have already emphasized in Section 3.3 that reachability is an important aspect of efficient flooding schemes as it is a tradeoff between saving in redundant rebroadcasts and reachability. Reachability in MANET flooding refers to the problem of estimating the percentage of nodes reached by the flooding scheme as defined in Section 3.3. However, little work is found in literature that characterize reachability of flooding in MANET based on analytical models [2]. However,

in the process of performing unicast using MANET flooding, we are interested in the problem of whether the destination is included in the set of nodes reached by the flooding scheme.

In graph theoretic terms, *reachability* refers to the problem of finding whether there exists a path from u to v given two vertices u and v in a graph. If there exists a path from a node u to another node v in a MANET according to the topology, it is intuitive that a frame originated at node u is able to reach node v via simple flooding. When the existence and the costs of direct edges between vertices are known the reachability problem in graph theory can be answered by computing the transitive closure of the graph [107]. Finding the shortest path is a closely related problem to finding the transitive closure.

Well known shortest path algorithms include Dijkstra, Bellman-Ford, A* and Floyd-Warshall. Some shortest path algorithms are for single source problems where paths are sort from a single node to all the other nodes, some are for single destination problems and others are for all pair solutions. Single source algorithms such as Dijkstra, Bellman-Ford and A* required to run n times to check whether all nodes are reachable from all the other nodes. When there is node mobility the snapshots of the network should be analyzed for reachable node pairs. In such cases a solution that gives all pair reachability information is more beneficial than single source solutions. Therefore all pair shortest path algorithms will be chosen. Floyd-Warshall algorithm [108] is considered as the standard all pair shortest path algorithm in [109] and this should be due to its simplicity and less pre-processing needs.

Reachability in MANET flooding is analyzed using a probabilistic model by Viswanath and Obraczka [2] to which we refer to as *Viswanath-Obraczka model*. Their analytical model is used to study the reachability achieved by simple flooding and probabilistic flooding. Their network model is same as that used by Takagi and Kleirock [89] in obtaining the optimal transmission range of a node in a multihop wireless network. The multihop communication model proposed in [2] is also based on the probability of successful transmission in CSMA derived by Wu and Varshney [92]. As broadcasts do not use RTS-CTS like collision avoidance mechanisms, collision is a critical problem in

Table 3.8: Comparson of algorithms for analyzing reachability of nodes in a given network topology

Algorithm	**condition**	**complexity**	**nature of paths**
Dijkstra	edge weights must be non negative	polynomial time solution $O(n^2)$ [110]	single source single target
Bellman-Ford	graph must not contain negative cycles	polynomial time $O(nm)$ [110]	single source paths
A*	requires a function to estmate internode distances	preprocessing costs high, some are NP-hard	(generalized Dijkstra) single source paths
Floyd-Warshall		$2n^3 - O(n^2)$ operations [109]	all pair paths
Hoffman-Winograd		n^3 comparisons and only $O(n^{\frac{5}{2}})$ additions and substractions	

n is the number of nodes, m is the number of arcs

CSMA-like medium access schemes and this leads to hidden terminal problem, which is highlighted as critical in multihop communication in wireless networks in [2, 92]. Viswanath-Obraczka model captures hidden terminal problem.

Rate of message propagation in MANET flooding Khelil [111] proposed an epidemic model to analyze message spreading in broadcasts considering the similarity between message spreading among MANET nodes and spreading of infectious diseases among living beings. The SI epidemic model in epidemiology is used for developing the above analytical model. An individual is mapped to one of the two compartments, namely Susceptible (S) and Infectious (I) in the SI model. Once infected, an individual remains infected forever and they keep on infecting others until the whole population gets infected. The SI model for packet broadcasting, defines a variable named *spread-*

Table 3.9: Selecting analytical models

model	**select/ reject**	**aspect being modeled**	**reason**
transmission graph	select	neighborhood due to distance and transmission ranges	ability to directly map network and graph aspects
evolving graph	select	model dynamics over time	ability to model mobility of nodes
connectivity graph	select	model the link generation and breakage with time	ability to model connecting and disconnecting wireless links with mobility
unit disk graph	reject	connection of nodes via wireless links	assumption that range is fixed
random graphs	reject	relate a global property of a graph when probability of having an edge changes	we analyze aggregated effect of local level activities of nodes e.g. total number of edges due to node degrees
connected dominating sets	reject	find a set of vertices to connect all nodes	we do not try to build virual backbones since it is a fixed stateful approach
reachability graph	select	check whether two given vertices are connected via one or more edges	ability to check whether a given pair of nodes in a MANET can communicate via flooding
Viswanath-Obraczka model	select	hidden terminal problem of CSMA, redundant frames by multihop flooding, reachability by multihop flooding, probabilistic flooding	directly relevant and applicable in our endcast
Epidemic model	reject	rate of message propagation in flooding	research focus is on redundancy and reachability rather than rate of propagation
Shortest path algorithms	select	check whether there exists a path	ability assess whether a given source destinatio pair is able to unicast

ing ratio, $i(t)$ that denotes the ratio between the number of nodes that received the message to the total number of nodes. i is similar to the metric RE defined in Section 3.3.

Selecting analytical models According to the nature of endcast on CSMA based wireless networks, the significant problems to analyze are hidden terminal problem due to MAC layer, time domain analysis due to RADs in flooding schemes, redundant frames due to flooding over broadcast links, and reachability issues due to suppression of rebroadcasts. The surveyed analytical models and concepts are summarized in Table 3.9 with the intention of utilizing them to build a theoretical model to analyze major aspects of endcast in Chapter 4.

3.8 Summary

We proposed to leverage flooding as a unicast mechanism in order to avoid costs of route discovery and maintenance in traditional MANET routing. After a broad survey of available flooding schemes we found out that probabilistic flooding and counter based flooding are candidate schemes for endcast in mobile-stateless manner. We then realized that counter based flooding has close analogy to cell proliferation control using chalone mechanism in the growth of the biological organs and selected counter based flooding for further investigation.

Then we explored suitable performance metrics to evaluate efficiency of flooding schemes and selected redundancy, reachability and delay metrics. Since the available metrics are designed to evaluate flooding schemes in their conventional use as network wide message dissemination we defined new set of metrics by combining broadcast protocol metrics with routing metrics.

Simulations are an indispensable technique in evaluating protocols. We surveyed available simulation studies with an emphasis on studies that evaluate flooding schemes and identified important simulation parameters and widely used values for the parameters. For example, we selected the definition of network density in terms of the average number of neighbors per node and density range of 4 to 20 as a meaningful range.

Analytical models are an essential tool to validate simulation results and draw generalized conclusions about the protocol performance. We explored a range of research work that analyze different aspects of MANETs in terms of theoretical models including reachability analysis using graph theory. We selected a probabilistic model which we refer to as *Viswanath-Obraczka* model because its ability to model CSMA transmission with hidden terminal problem, and its facilities to assess reachability and redundant frames in simple flooding and probabilistic flooding. However, this model cannot be readily applied to assess counter based flooding because of the time dependent rebroadcast decision in counter based scheme cannot be modeled using original Viswanath-Obraczka model. Therefore, we have to modify the model in such a way that time domain is included. We identified time evolving graphs as a candidate model for incorporating time domain. If time aspect is included in the model it will enable us to analyze node mobility as well.

CHAPTER IV

RESEARCH METHODOLOGY

4.1 Introduction

We proposed that flooding can be leveraged to perform unicast in MANETs in Section 2.3 in mobile-stateless routing paradigm introduced in Chapter 1. However, flooding causes broadcast storms and floods which will be analyzed on a theoretical basis in this chapter. Note that we target the flooding scheme at link layer as stated in Chapter 1 so that the data unit is referred to as frames.

4.2 Unicast via simple flooding

Ideally, a given data frame should be forwarded only by the nodes in the best path from a source to the destination in the most efficient unicast mechanism in any multihop network. For example, a data frame originated at node A in Figure 4.1 destined to node H should go through only C and G. However, in wireless networks, data propagation is broadcast based. Therefore, all the neighbors of the nodes in the path receive the frame even in a protocol that manages to propagate it along the best path. For instance, all the nodes in the transmission range of A, C and G also receive the frame. When the frame is flooded by A into the network, nodes B, D, E and F also receive and rebroadcast it in an action that is redundant. It can be hypothesized that the waste of resources for unwanted rebroadcast frames becomes higher causing storms when the network is

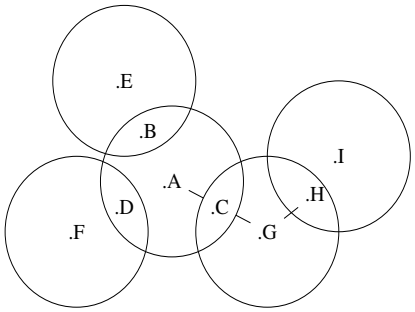

Figure 4.1: Problem of unicast via flooding

Table 4.1: Accumulation of frames in simple flooding

rebroadcast level	circles covering the boundary	received frames in network	new reaches
0	0	n	
1	3	$n \times n$	$3 \times 0.41n$
2	5	$3n \times 0.41n$	$5 \times 0.41n$
3	7	$5n \times 0.41n$	...

dense.

Suppose that there are n neighbors on average, uniformly distributed in radio range of each node. Then a broadcast of node A will be received by n nodes. C also will have n number of nodes in neighborhood. However, there will be an overlap between the neighbors of A and C so that the common neighbors will receive the rebroadcast of the same frame by C as redundant frames. According to Tseng et al. [4] area-wise overlap of two transmission ranges on average is 59% of the transmission region. Therefore, when only A and C are considered a rebroadcast of C will cause $0.59n$ number of nodes to receive the frame redundantly. When all the n neighbors of A rebroadcast, then the redundant frames will be $0.59n^2$. Even if we consider the rebroadcasting of only the immediate neighbors of the source node the redundant frames shows $O(n^2)$ growth.

A node at the second level of rebroadcasting, for example, G in Figure 4.1 will also cause $0.59n$ number of redundant frames within its coverage area. Therefore, the number of nodes at the second level of rebroadcasting n_2 will cause $0.59nn_2$ such redundant frames. Similarly, n_i number of nodes that will rebroadcast at level i will

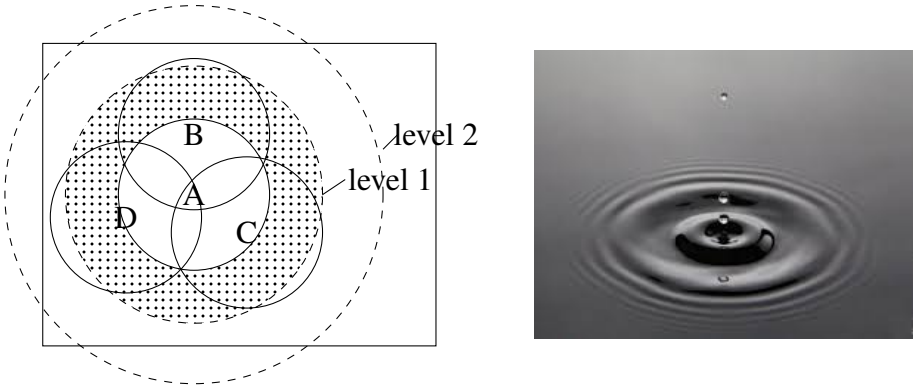

Figure 4.2: Geometric estimation of reached nodes at each rebroadcast level

cause $0.59nn_i$ number of redundant frames. The accumulated redundant frames by each level of rebroadcast up to level l is given by Expression 4.1.

$$\sum_{i=0}^{l} 0.59nn_i \tag{4.1}$$

As shown in Figure 4.2 source, A will cover its transmission range by the original broadcast. The neighbors of A, namely, B, C, and D will rebroadcast at rebroadcast level 1 so that approximately the area within the dashed circle labeled "level1" will be covered. This way the frames will propagate similar to how a drop of water fallen on a still pool will cause a wave as in Figure 4.2, thus we termed the propagation of frames via flooding as a *flooding wave*.

According to Figure 4.2, the circumference of A's radio range circle can be covered by around three radio range circles each of which is overlapped with A's range by 59%. Each radio range circle will give additional coverage of 41% so that $0.41n$ number of nodes will be residing in that area. Therefore, there will be $3 \times 0.41n$ nodes altogether newly receiving the rebroadcasts of A's neighbors. These are the nodes that reside in the dotted area in Figure 4.2. Only these nodes will rebroadcast the frame at level 2 because in simple flooding the nodes rebroadcast only when a frame is received for the first time. Similarly, circumference of level 1 circle can be covered by about 5 transmission range circles and circumference of level 2 circle by about 7 circles. The propagation of the flooding wave is quantified in Table 4.1.

According to Table 4.1 four sample networks characterized by neighborhood 5, 10,

Table 4.2: Accumulation of frames in simple flooding with network density

neighborhood	rebroadcast level 0	level 1	level 2	level 3	level 4
5	5	25	30.75	51.25	71.75
10	10	100	123	205	287
15	15	225	276.75	461.25	645.75
20	20	400	492	820	1148

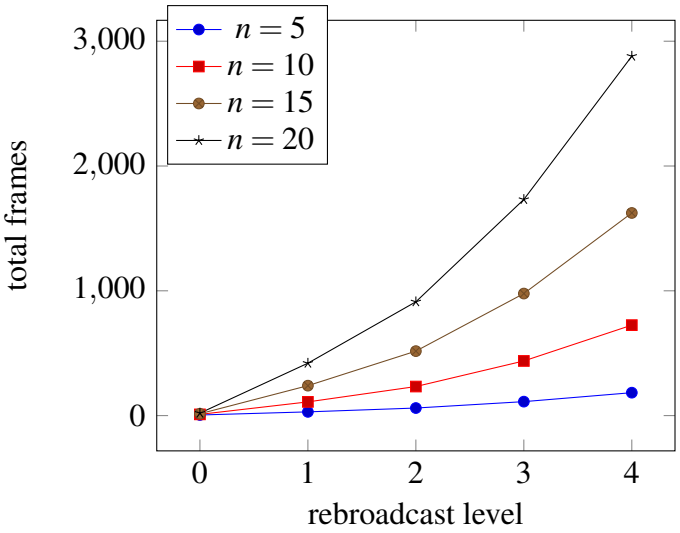

Figure 4.3: Total number of frames received in the network by propagation of simple flooding for networks having different average neighborhood, n

15 and 20 were analyzed. The resulting number of frames received in the network due to each level of rebroadcast is shown in Table 4.2. Figure 4.3 shows the accumulated number of frames up to each level of rebroadcast.

Figure 4.3 shows that the redundant frames accumulated in the network grows exponentially with the rebroadcast level. The rate of growth is higher when the network is dense in terms of neighborhood size. This verifies our hypothesis that when networks become dense the storm condition caused by unnecessary rebroadcasts is intensified.

In order to direct the flooding wave towards the destination, we propose to use totally local state information to conform to mobile-stateless routing paradigm introduced in Chapter 1. However, global information is required to build the best path from a source to the destination. We cannot build definitive best paths since we use

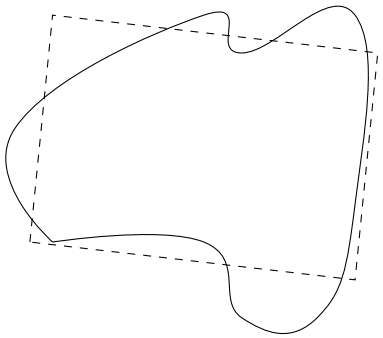

Figure 4.4: Playground approximation by rectangular regions

totally local information in nodes to make the data forwarding decision. We explored available flooding schemes in Chapter 3 with the intention of developing a scheme for unicast in dense MANETs. Consequently, we identified counter-based flooding as a scheme that regulates the growth of accumulated frames in the network similar to chalone mechanism that controls biological cell proliferation in the growth of the organs.

Furthermore, after reaching the destination H, the flooding wave still propagates to I and beyond in Figure 4.1 if a specific mechanism is not in place to inhibit it. The propagation of frames beyond the destination is the flood situation and we identified negative acknowledgements in Chapter 2 as a mechanism to mitigate it.

Similar to biological cells that get accumulated in an organ due to proliferation, data frames also get accumulated in the network due to rebroadcasting. Efficient flooding suppresses redundant rebroadcasts so that the total number of copies of the same frame accumulated in the network is a main metric to evaluate flooding schemes. It can be noted from above explanation that accumulation of frames due to flooding schemes depends on the MANET parameters such as neighborhood, and thus the MANET is parameterized in Section 4.3

4.3 Parameterizing a MANET that unicast via simple flooding

According to Figure 4.3, it is clear that neighborhood is a prominent parameter that affects the number of accumulated frames due to frame propagation in flooding MANETs. We borrow the definition of network density in Section 3.4, which is in terms of the number of neighbors per node so that the accumulated number of packets can be directly related to network density.

The network topology in terms of neighborhood can be given by the *adjacency matrix* as shown in Figure 4.5. A topology is given by the number of nodes (N), node placement, playground size and transmission range (R). The adjacency matrix can thus be extracted from this topology by getting the Euclidean distance between node pairs and checking whether the distance is less than R. This corresponds to the graph representation defined as *transmission graph* in Section 3.7.

Playground refers to the physical space that the nodes occupy. In real scenarios, the playground usually takes an irregular shape as shown in the example in Figure 4.4. For convenience, we assume a rectangular playground of size $(X \times Y)$. However, we can approximate irregular playgrounds with one or more rectangular regions as shown in 4.4.

Transmission range is the measure of region covered by the direct transmission by a node. In reality, devices cannot give a perfect circular region with same transmission radius although the transmitter is of the same type and of the same specifications. This is mainly due to the effect of environment such as obstacles and the orientation of physical environment that affect the radio wave propagation. For example, in a corridor that includes metal bars will result in a longer transmission distance as the corridor acts as a waveguide. However, to simplify the analysis we assume a circular transmission region with same radius R for all nodes.

	$h0$	$h1$	$h2$	$h3$	$h4$	$h5$	$h6$	$h7$	$h8$	$h9$	$h10$	$h11$	$h12$	$h13$	$h14$	$h15$	$h16$	$h17$	$h18$	$h19$
$h0$	0	∞	∞	∞	∞	∞	1	∞	∞	∞	∞	∞	∞	1	∞	∞	∞	∞	1	∞
$h1$	∞	0	∞	∞	∞	1	∞	1	1	1	∞	∞	1	1	1	1	1	1	1	∞
$h2$	∞	∞	0	∞	∞	∞	∞	∞	∞	∞	∞	1	∞	∞	∞	1	1	∞	∞	∞
$h3$	∞	∞	∞	0	1	∞	∞	1	1	1	1	∞	∞	∞	∞	∞	∞	∞	∞	∞
$h4$	∞	∞	∞	1	0	∞	∞	∞	∞	∞	∞	∞	∞	∞	∞	∞	∞	∞	∞	∞
$h5$	∞	1	∞	∞	∞	0	∞	1	1	1	∞	∞	1	∞	1	∞	1	∞	∞	∞
$h6$	1	∞	∞	∞	∞	∞	0	∞	∞	∞	∞	∞	∞	1	∞	∞	1	1	1	∞
$h7$	∞	1	∞	1	∞	1	∞	0	1	1	1	∞	1	∞	1	∞	∞	∞	∞	1
$h8$	∞	1	∞	1	∞	1	∞	1	0	1	1	∞	1	∞	1	∞	∞	∞	∞	1
$h9$	∞	1	∞	1	∞	1	∞	1	1	0	∞	∞	1	1	1	∞	1	1	1	∞
$h10$	∞	∞	∞	1	∞	∞	∞	1	1	∞	0	∞	1	∞	1	∞	∞	∞	∞	1
$h11$	∞	∞	1	∞	∞	∞	∞	∞	∞	∞	∞	0	∞	∞	∞	1	1	∞	∞	∞
$h12$	∞	1	∞	∞	∞	1	∞	1	1	1	1	∞	0	∞	1	∞	∞	∞	∞	1
$h13$	1	1	∞	∞	∞	∞	1	∞	∞	1	∞	∞	∞	0	∞	∞	1	1	1	∞
$h14$	∞	1	∞	∞	∞	1	∞	1	1	1	1	∞	1	∞	0	∞	∞	∞	∞	1
$h15$	∞	1	1	∞	∞	∞	∞	∞	∞	∞	∞	1	∞	∞	∞	0	1	∞	∞	∞
$h16$	∞	1	1	∞	∞	1	1	∞	∞	1	∞	1	∞	1	∞	1	0	1	1	∞
$h17$	∞	1	∞	∞	∞	∞	1	∞	∞	1	∞	∞	∞	1	∞	∞	1	0	1	∞
$h18$	1	1	∞	∞	∞	∞	1	∞	∞	1	∞	∞	∞	1	∞	∞	1	1	0	∞
$h19$	∞	∞	∞	∞	∞	∞	∞	1	1	∞	1	∞	1	∞	1	∞	∞	∞	∞	0

Figure 4.5: Adjacency matrix of a sample network

The matrix in Figure 4.5 corresponds to a sample network of 20 nodes with each node having a transmission range of 40m and the nodes are randomly placed on a $85m \times 85m$ playground.

Node placement depends on the application scenario and the physical environment. For example, in a disaster relief camp, families will stick together and there will be queues for some services from time to time. However, we assume random uniform placement of nodes throughout the playground for simplifying the analysis.

Node distribution Physical area and the number of nodes residing in that area are related in different ways depending on the node distribution. Counting the number of nodes in regions of planes when nodes are placed randomly on the plane is an important problem addressed particularly in adhoc, sensor and cellular networks. The branch of study that captures this problem is *spatial point processes* under stochastic geometry. When a set of nodes are placed randomly on a plane, estimating the number of nodes residing in a specific region can be formulated as a *counting process* coming under stochastic processes.

We formulate the problem as $N(a)$, $a \geq 0$ where a is the area of the circular region centered at the flooding source and $N(a)$ is the number of nodes residing in a region with area a. Due to following characteristics of $N(a)$, the problem in fact represents a counting process:

- $N(a) \geq 0$
- $N(a)$ is integer valued
- If $a_1 < a_2$ then $N(a_1) < N(a_2)$ where a_1 and a_2 are areas of circular regions centered at the source.
- For $a_1 < a_2$, $N(a_2) - N(a_1)$ is the number of nodes added by the area $a_2 - a_1$, the increments in number of nodes at different regions given by increments of a are independent.

In the considered MANET scenario, we are given a $X \times Y$ playground with N nodes randomly placed on it. We also assume that the network is dense so that no node is isolated and the nodes are dispersed throughout the playground with no significantly vacant areas. From transmission graph we know how many nodes are placed within circles of radius R centered at each node as that number equals the neighborhood (N_{neigh}). Therefore, it can be assumed that if we place a circle of radius R anywhere within the playground there will be N_{neigh} number of nodes residing in it and for simplicity we ignore the exceptions at the boundary of the playground for this model. Since the average number of nodes residing on any region is known, this problem can be modeled as a Poisson process in which λ is the average number of nodes per unit area given by $\frac{N_{neigh}}{\pi R^2}$ and thus $\lambda > 0$. Therefore, the number of nodes in any interval of b is Poisson distributed with average λb. That is for all $a, b \geq 0$

$$P\{N(a+b) - N(a) = n\} = e^{-\lambda b}\frac{(\lambda b)^n}{n!}, n = 0, 1, \ldots \tag{4.2}$$

4.4 Graph based model for flooding schemes

Propagation of a data frame in a MANET via flooding is modeled as the evolution of a graph rooted at the source as shown in Figure 4.6 according to Viswanath-Obraczka model [2] and we term the resulting graph as the *flooding graph*. N_{xy} denotes the nodes that are x hops away from the source and y simply index the nodes at that level. Further, x represents the rebroadcast level, for example the immediate neighbors or the one hop neighbors of the source will be the nodes to rebroadcast the frame for the first time. Each edge (u, v) represents the reception of a frame by a node v due to a broadcast of node u. We build our model on this graph realization of flooding in MANETs.

According to Figure 4.6, it is visible that the number of frames accumulated in the network is equal to the number of edges in the graph. Number of edges in turn depends on MANET parameters such as network topology and neighborhood.

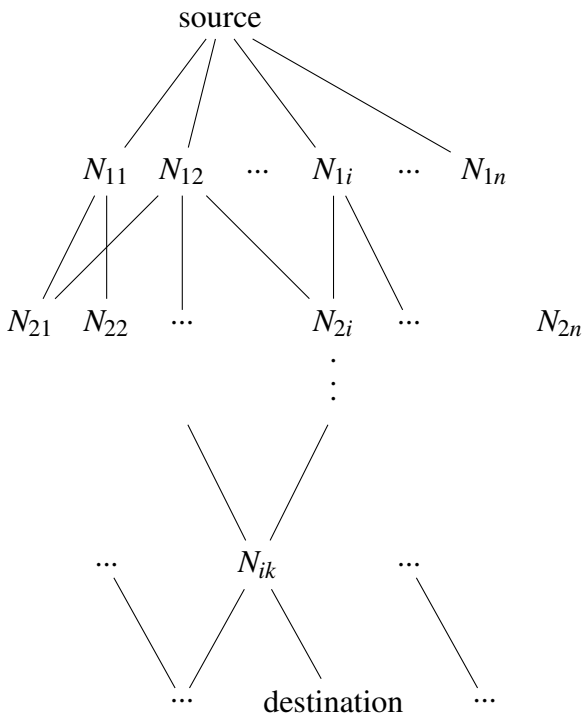

Figure 4.6: Redundant rebroadcasting modeled as graph evolution, N_{xy} denotes node at x hops away from source with y as node index at that level

Table 4.3: Metrics and definitions to describe graphs

Symbol	**Definition**
G	an undirected graph
N	number of nodes in a graph
N_x	number of nodes in a tree at level x
E	number of edges in a graph
E_x	number of edges in a tree at level x
δ	diameter of the graph
deg_v	outdegree: number of edges incident to the node v
$\overline{deg}$	average outdegree of the nodes of a graph
hop_x	hop count at level x of rebroadcasting

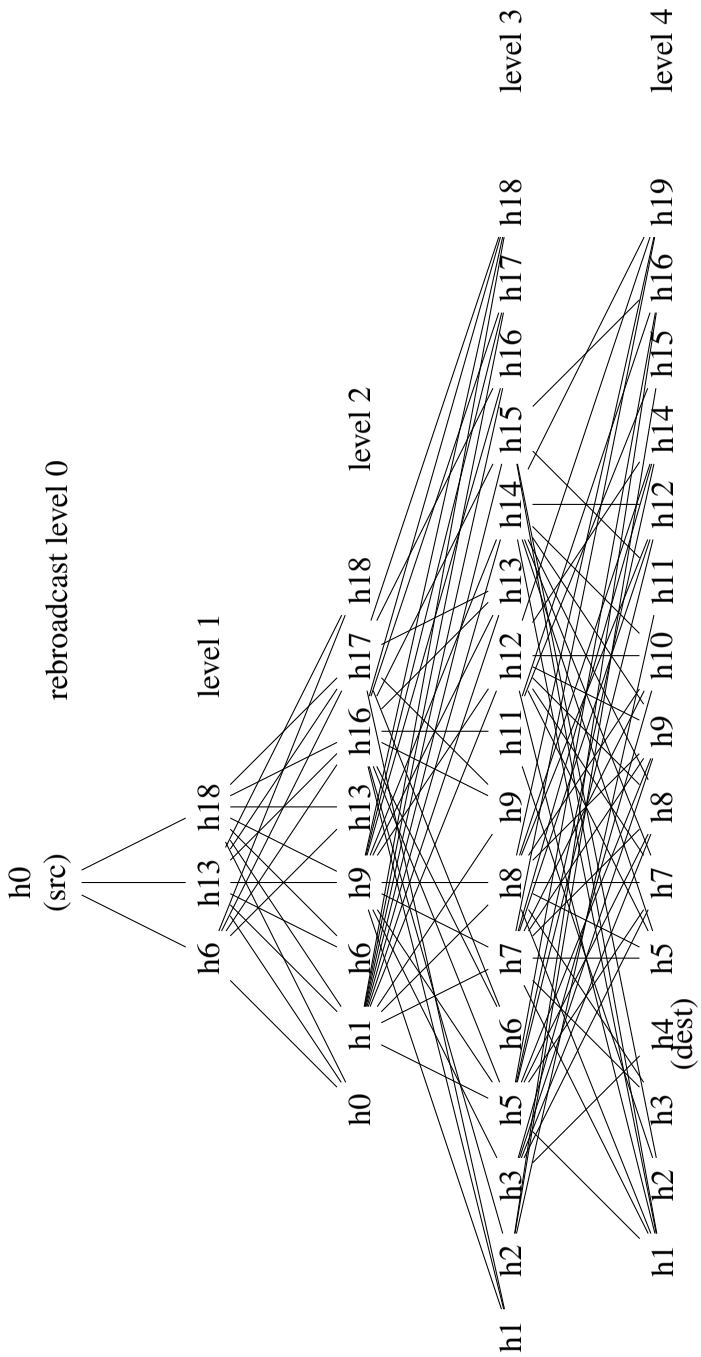

Figure 4.7: Redundant rebroadcasting modeled as graph evolution for the topology given in adjacency matrix in Figure 4.5 for unicast from host0 to host4

The tree structured graph in Figure 4.7 corresponds to the sample network given by adjacency matrix in Figure 4.5. Figure 4.7 illustrates the propagation of a frame originated by h0 destined to h4 according to SNCF or simple flooding. The notations and definitions of graphs in Table 4.3 will be used for the following descriptions.

4.4.1 Number of edges in flooding tree

A data frame propagates in a sequence of stages termed *retransmission level* by Viswanath and Obraczka [2], which we call *rebroadcast levels*. According to Figure 4.7, the original broadcast by the source h0 is considered as the rebroadcast level 0. This broadcast is received by the neighbors of h0, thus at this level the number of edges is same as the outdegree of h0. The immediate neighbors, namely h6, h13 and h18 will rebroadcast it at rebroadcast level 1. This results in an increment in number of edges E by sum of outdegrees of h6, h13 and h18. At rebroadcast level 2, the neighbors of h6, h13 and h18 receive the frame. However, the frame is not rebroadcast by h0, h6, h13 and h18 as they have already broadcast it as per the specification of SNCF scheme. It can be concluded that E increases by the sum of outdegrees deg_v of *rebroadcasting nodes* at each rebroadcast level. The number of rebroadcasting nodes is also important to calculate Saved ReBroadcasts (SRB) given in Section 3.3.

The graph in Figure 4.7 was obtained using simulation results. We develop a mathematical model to estimate the number of edges at each level of rebroadcasts in the following subsections. We use geometric properties of the MANET scenario for the mathematical model. We obtain the total number of edges at each level of rebroadcasts using the developed mathematical model and compare it with simulation results at the end of this section.

It is important to quantify number of edges E_i at each level of rebroadcast to characterize propagation of a data frame by flooding schemes. For example, a complete graph having N vertices will have $N(N-1)/2$ number of edges and a binary tree will have 2^l edges at each level where l is the level number. However, the graph that models the propagation of flooding is complex as each node has a different outdegree. Furthermore, multiple edges from an upper level may be incident to a node at lower level due

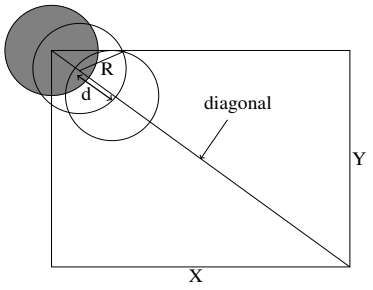

Figure 4.8: Maximum hop count calculation for a rectangular playground of $X \times Y$, R-transmission radius, d-distance between a transmitting node and a neighbor.

to overlapping of neighborhood. For example, h1 is a neighbor of both h13 and h18 in Figure 4.7. When the network becomes dense it can be assumed that the number of such overlaps are higher.

4.4.2 Span of flooding tree

The tree abstracted in Figure 4.6 spans for a number of levels equal to the network diameter given in terms of number of hops [2]. The maximum number of levels that the flooding tree will span is equal to the maximum hop count of the shortest path of all node pairs when simple flooding is used. This maximum hop count in turn will be recorded for the node pair located maximum distance apart, for example the node pair at the opposite ends of the diagonal of a rectangular playground as shown in Figure 4.8. When the transmission range of every node is R and the size of the playground is $X \times Y$, then the maximum hop count for the shortest paths is given by Equation 4.3.

$$h_{max} = \frac{\sqrt{X^2 + Y^2}}{d_{av}} \tag{4.3}$$

In Equation 4.3 d_{av} is the average distance between a transmitting node to its neighbors where $0 < d_{av} < R$ and d_{av} will be estimated later in this section.

It is required to estimate the number of nodes n_i reached at each level of rebroadcast $level(i)$ where $i = 0, ..., h_{max}$. However, only a sub set of n_i will rebroadcast in efficient flooding. We can estimate the number of rebroadcasting node m_i depending on the flooding scheme. For example, m_i in simple flooding is the number of nodes that

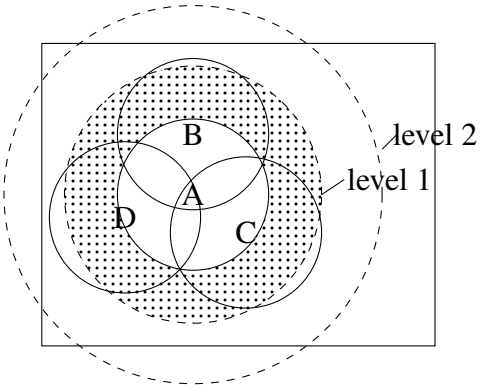

Figure 4.9: Geometric estimation of the area of regions that receive the frame at each rebroadcast level

have not rebroadcast the message before. Therefore, Equation 4.1 that calculates the number of edges in flooding graph is modified as Equation 4.4. At level 0 in Equation 4.1 there is only the source causing $n_0 = m_0 = 1$ and $deg_v = deg_{src}$ where deg_{src} is the neighborhood of the source. Therefore, the number of edges in flooding tree can be obtained using Equation 4.5.

$$E = \sum_{i=0}^{h_{max}} m_i deg_v \tag{4.4}$$

$$E = deg_{src} + \sum_{i=1}^{h_{max}} m_i \overline{deg} \tag{4.5}$$

We use a geometric method to estimate the additional area covered by each rebroadcast level when multiple neighbors rebroadcast, for example the dotted area shown in Figure 4.9. Average additional coverage acquired by rebroadcast of a single neighbor is derived by Tseng et al. in [4] as previously explained in Section 3.2.2. We use this result in our calculations. The flooding wave in MANET will propagate in such a way that all the N nodes are covered when h_{max} number of rebroadcast levels are finished.

4.4.3 Nodes covered by the first level of rebroadcast

We have to estimate average increment of area b by rebroadcast of all the neighbors of A. That is the area difference between coverage area of A and the area of level 1

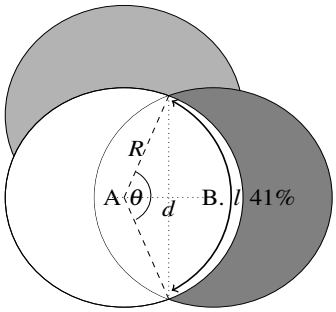

Figure 4.10: Estimating the average area covered by rebroadcast level 1

circle or the dotted area in Figure 4.9. It is proved in [4] that the average additional area covered by the rebroadcast of a single neighbor is 41% of radio range as shown by dark gray area in Figure 4.10. When all such additional coverage areas by the rebroadcast of all neighbors of A are considered the result should be equal to b. We need to estimate how many circles will cover the circumference of the coverage area boundary of A. An arc of length l will be covered by a single neighbor resulting in a number of additional coverage areas equal to $\frac{2\pi R}{l}$. Here $l = R\theta$.

From Figure 4.10;

$$\theta = 2\cos^{-1}\frac{d}{2R} \tag{4.6}$$

$$l = 2R\cos^{-1}\frac{d}{2R} \tag{4.7}$$

Therefore, the number of arc lengths k that will cover the circumference of a circle of radius R is given by $2\pi R/l$ which will be simplified to Equation 4.8;

$$k = \frac{\pi}{\cos^{-1}\frac{d}{2R}} \tag{4.8}$$

Since the average additional area covered by rebroadcast of a single neighbor is $0.41\pi R^2$ [4] the average additional area b covered by all neighbors of A will be given by $0.41k\pi R^2$ only if the maximum number of neighbors (highest node degree) $deg_{max} \geq k$, which simplifies to Equation 4.9;

$$b = \begin{cases} 0.41k\pi R^2, deg_{max} \geq k \\ \\ 0.41deg_{max}\pi R^2, deg_{max} < k \end{cases} \tag{4.9}$$

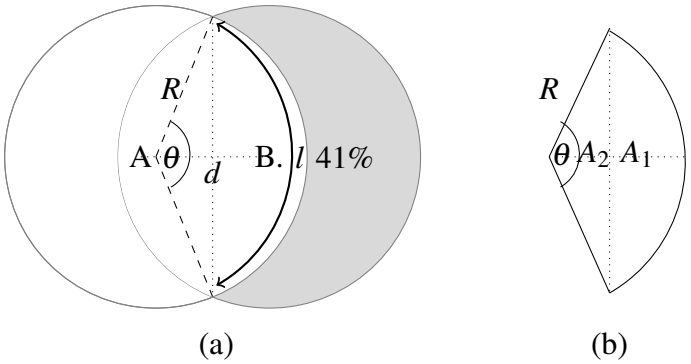

Figure 4.11: Estimating average distance d_{av} between source and a neighbor

Here d denotes the distance between A and any neighbor B. Note that d can vary from 0 to R. The lower bound of b is when $d = 0$ whereas the upper bound is when $d = R$. Average distance d_{av} corresponds to the case that the transmission ranges of A and B overlap by 59% of area.

According to Figure 4.11(b) total area of the wedge is $\frac{R^2\theta}{2}$ and $A_1 = \frac{R^2\theta}{2} - A_2$. Overlapping area is $2A_1$ and b' is estimated by Equation 4.12.

$$A_2 = \frac{Rd\sin\frac{\theta}{2}}{2} \tag{4.10}$$

$$A_1 = \frac{R^2\theta - Rd\sin\frac{\theta}{2}}{2} \tag{4.11}$$

Intersection of transmission ranges of A and B denoted by $b' = 2A_1$;

$$b' = R^2\theta - Rd\sin\frac{\theta}{2} \tag{4.12}$$

$$\cos\frac{\theta}{2} = \frac{d}{2R} \tag{4.13}$$

$$\sin\frac{\theta}{2} = \sqrt{1 - \frac{d^2}{4R^2}} \tag{4.14}$$

Using $\cos\theta = 2\cos^2\frac{\theta}{2} - 1$;

$$\cos\theta = \frac{d^2}{2R^2} - 1 \tag{4.15}$$

Substituting in Equation 4.12;

$$b' = 2R^2 \cos^{-1}(\frac{d}{2R}) - \frac{d}{2}\sqrt{4R^2 - d^2} \tag{4.16}$$

Equation 4.12 should be solved for $b' = 0.59\pi R^2$ to calculate average distance, d_{av};

$$0.59\pi R^2 = 2R^2 \cos^{-1}(\frac{d_{av}}{2R}) - \frac{d_{av}}{2}\sqrt{4R^2 - d_{av}^2} \tag{4.17}$$

The area b' accounts for around 59% of πR^2 for the average case resulting in Equation 4.17. When the equation was solved for the sample 20-node network, it resulted in 26m of average distance (d_{av}) between A and B. For this value of d, the number of arc lengths k that covers the circumference of the level 0 circle according to Equation 4.8 was 2.5. Note that k results in 2.5, which is a fractional number and it is acceptable as we only consider arc lengths that cover the circumference of radio range circle and not necessarily the number of circles, which will be 3 for this case.

In the considered sample MANET, we are given a $85m \times 85m$ playground with 20 nodes randomly placed on it. As previously stated in Section 4.3, we assume that no node is isolated and the nodes are dispersed throughout the playground. From transmission graph described by adjacency matrix in Figure 4.5, we know that the number of nodes placed within circles of radius R centered at each node is the neighborhood or outdegree deg_v in graph theoretic terms. The highest node degree deg_{max} for the sample 20-node network was 11. The probabilities of having node numbers 1 through 11 were calculated using Equation 4.2 to obtain the probability mass function shown in Figure 4.12. The average number of nodes newly reached at rebroadcast level 1 by the flooding wave was calculated using Equation 4.18 for discrete random variables, where n is the number of nodes and $p(n)$ is the probability that there exists n number of nodes in a considered region. Thus, around six nodes were found to be newly reached by the flooding wave at the first level of rebroadcast.

$$E[n] = \sum_{n=0}^{\infty} np(n) \tag{4.18}$$

For the $d_{av} = 26m$ found above, we estimate the area covered by level 1 circle in addition to the area covered by the original broadcast of the source using Equation 4.9 (similar to the dotted area in Figure 4.9).

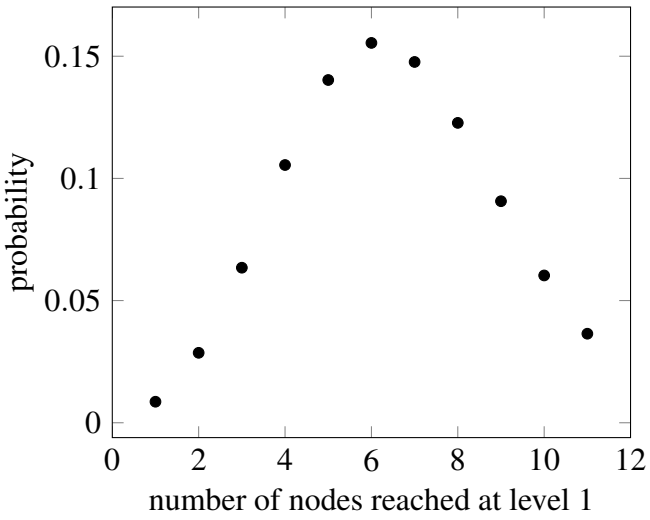

Figure 4.12: Probability mass function for the number of nodes additionally covered by rebroadcast level 1 for sample 20-node network

Table 4.4: Theoretical results for flooding propagation for 20-node sample network

level i	**area covered** A_i (m^2)	**rebroadcast radius** R_i (m)	**# arc lengths on circumference** k_i	**# new nodes** n_i	**# total edges** E
0	5027	40	2.53	3(= d_{src})	3
1	10249	57	3.62	6	22.2
2	17706	75	4.77	6	61.5
3	27507	94	5.93	4	100.8

transmission radius = 40m
average distance from a transmitting node to a neighbor = 26m
θ when average additional coverage is 41%=2.48 radians (142°)
$\overline{deg}$ average node degree=6.4

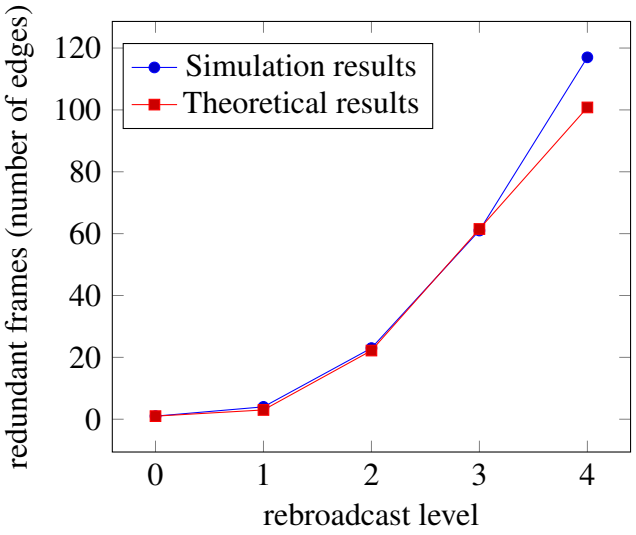

Figure 4.13: Redundant rebroadcast frames with rebroadcast levels in simple flooding for a sample 20-node network

4.4.4 Nodes covered by next levels of rebroadcast

The additional area covered by rebroadcast level 1 is added to the coverage of the source to get the area covered by level 1 circle in Figure 4.9. This gives the Equation 4.19 where b is given by Equation 4.9;

$$A_{level1} = \pi R^2 + b \tag{4.19}$$

$$R_{level1} = \sqrt{\frac{A_{level1}}{\pi}} \tag{4.20}$$

$$C_{level1} = 2\pi R_{level1} \tag{4.21}$$

$$k_{level2} = \frac{\pi R_{level1}}{R\cos^{-1}\frac{d}{2R}} \tag{4.22}$$

Next, the circumference C_{level1} of level 1 circle is calculated from the area of the circle using Equations 4.19, 4.20 and 4.21. Then, the number of arc lengths of radius R that covers the circumference referred to here as k_{level2} is estimated using Equation 4.22. The additional area b_2 that the second rebroadcast will cover is estimated using

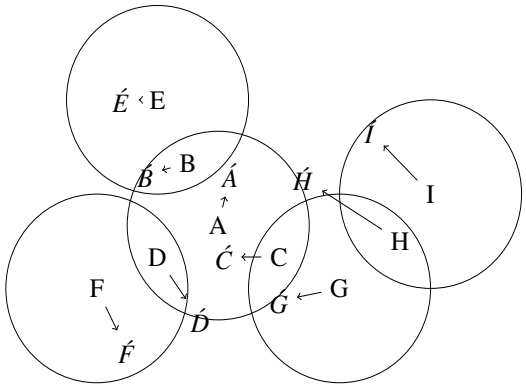

Figure 4.14: Problem of unicast via flooding in the presence of mobility

Equation 4.9. Next, the probabilities that there are 1 through deg_{max} number of nodes residing in the area b_2 are calculated using Equation 4.2 to obtain the probability mass function. Thereafter, the number of newly reached nodes by the second rebroadcast is obtained using Equation 4.18. This process is repeated for all the other levels of rebroadcasts until the level h_{max}. After following the complete procedure on the sample 20-node network, we obtained the results in Table 4.4.

As shown in Figure 4.13 the total number of frames accumulated in the network by the time each rebroadcast level finishes, grows exponentially. Moreover, both the theoretical results and the simulation results show the same behavior. However, towards the last rebroadcast level, theoretically estimated number of frames grows in a lesser amount than simulation results. This should be because we used $\overline{deg}$ in place of actual node degrees in the theoretical model.

4.4.5 Effect of node mobility

Consider the following example scenario. In the sample network in Figure 4.14, assume the nodes A through I move in the directions given by arrows and the new positions of the nodes are denoted by $\acute{A}$ through $\acute{I}$ by the time t_1. The node placements at time t_0 and t_1 are considered separately in Figure 4.15. According to Figure 4.15, we can extract the transmission graph and time-index the edges to get the corresponding *time evolving graph* as shown in Figure 4.16.

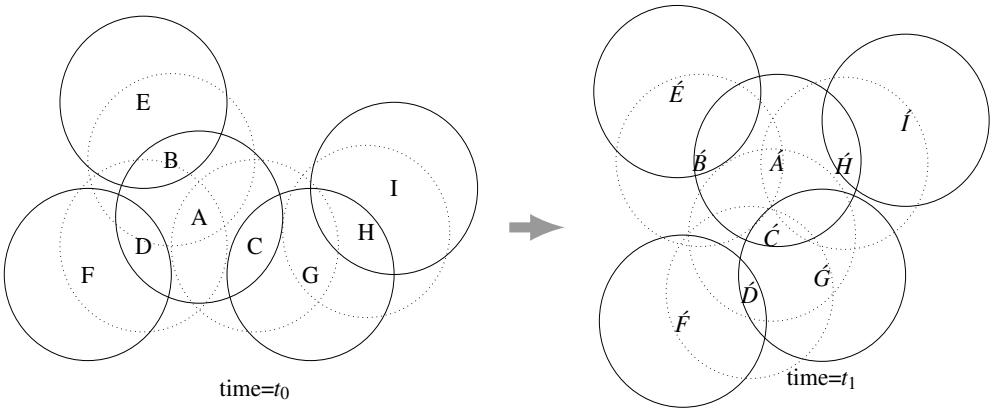

Figure 4.15: Network configurations at two time instances while the nodes are moving

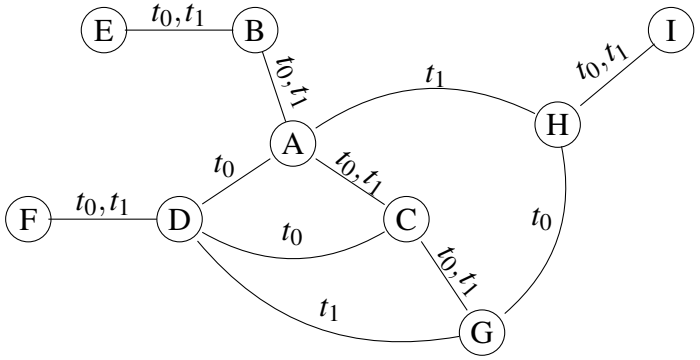

Figure 4.16: Time evolving graph due to mobility

If the nodes are static, a frame originated at A will propagate via simple flooding as shown in Figure 4.17 (a). When the nodes are mobile, the frame propagation should be analyzed with respect to time as in Figure 4.17 (b). If node A originates a frame and broadcasts it at $t = t_0$, nodes B, C and D will receive almost at $t = t_0$ ignoring the propagation delays compared to the time taken for the node movements and random assessment delays T_{RAD} (Section 3.2.2). The nodes B, C and D rebroadcast at $t < t_0$ and we assume the rebroadcasting times are close to t_0. By the time t_0 the links indexed by t_0 are available. Therefore, node E receives the frame from B, F receives from D, G receives from C and A receives redundantly from B, C and D. If the receiving nodes rebroadcast at times slightly offset from t_1 the frame will reach nodes that are connected by links indexed by t_1. Accordingly, nodes H and I also can be reached when the nodes are static. Mobility causes the breaking of the link (G,H). Therefore,

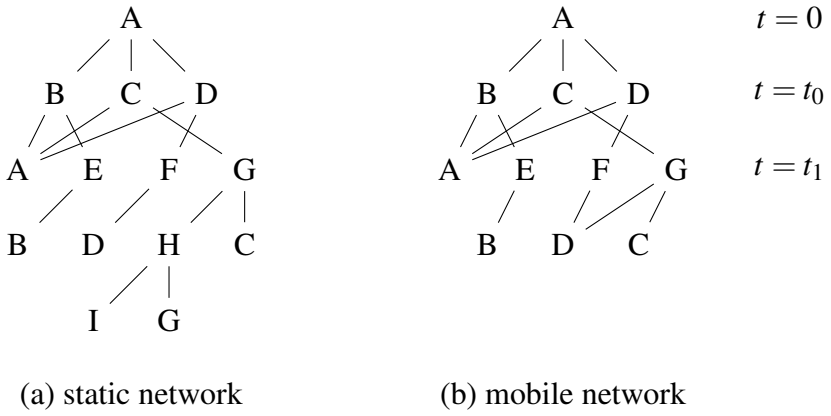

(a) static network (b) mobile network

Figure 4.17: Flooding graphs for simple flooding in static and mobile networks

H and I become unreachable due to mobility.

In order to derive generalized mathematical expressions for the number of nodes covered by each level of retransmission, we use *the probability of complete transmission* in single hop communication of moving nodes, derived by Cho and Hayes [95] as previously introduced in Section 3.6.2. Cho and Hayes [95] introduce a mobility model, which they call *constant velocity (CV) model* in which the nodes move at constant speed linearly at different angles but without changing the direction while moving (Section 3.6). As explained in Section 3.6 we use random waypoint (RWP) mobility model for our simulative analysis to evaluate the impact of mobility on performance of flooding schemes. In each movement epoch of RWP mobility, a node moves at constant speed along a straight line towards a destination point without changing the movement angle. Therefore, RWP can be decomposed into epochs that are modeled by CV mobility model.

A moving node N_0 succeeds in transmitting a frame completely to another moving node N_k in a single hop communication, only if N_k moves across the transmission region of N_0 throughout the time period of transmission of the frame (T_{comm}). The movement of N_k across the circular transmission region of N_0 is visualized in Figure 4.18 as already described in Section 3.6.2. According to Figure 4.18, node N_0 must start transmission after N_k starts traversing the distance Y and finish the transmission before N_k exits the transmission region of N_0. The time taken to travel the distance Y is

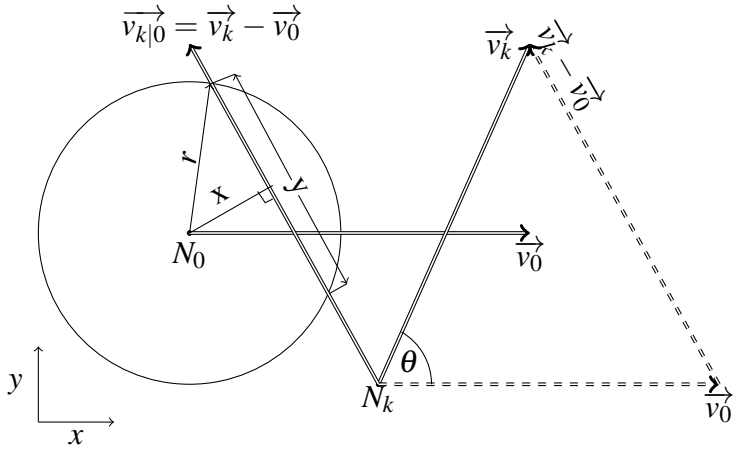

Figure 4.18: Motion of node N_k passing through the transmission region of node N_0 [95]

regarded as the link duration (T_{LD}) between N_0 and N_k, and the event of N_0 transmitting to N_k that crosses the transmission region of N_0 is described by (X, Θ).

The transmission must start at a time t where $0 \leq t \leq T_{LD}(x,\theta) - T_{comm}$ for a message to be completely transmitted before N_k exits from the region with a message transmission time T_{comm}. Accordingly, the conditional probability of complete transmission p_{comp} is given by Equation 4.23.

$$p_{comp}(T_{comm}|x,\theta) = \frac{max[T_{LD}(x,\theta) - T_{comm}, 0]}{T_{LD}(x,\theta)} \tag{4.23}$$

The total probability of complete transmission is given by Equation 4.24. Here, $g_{X,\Theta}(x,\theta)$ is the joint probability function of the event of transmitting a message by N_0 to N_k that crosses the communication region of N_0.

$$p_{comp}(T_{comm}) = \int_0^{\pi} \int_0^{r} p_{comp}(T_{comm}|x,\theta) g_{X,\Theta}(x,\theta) dx d\theta \tag{4.24}$$

Calculating $g_{X,\Theta}(x,\theta)$: Cho and Hayes [95] cite Little's theorem, which states that the average number of customers in a system is equal to the product of the arrival rate of the customers to the system and the average time that the customers spend in the system. By applying Little's theorem to single hop wireless communication in the presence of mobility, $g_{X,\Theta}(x,\theta)$ is found to be proportional to $v_{k|0}(\theta).T_{LD}(x,\theta)$ where

$v_{k|0}(\theta)$ denotes the relative velocity of N_k with respect to N_0. Using Equation 4.25, $g_{X,\Theta}(x,\theta)$ is obtained as in Equation 4.26.

$$T_{LD}(x,\theta) = \frac{Y(x)}{v_{k|0}(\theta)} \tag{4.25}$$

$$g_{X,\Theta}(x,\theta) = \frac{Y}{\int_0^{\pi}\int_0^{r} Y dx d\theta} \tag{4.26}$$

According to Figure 4.18,

$$Y(x) = 2\sqrt{r^2 - x^2} \tag{4.27}$$

Solving Equation 4.26;

$$g_{X,\Theta}(x,\theta) = \frac{\sqrt{r^2-x^2}}{\int_0^{\pi}\int_0^{r}\sqrt{r^2-x^2}dxd\theta}$$

$$\int_0^{\pi}\int_0^{r}\sqrt{r^2-x^2}dxd\theta = r\int_0^{\pi}\int_0^{r}\sqrt{1-(\frac{x}{r})^2}dxd\theta$$

$$= r\int_0^{\pi}\int_0^{\frac{\pi}{2}}(r\cos^2\alpha)d\alpha d\theta$$

where $\frac{x}{r} = \sin\alpha$, therefore, $dx = r\cos\alpha d\alpha$ and $\alpha : 0 \to \frac{\pi}{2}$ as $x : 0 \to r$.

$$= r^2\int_0^{\pi}\int_0^{\frac{\pi}{2}}\frac{(2\cos^2\alpha - 1 + 1)}{2}d\alpha d\theta$$

$$= \frac{r^2}{2}\int_0^{\pi}\int_0^{\frac{\pi}{2}}(\cos 2\alpha + 1)d\alpha d\theta$$

$$= \frac{r^2}{2}\int_0^{\pi}(\frac{\sin 2\alpha}{2} + \alpha)\Big|_0^{\frac{\pi}{2}}d\theta$$

$$= \frac{r^2\pi}{4}\int_0^{\pi}d\theta = \frac{r^2\pi^2}{4}$$

Therefore,

$$g_{X,\Theta}(x,\theta) = \frac{4\sqrt{r^2-x^2}}{r^2\pi^2} \tag{4.28}$$

In Equation 4.23,

$$max[T_{LD}(x,\theta) - T_{comm}, 0] = \begin{cases} T_{LD}(x,\theta) - T_{comm},\ T_{LD}(x,\theta) > T_{comm} \\ 0,\ otherwise \end{cases}$$

Therefore,

$$p_{comp}(T_{comm}|x,\theta) = \begin{cases} \frac{T_{LD}(x,\theta) - T_{comm}}{T_{LD}(x,\theta)},\ T_{LD}(x,\theta) > T_{comm} \\ 0,\ otherwise \end{cases}$$

According to the definition of CV mobility in Section 3.6.2, the velocity can be represented by $\overrightarrow{v_k} = v(\overrightarrow{i}\cos\theta + \overrightarrow{j}\sin\theta)$. The direction of node N_0 is $\theta_0 = 0$. denoted by $\overrightarrow{v_{k|0}} = \overrightarrow{v_k} - \overrightarrow{v_0}$. The magnitude of $\overrightarrow{v_{k|0}}$ is $v_{k|0} = v\sqrt{2-2\cos\theta} = 2v\sin\frac{\theta}{2}$. By substituting this result and Equation 4.27 in Equation 4.25,

$$T_{LD}(x,\theta) = \frac{\sqrt{r^2 - x^2}}{v\sin\frac{\theta}{2}}$$

Therefore,

$$p_{comp}(T_{comm}|x,\theta) = \begin{cases} 1 - \frac{T_{comm}}{T_{LD}(x,\theta)},\ T_{LD}(x,\theta) > T_{comm} \\ 0,\ otherwise \end{cases}$$

$$p_{comp}(T_{comm}|x,\theta) = \begin{cases} 1 - \frac{T_{comm} v\sin\frac{\theta}{2}}{\sqrt{r^2 - x^2}},\ T_{LD}(x,\theta) > T_{comm} \\ 0,\ otherwise \end{cases} \tag{4.29}$$

By substituting Equations 4.29 and 4.28 in Equation 4.24 when $T_{LD}(x,\theta) > T_{comm}$;

$$p_{comp}(T_{comm}) = \frac{4}{r^2\pi^2}\int_0^{\pi}\int_0^{r}(\sqrt{r^2 - x^2} - T_{comm} v\sin\frac{\theta}{2})dxd\theta$$

$$p_{comp}(T_{comm}) = \frac{4}{r^2\pi^2}\int_0^{\pi}(\int_0^{r}(\sqrt{r^2 - x^2}dx - \int_0^{r} T_{comm} v\sin\frac{\theta}{2})dx)d\theta$$

As already calculated $\int_0^r(\sqrt{r^2 - x^2}dx = \frac{r^2\pi}{4}$;

$$p_{comp}(T_{comm}) = \frac{4}{r^2\pi^2}\int_0^{\pi}(\frac{r^2\pi}{4} - T_{comm} v\sin\frac{\theta}{2}(x)\Big|_0^r)d\theta$$

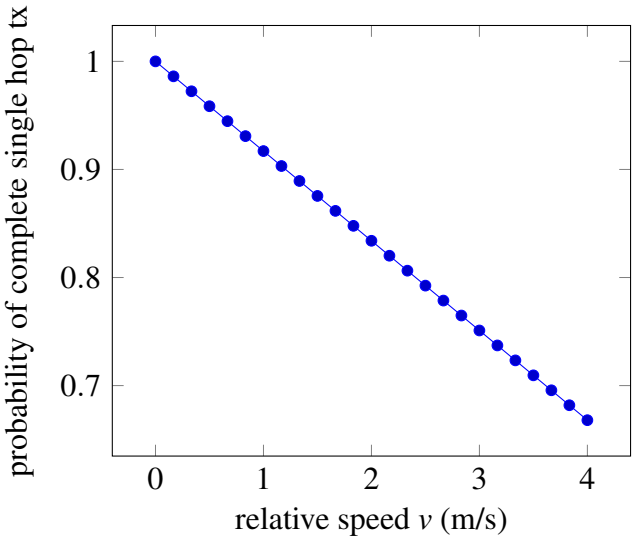

Figure 4.19: Probability of complete transmission of a 1024 Byte frame at 2 Mbps by a mobile node having transmission radius of 40 m in single hop communication with another mobile node when the speed of relative mobility varies

$$p_{comp}(T_{comm}) = \frac{4}{r^2\pi^2}\int_0^{\pi}(\frac{r^2\pi}{4} - rT_{comm}v\sin\frac{\theta}{2})d\theta$$

$$p_{comp}(T_{comm}) = \frac{4}{r^2\pi^2}(\frac{r^2\pi}{4}\theta + 2rT_{comm}v\cos\frac{\theta}{2})\Big|_0^{\pi}$$

$$p_{comp}(T_{comm}) = \frac{4}{r^2\pi^2}(\frac{r^2\pi^2}{4} - 2rT_{comm}v)$$

$$p_{comp}(T_{comm}) = 1 - \frac{8}{r\pi^2}T_{comm}v \tag{4.30}$$

For nodes having transmission radius of $40m$, Y varies from 0 to $80m$. When nodes move with a speed between 1 to 2 m/s, the maximum relative velocity is achieved when two nodes with speeds 2 m/s move in opposite directions so v varies from 0 to 4 m/s. We also consider the basic data rate of 2 Mbps at which broadcast communication happens according to IEEE 802.11 specifications as previously presented in Section 3.4. Let the frame size be 1024 Bytes as in IEEE 802.11 specifications and be fixed. It takes around 4 s to transmit a 1024 Byte frame at a rate of 2 Mbps. Probability of complete transmission of a frame with $T_{comm} = 4s$ varies with the magnitude v of

relative velocities according to Equation 4.30 and this variation is visualized in Figure 4.19 when v varies from 0 to 4 m/s.

At a macroscopic level, the movement of nodes in and out of the transmission range of a transmitting node is important to quantify the number of frames accumulated in the network. For example, if node A originates a frame in Figure 4.15 at $t = t_0$ it can be assumed that A's neighbors at $t = t_0$ receive it with a probability over 0.7, according to Figure 4.19 assuming the parameters such as movement speeds is 1 to 2 m/s, data rate is 2Mbps, and frame size is 1024B.

4.5 Storm control

Storm can be controlled using an appropriate mechanism that suppresses rebroadcasts such as efficient flooding. A broad survey of such efficient flooding schemes is given in Chapter 3 and threshold driven counter based scheme was identified as the best scheme for storm control as summarized in Table 3.1. This decision is inspired by the similarity between counter based flooding scheme and the chalone mechanism that regulates cell proliferation in the growth of the organs (Section 2.3). In counter based flooding scheme, a node on the receipt of a frame will buffer it and wait for a random period of time known as RAD (Section 3.2.2). During the RAD that we denote as T_{RAD}, the node will count the number of times the same frame is received subsequently. The node will rebroadcast the frame only if this counter C is less than a pre determined threshold K as explained in Sections 3.2.

4.5.1 Graph based analysis of counter based flooding

Let us analyze the same sample 20-node network described by the adjacency matrix in Figure 4.5, when it runs counter based flooding with a threshold of one ($K = 1$). In this scenario, a node will rebroadcast a received data frame only if it will not receive the frame again during its random wait period T_{RAD}. The following sequence of actions will occur when counter based flooding is applied on the sample network:

The nodes h6, h13 and h18 receive the frame at time t_0 from the source for the first time. These three nodes will wait for a T_{RAD} after buffering the frame. Assuming h13 waits the least among the three nodes, h13 will rebroadcast and the neighbors of h13 receive the frame. This is denoted by labeling the set of edges going out from h13 as t1. When the edges are time-indexed, the graph can be considered a *time evolving graph* as explained in Section 3.7.

Lets assume that the level 1 rebroadcast of h13 is heard by all its neighbors by the time h18 gets timeout after receiving the frame from the source. Since h18 is also a neighbor of h13, h18 now records that it received the same frame again. Since the threshold is one and h13 received the frame again, h13 refrains from rebroadcasting the frame in the buffer. Similarly, h6 also decides not to rebroadcast. Therefore, only one node, namely h13 will rebroadcast at level 1. If h6 and h18 wait for a period less than the time required for neighbors of h13 to receive the rebroadcast, then all three will end up rebroadcasting as in simple flooding. Assuming the timeouts are scheduled with adequate time gaps, we will get the tree in Figure 4.20.

At level 2, although h1, h2, h5, h6, h9, h11, h13, h15, h17 and h18 receive the frame, h13 ignores the frame as it has already rebroadcast it. Further, h6 and h18 have received the frame from h18 while the frame was still in buffer thus frame count is not less than the threshold when the timeout occurs. Therefore, h1, h2, h5, h9, h11, h15 and h17 buffer the frame. Consider that the random wait period for h9 is the least so that h9 will rebroadcast at level 2 first.

The rebroadcast of h9 is received by h1, h3, h5, h7, h8, h12, h13, h14, h16, h17 and h18. The transmission of h9 is most likely to reach h1, h16, h17 and h18 while waiting with the frame buffered at level 2. Therefore, h1, h16, h17, h18 will not rebroadcast as the count is not less than the threshold. Node h6 also will not rebroadcast as it has already discarded the frame. Also h13 will discard the frame as it has already rebroadcast. Therefore, it will be only h9 that rebroadcasts at level 2. Furthermore, the nodes h3, h5, h7, h8, h12 and h14 are the tentative nodes to rebroadcast at level 3 and they will buffer the frame.

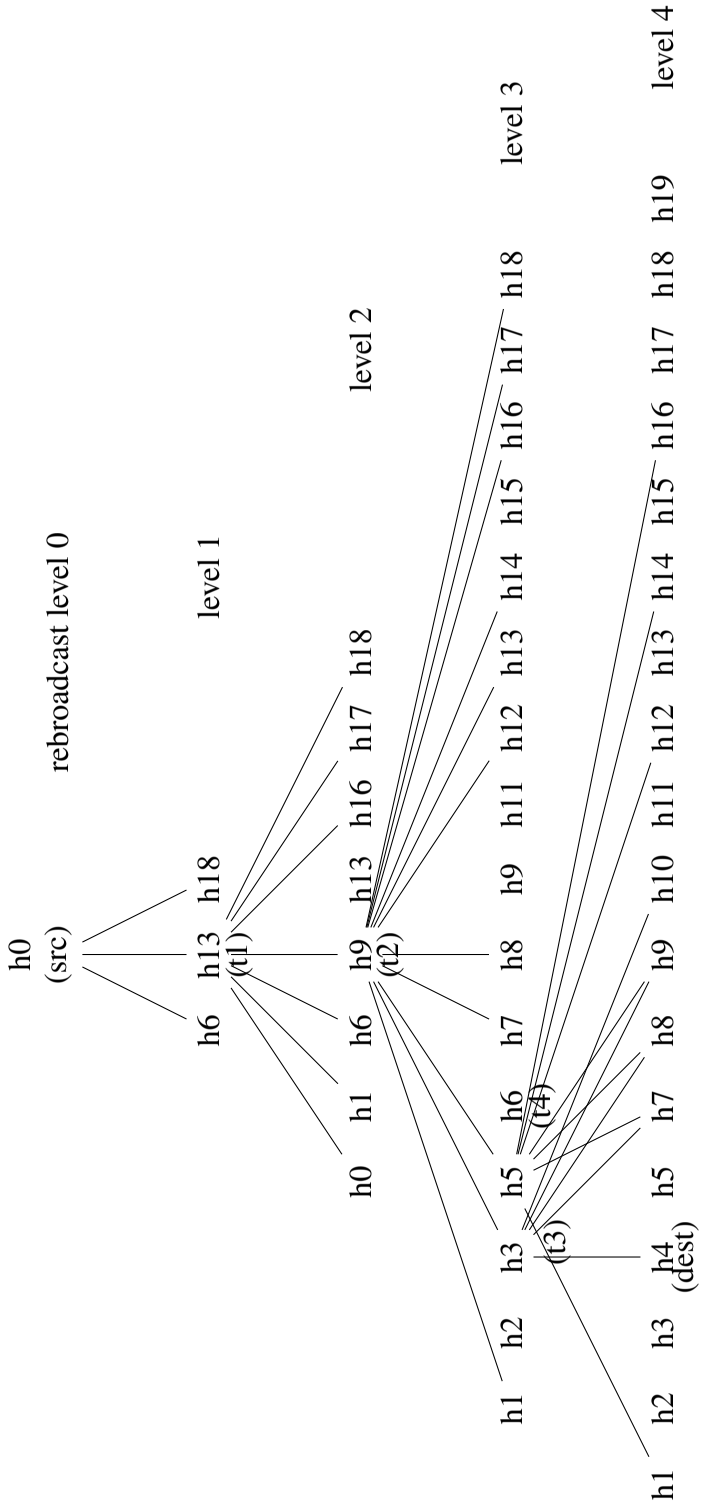

Figure 4.20: Redundant rebroadcasting in counter based flooding modeled as graph evolution for the topology given in adjacency matrix in Figure 4.5 for unicast from host0 to host4

Assume that h3 is the first to rebroadcast at level 3. This manages to reach the destination h4. The nodes h7 and h8 also receive the rebroadcast of h3 while the frame is still in buffer. However, h5, h12 and h14 are tentative rebroadcasters when their waiting times elapse. Let h5 rebroadcast after h3. Then h12 and h14 will refrain from rebroadcasting at level 3.

The tree will be different when the random waiting periods of nodes elapses in a different order than what gave the tree in Figure 4.20. According to the tree in Figure 4.20, the number of edges caused by each rebroadcast level gives the plot in Figure 4.21. According to Figure 4.21, counter based flooding effectively reduces the number of redundant frames compared to simple flooding as the counter based flooding gives a slow growing curve where as simple flooding gives an exponentially growing curve.

According to the above graph based analysis, the following conclusions can be drawn to assist in building a generalized model for counter based flooding:

- The nodes at each rebroadcast level in the simple flooding tree (Figure 4.7) are the tentative rebroadcasters in counter based flooding because the nodes are likely to rebroadcast at a particular level (hop count) depending on their physical location relative to the source. Therefore, we interpret rebroadcast level in counter based flooding tree as the potential level for a node to rebroadcast. For example, referring to the graph corresponding to simple flooding in Figure 4.7, h6, h13 and h18 are able to rebroadcast at level 1 as they are physically located in the neighborhood of the source. However, according to the specification of counter based flooding it is required that $C < K$ for a node to rebroadcast. If $K = 1$ only one of them will end up rebroadcasting (e.g. h13 in Figure 4.20), because the rebroadcast of any one of the nodes makes $C = 1$ for the other two nodes if T_{RAD}s of the nodes have adequate gap to receive each others' broadcasts.

- In contrast to the case of simple flooding, the graph model for counter based flooding requires to incorporate time dimension. We index the set of edges by time at which the frame is received by the receiving node so that we can determine which set of neighbors will rebroadcast upon expiring the T_{RAD}. The set of nodes that actually rebroadcast is decided by how many fellow tentative re-

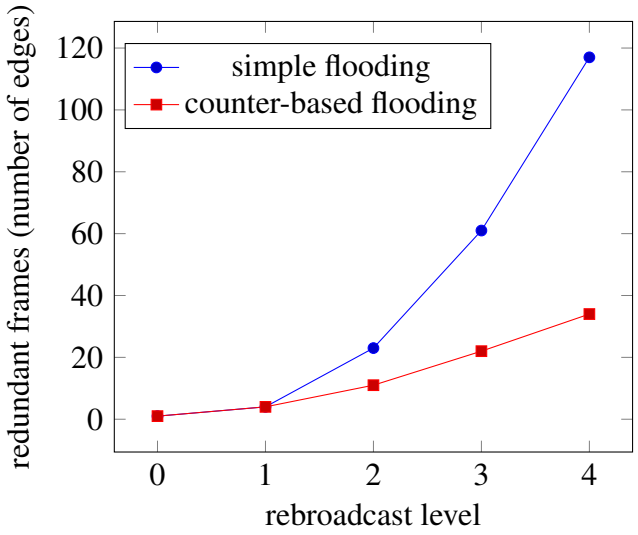

Figure 4.21: Simulation results for redundant rebroadcast frames with rebroadcast levels in simple flooding and counter based flooding with threshold 1 for a sample 20-node network

broadcasters in the same level will send a frame within T_{RAD} of that node. The order in which T_{RAD} expires for nodes in the same level matters and the tree is structured in a different configuration when this order varies.

- The fact that a destination is reachable or not, depends on the set of nodes that actually rebroadcast according to the order of T_{RAD} and the threshold K. There is a risk that a destination that is reachable via simple flooding, is never reached by counter based flooding, for example node h4 will not be reached if node h3 had a longer T_{RAD} and thus h3 refrains from rebroadcasting as C is not less than K.

4.5.2 Mathematical model for counter based flooding

We develop a mathematical model to estimate the redundant frames caused by counter based flooding with the insights gained by analyzing the sample network and the related work surveyed in Chapter 3. In the previous section we realized that the following modifications must be made to the graph based model of simple flooding in order to model counter based flooding.

- Index each edge (u, v) with the time at which a frame is received by node v thus converting the graph into a time evolving graph. This time domain representation is required to interpret any flooding scheme that involves a RAD including counter based flooding.

- We redefined rebroadcast level for counter based flooding above as the level or the hop count from the source, at which a node is likely to rebroadcast. Therefore, at each rebroadcast level, the nodes that receive a frame become *potential rebroadcasters*.

Estimating number of rebroadcasting nodes Let the number of potential rebroadcasters be n_i where i denotes the level of tentative rebroadcast. Accordingly, the numbers of nodes that are potential in rebroadcasting at each rebroadcast level in the sample network is same as the number of newly reached nodes in Table 4.4 corresponding to simple flooding.

According to Viswanath-Obraczka model for probabilistic flooding (Section 3.2.1), the number of nodes that rebroadcast at each level of rebroadcast is obtained by multiplying the newly reached nodes in that level by the probability of rebroadcasting of a node. Similarly, we also estimate a probability of rebroadcasting for counter based flooding by each node and let that be denoted by P_{tx}. Therefore, number of nodes that will decide to rebroadcast at each level m_i will be, $m_i = P_{tx} n_i$.

The probability that a node decides to rebroadcast depends on the frame count C from the time at which the frame is received for the first time until the time at which T_{RAD} expires. A node will rebroadcast only when $C < K$ so that P_{tx} also depends on K. Following analyses are aimed as quantifying P_{tx}.

Geometrically modeling the counter value Consider the scenario in which node A in Figure 4.22 broadcasts a frame. The nodes B, C, and D receive it. All three of these nodes are tentative rebroadcasters at level 1. Let one of them rebroadcast, for example B. This rebroadcast will be received by nodes within B's range. The nodes that are in the intersecting area of A's coverage and B's coverage have already received A's

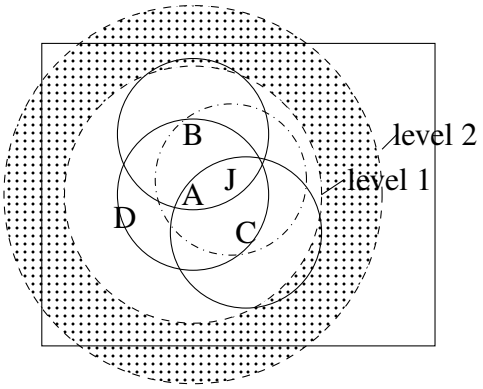

Figure 4.22: Geometric estimation of counter value by rebroadcast of neighbors

transmission. Therefore, B's transmission causes counter to increase by one for these nodes. The maximum counter value that a node in A's coverage will experience due to rebroadcast at level 1 will be the number of radio ranges of A's neighbors that intersect in such a way that the node is located in the intersection area. For example, node J is at a position inside the intersection area of B's and C's coverage circles. Since J is also in the range of A, J has already received the original broadcast of the frame from A. Subsequently, J receives the rebroadcast of both B and C also, thus recording a counter value of two. For node J to receive a transmission from B, distance between B and J should be less than R which is the transmission radius and similarly the distance between C and J should also be less than R assuming fixed radio range R for all nodes.

According to the above analysis, a counter value in any node $h[i]$ is equal to the number of rebroadcasting nodes that will cover $h[i]$ with their radio ranges. The condition for $h[i]$ to reside in any other node's radio range is that the distance of $h[i]$ from that node should be less than R if R is the fixed radio range of all nodes.

There are attempts to analytically estimate related quantities such as intersection area of many circles [112], probability distribution function of internode distances of points placed in a sphere [113], and neighbor distances using probabilistic model [114]. These calculations are cumbersome and cannot maintain the problem at a practically tractable level [114, 112, 113], for example, it is challenging to estimate the intersection area of many circles because there are large number of possible configurations of overlapping with each configuration resulting in a different geometric expression

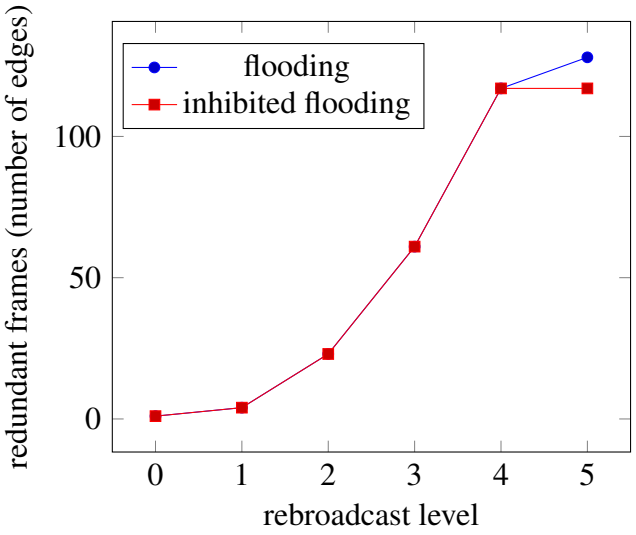

Figure 4.23: Redundant rebroadcast frames with rebroadcast levels in simple flooding for a sample 20-node network after reaching the destination

for area [112]. Therefore, Monte Carlo simulations are used to obtain a numerical approximation for such calculations and also used for verifying analytical results.

Counter based flooding is analytically explored in Chapter 6 based on the concepts and insights developed in this section.

4.6 Flood control

Although suppression of rebroadcasts gives a reduction in storm situation (Figure 4.21), the frame continues to propagate thus leaving the *broadcast flood problem* unsolved as seen in Figure 4.23. We use negative acknowledgment to control flood. Although destination is reached by maximum of h_{max} levels of rebroadcasts the flooding tree continues to grow until all the nodes that fulfill the conditions for rebroadcast, have finished rebroadcasting. For example, in Figure 4.7 the destination is reached by the rebroadcast at level 3. However, h10 and h19 that receive the frame for the first time at level 4 continue to rebroadcast at level 4. This adds 6 frames received by neighbors of h10 and 5 frames by neighbors of h19. If h4 sends out a message to inform the nodes that they must not rebroadcast, then we could have saved these 11 messages.

However, the negative acknowledgement frame that we term as *inhibitor* will propagate as another flood. This negative acknowledgement scheme should be optimized in terms of resource consumption. For example, the inhibitor frame size should be smaller than the data frame, should propagate faster than the data flooding wave to inhibit as many rebroadcasts as possible. Inhibitor should not propagate far beyond the area that the data flooding has covered. The design of inhibitor scheme is included in the protocol design in Chapter 5.

4.7 Summary

In this chapter, we derived a graph model to represent a MANET that runs a given flooding scheme as follows:

- Given the location map of the nodes, draw circles of radius r around each node where r is the variable transmission ranges of nodes. In other words, compare the distances between node pairs to check whether they are within the transmission ranges of each other.
- Get the adjacency matrix for the network where nodes are adjacent or have direct wireless links if two nodes are within transmission ranges of each other.
- Given a source destination pair for unicast, build the *flooding graph* $G(V,E)$, in which nodes are the vertices V and an edge (u,v) is added if the flooding scheme causes a frame to propagate from node u to v: If it is a static network with simple flooding or probabilistic flooding the graph is a tree with rebroadcast levels. If the nodes move or the flooding scheme includes a RAD, the graph is a *time evolving flooding graph* in which edges are time indexed.
- The number of frames caused by flooding scheme is given by the total number of edges in the *flooding graphs* and the number of time indices on the edges in the *time evolving flooding graphs*.

- Propagation of the frames via flooding schemes is quantified by the growth in the number of frames with rebroadcast level in flooding graphs and the number of time indices with time in time evolving flooding graphs.

This process is doable in a small sized network but not feasible for dense networks. Therefore, we developed a geometric method to estimate the number of edges added to a flooding graph at each level of rebroadcast.

It is shown by prior research that the average additional area covered by a rebroadcast of an immediate neighbor is 41% of the communication region of a node. This result is obtained by considering the overlap between two equal circles that intersect when the centers are placed at distances between 0 and radius R. We extend the idea when multiple neighbors rebroadcast by considering the intersection of multiple radio range circles of neighbors with the radio range circle of a node. We place radio range circles of the neighbors at the intersection distance that gives 41% additional coverage by each circle. We estimate how many such circles are required to cover the circumference of the radio range circle of a node in terms of arc lengths. Then, we multiply the number of arc lengths by 41% to get the total additional area covered by rebroadcast of all the neighbors.

We drew insights to develop a model to analyze counter based flooding that will be elaborated in Chapter 6. We also conceptualized how an inhibition scheme should be designed to control broadcast flood situation that will be explained in Chapter 5.

CHAPTER V

PROPOSED PROTOCOL

5.1 Introduction

In this chapter, we propose a protocol to perform unicast in dense MANETs in such a way that the nodes do not have to maintain global network states such as routing tables and there are no special nodes to undertake routing and control. The proposed protocol is targeted at MANET scenarios that have the following characteristics as previously explained in Section 1.1:

- No routing infrastructure such as special beaconing nodes
- Potentially large number of transmitting nodes
- Minimum amount of state information held by each node
- Stored state information is only locally relevant and subject to rapid change and frequently become invalid

After a broad survey of traditional routing approaches in Chapter 2, we rejected the fixed-stateful routing approaches as a solution to routing problem in dense MANETs due to the costs of discovering and maintaining routes or topological structures. In Section 2.3 we built the hypothesis that unicast can be achieved via blind rebroadcasting and the inefficiencies should be mitigated using suitable control mechanisms in such

a way that the scheme conforms to the mobile-stateless routing paradigm. Blindly rebroadcasting and its descendant, simple flooding causes two significant performance problems, namely the *broadcast storm problem* and the *broadcast flood problem* introduced previously in Section 2.3 and theoretically elaborated in Sections 4.5 and 4.6.

Nature-inspired solutions have proven to perform satisfactorily in a plethora of real world problems in the literature as briefed earlier in Section 2.3, in which the inspirations are drawn from ant colonies, honey bees, human immune system and more. We also surveyed natural systems that show similar characteristics of a blindly rebroadcasting MANET (Section 2.3) and identified *cell proliferation* in the growth of biological organs as the best analogy. We will explain the concepts in cell proliferation and its regulatory mechanisms in this chapter with a mapping between MANET concepts and cell biological concepts.

According to the nature of broadcast flood situation, we identified negative acknowledgement as the best mechanism to mitigate broadcast flood problem according to Section 2.3. In this mechanism, a control message is used to catch the flooding wave and stop its propagation beyond the destination and we present such a flood control mechanism also in this chapter.

Widely available commodity wireless networking hardware is compliant with IEEE 802 standards. According to the IEEE 802 specifications the protocols are targeted at Layer 1 and 2 in the ISO OSI protocol stack. The recently amended IEEE 802.11 Mesh Network standards emphasize the suitability of routing functionality for mesh type wireless networks at the Link Layer. To distinguish between routing at layer 2 from that at layer 3, IEEE 802.11 introduces the term *path selection* [8]. The convention of routing at link layer has been arrived at around 2006 in IETF MANET groups and the active MANET research communities. We also follow the trend and propose our protocol to operate at the Link layer thus we use the term *frame* for the data units in our protocol and work with MAC addresses.

Table 5.1: Comparison of cell proliferation with blind rebroadcasting

cell proliferation	**blind rebroadcasting**
It is local to the micro environment of the cells and uses information either by direct signaling or by indirect signaling via the micro environment	Each node has no state information about the topology or the neighborhood of the nodes
Cells are identical to each other and goes through the same life cycle	Every node performs the same simple task of forwarding a received data packet
Each cell divides into two so that the number of cells should grow exponentially if there are no regulatory mechanisms	Total number of packets in the network grows exponentially
Cells are organized into a dense population in a biological organ	Large number of interacting nodes in the network

5.2 Controlling redundant rebroadcasts

Cell proliferation was identified as an analogy to blind rebroadcasting in Section 2.3.1.9. A grown organ in human body is made out of a dense population of biological cells. The organs originate from a small number of *stem cells* and these cells divide themselves repetitively in the process called *cell proliferation* [53].

Definition of cell proliferation: Cell proliferation is the process that results in an increase of the number of biological cells when each cell divides into two identical cells by the completion of cell life cycle [53, 115, 116]. Cell proliferation is analogous to re-broadcasting of packets in a MANET according to Table 5.1.

It is an interesting question to ask “On what basis our ears end up growing into a particular size?”. The nature has its regulatory mechanisms for controlling the cell division in an organ. These biological regulatory mechanisms are surveyed in following sections with the intention of identifying suitable mechanisms to manage redundant broadcasts in a dense MANET in compliant with mobile-stateless paradigm.

5.2.1 Growth regulation in organs

According to Lui and Baron [53], the human body has a growth deceleration mechanism driven at the physiological level by growth itself and at a molecular level by a cell intrinsic genetic program. This claim is supported by Finkielstain et al. [115]. Lui and Baron in [53] further elaborate that the local communication mechanisms play the central role in growth deceleration rather than the systemic mechanism. Bryant and Simpson in [116] also highlight the evidence for organ intrinsic mechanisms in growth control in organs. However, the growth deceleration program is not cell autonomous but it depends on the interaction of the cell with the extra-cellular micro environment [53].

5.2.1.1 Using growth as the inhibitor of growth

The genetic program explained in [53] is responsible for growth inhibition according to the inputs related to growth itself such as the number of accumulated cells, organ functionality and the number of cell divisions undergone. This genetic program up or down-regulates growth promoting genes according to a negative feedback loop. The hypothesis that the growth itself causes growth inhibition is also proved by Forcinito et.al in [117].

5.2.1.2 Terminal conditions of growth

According to Lui and Baron [53] the *growth program* described above down-regulates the growth-promoting genes when (i) the accumulated number of cells reach the saturation level, (ii) the organ is adequately grown to perform the intended functionality or (iii) the number of divisions undergone is equal to the particular number set during the embryonic stage.

5.2.1.3 Growth sensing mechanisms

Individual cells sense the growth in terms of number of accumulated cells by means of the concentration of some secreted molecules known as *chalones* [53]. Bullough [118] coined the term chalone and hypothesized it as the inhibitors of cell growth

by negative feedback to control the size of a tissue. A number of studies provide experimental evidence in support of this hypothesis [119, 120, 121, 122]. Growth in terms of the level of functionality is sensed for example in the liver by flux of bile acids. Bile acids are synthesized in the liver and secreted into the small intestine to facilitate digestion. Bile acid is then reabsorbed and returned to the liver. The number of cell divisions undergone is measured using cell cycle counting mechanisms such as telomere shortening [53].

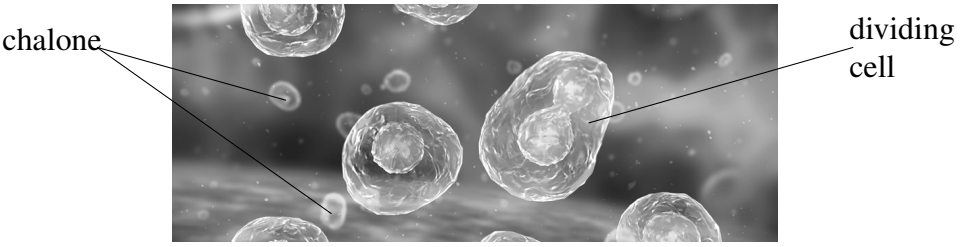

Figure 5.1: Chalone mechanism for cell proliferation control

Chalone mechanism The term *chalone* is commonly used to identify certain soluble factors in biological systems, the concentration of which is directly proportional to the number of cells. Chalones are secreted by each individual cell and its concentration increases proportional to the number of cells with cell proliferation. The cells sense the chalone concentration in its micro environment. When the chalone concentration reaches a particular level such that the organ has adequately grown, the individual cells decide not to divide. This concept is visualized in Figure 5.1.

5.2.2 Biological system to MANET mapping

We map a biological cell to a data frame in a node as in Table 5.2. Cells increase in number due to proliferation and similarly, the frames in a MANET increase in number when the nodes rebroadcast the frame and the neighboring nodes receive it. The number of cells in the organ is represented by the chalone concentration. A similar local measure should be devised for a MANET to estimate number of frames in the network. According to Figure 5.2 and as also shown in Section 4.2, increase in the frame count

Table 5.2: Mapping from biological system to MANET

Biological System	**MANET**
Biological cell	Data frame in a node
Cell division	Frame rebroadcasting
Chalone	The received data frames from the neighbors. Neighbors are the nodes within the transmission range of a node.
Chalone concentration	Number of neighboring nodes who have already broadcast the Data Frame.

depends on the neighborhood of the rebroadcasting nodes. Therefore, the growth of the number of frames can be estimated using the number of neighbors, though the total number of accumulated frames cannot be known using local mechanisms.

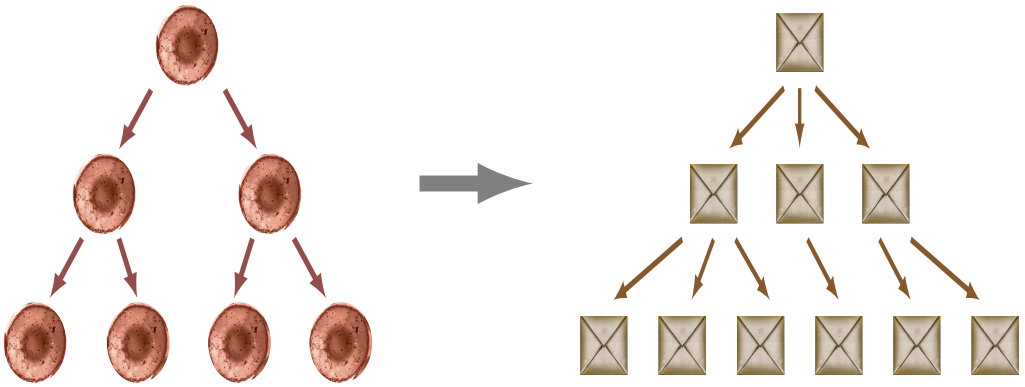

Figure 5.2: Cell proliferation Vs message rebroadcasting

A conventional method to obtain neighborhood information in MANETs is to periodically exchange beacon frames. However, it is undesirable to use local beaconing for neighbor information gathering due to collisions and contention in dense neighborhood as previously presented in Chapter 2. A node is able to sense the number of neighbors who rebroadcast the same frame by looking at the received frames. Therefore, the received frames themselves act as chalone that interpret the neighborhood as a cue about the accumulated frames in the network. For instance, if a node receives the same frame from many neighbors, the node may not reach new nodes by rebroadcasting that frame. The rebroadcast will be received by the neighbors only as redundant

frames.

A node decides to rebroadcast a received frame depending on the number of redundant copies of the same frame received from elsewhere. If the count of redundant frames reaches a threshold the node decides not to rebroadcast. This is similar to chalone mechanism. We borrow the term *chalone* for the actions regarding the neighborhood in MANETs to denote the inspiration from chalone mechanism in cell proliferation.

5.2.3 Operational model of the bio-inspired system

In general, the functional behavior of cell biological systems are modeled in terms of cellular automata as in [123, 124, 125, 126]. Similarly, the operation of biologically inspired broadcasting model for MANETs is interpreted based on cellular automata in this section.

Cellular automata (CA) are defined as mathematical idealization of problems or physical systems in which space and time are discrete and the physical values take on finite set of discrete values [127]. This was invented by John von Neumann in 1940s as a result of biological motivation with an intention to design self-replicating artificial systems. Power of CA lies in its fundamental properties that are also found in the physical world: CA are massively parallel, homogeneous and all interactions are local [128]. Therefore, a variety of physical and biological systems have successfully been modeled and simulated using CA [129, 124, 130, 131, 132].

One-dimensional two-state CA is extensively elaborated in [127]. Formalism of CA is found in [133] for multi-dimensions which is an exhaustive algebraic treatment of the subject. The type of CA of our interest is two-dimensional as the nodes in the MANET lie effectively on a plane. Packard and Wolfram [134] further analyze two-dimensional CA and cite [133] for *additive two-dimensional* CA. According to [134], a two-dimensional CA consists of a regular lattice of sites. Each site takes on k possible values. Each site is updated in discrete time steps according to a set of rules, ϕ that depends on the values of sites in some neighborhood around it at the previous time step. Packard and Wolfram [134] addresses the special class of ϕ known as *totalistic*

rules in which the values of a site depends only on the sum of values of the neighbors.

Our CA model of MANET is also viewed as a regular lattice on which mobile nodes are randomly placed. Each site takes only two values: 1 to denote that the node has rebroadcast a specified data frame and 0 to represent that the node has not rebroadcast. Neighborhood for our CA is the circular region captured by the radio range of a mobile node. Any node within the range will respond as a neighbor. We apply *totalistic rule* in which we count the total number of neighbors who have rebroadcast a specific data frame. The number of neigbors who have rebroadcast (state 1) is given by the number of frames received from the neighborhood. If this number exceeds a predefined threshold a node can decide not to rebroadcast a data frame in hand and we name this number as *the chalone threshold*. This will be the cellular automata rule.

We designed the simulation software for the protocol in a modular architecture by considering the cellular automata based representation of the protocol. Each node independently runs the same simple set of actions (Figure 5.3): if a frame is received for the first time buffer it, wait, count the number of frames received subsequently, when the waiting time elapses evaluate the rule "counter is less than the threshold?", if less then rebroadcast (state 1), else discard (state 0). The set of actions are the same for both the data frames and the inhibitor frames.

A default set of values for chalone threshold and minimum and maximum waiting times will be given in the protocol by assuming a general case of MANET scenario. Example MANET scenarios such as a meeting room or a disaster relief camp is characterized by the physical area the nodes occupy, number of nodes that may reside and transmission ranges of the nodes.

5.3 Protocol architecture and design

The protocol consists of two phases: storm control mechanism and the flood control mechanism.

Storm control mechanism

Our conservative frame rebroadcast scheme which we call the *storm control mechanism* operates as follows: when a node receives a data frame for the first time, it enqueues the frame and creates a record in its frame log. Then it waits for a time period which we call *chalone wait* to denote that the node is listening for the neighbor information. If the same data frame is received subsequently during the chalone wait the senders' addresses are also recorded for that frame. Thus the log record includes the list of neighbors who have already rebroadcast the frame. When the chalone wait time elapses, the node evaluates the number of rebroadcast neighbors to see whether it exceeds a pre-defined threshold that we name *chalone threshold*. If the number of rebroadcasting neighbors does not exceed the threshold the node dequeues the frame by rebroadcasting it. Otherwise the frame gets discarded. According to the specification of counter-based scheme in [4] as previously explained in Section 3.2, our approach can also be characterized broadly as counter-based flooding. The details and specificities are worked out in Section 5.3.

The forwarding decision is made per frame basis by referring to the frame log of the form in figure 5.4. A data frame is uniquely identified by the source MAC, destination MAC, and a sequence number generated by the source which altogether is considered as the *Frame ID*. *Data state* carries the information such as whether the data is discarded or rebroadcast. *Control state* is to record any control message sent or received about the frame.

Flood control mechanism

Though the above threshold based mechanism rebroadcasts the data frame in a conservative manner the frame will continue to flood outwards in the MANET starting from the source node. Therefore, upon received by the intended destination this flooding wave must be stopped.

Our adaptive frame inhibition scheme which we call the *flood control mechanism* operates as follows: a node sends a control frame named *inhibitor* as soon as it receives a data frame destined to itself. Any other node that receives an inhibitor forwards it

only if there exists any record of the data frame that the inhibitor corresponds to. In order to reduce the number of inhibitors forwarded by nodes the storm control mechanism above is followed. However the wait time referred in this case as *inhibitor wait* is considerably low compared to chalone wait time. Thus the proposed inhibition scheme is initiated by the destination and it propagates faster than the flooding wave only for the purpose of catching the flooding wave and not to propagate beyond the flooded area. Figure 5.3 illustrates the storm control mechanism and initiation of flood control.

Variables and justifications

Following variables may be set with default values when the endcast scheme is installed into devices by assuming or by letting the user select a MANET scenario, which is described by the approximate number of devices and the physical area.

Chalone wait

Chalone wait can be recognized as a random assessment delay (RAD) defined in [5]. Common practice of setting a RAD is to specify a maximum delay (T_{max}) and RAD is chosen uniformly from the range 0 to T_{max} [5]. This randomization avoids collisions. However, chalone wait should not be 0 but large enough to receive as many neighbor responses as possible and should not be too large to introduce an unacceptable end to end delay for the frame.

T_{max} is set to 0.001 s, 0.01 s, 0.05 s and 0.1 s in the simulative study to compare broadcast protocols in [5]. T_{max} is set to 0.01 s in the simulative setup in [68]. Delay and backoff intervals in the Rene mote testbed for flooding experiments are randomly picked from the range 0.006 s to 0.01 s. In [63] the maximal transmission latency is calculated by dividing the transmission range from transmission speed. IEEE 802.11 standard specifies the speed of radio waves propagating in free space as $300m/\mu s$. We set the T_{max} to be the worst case time duration for two nodes at two ends of the playground will take to communicate by dividing the maximum distance between nodes by transmission speed.

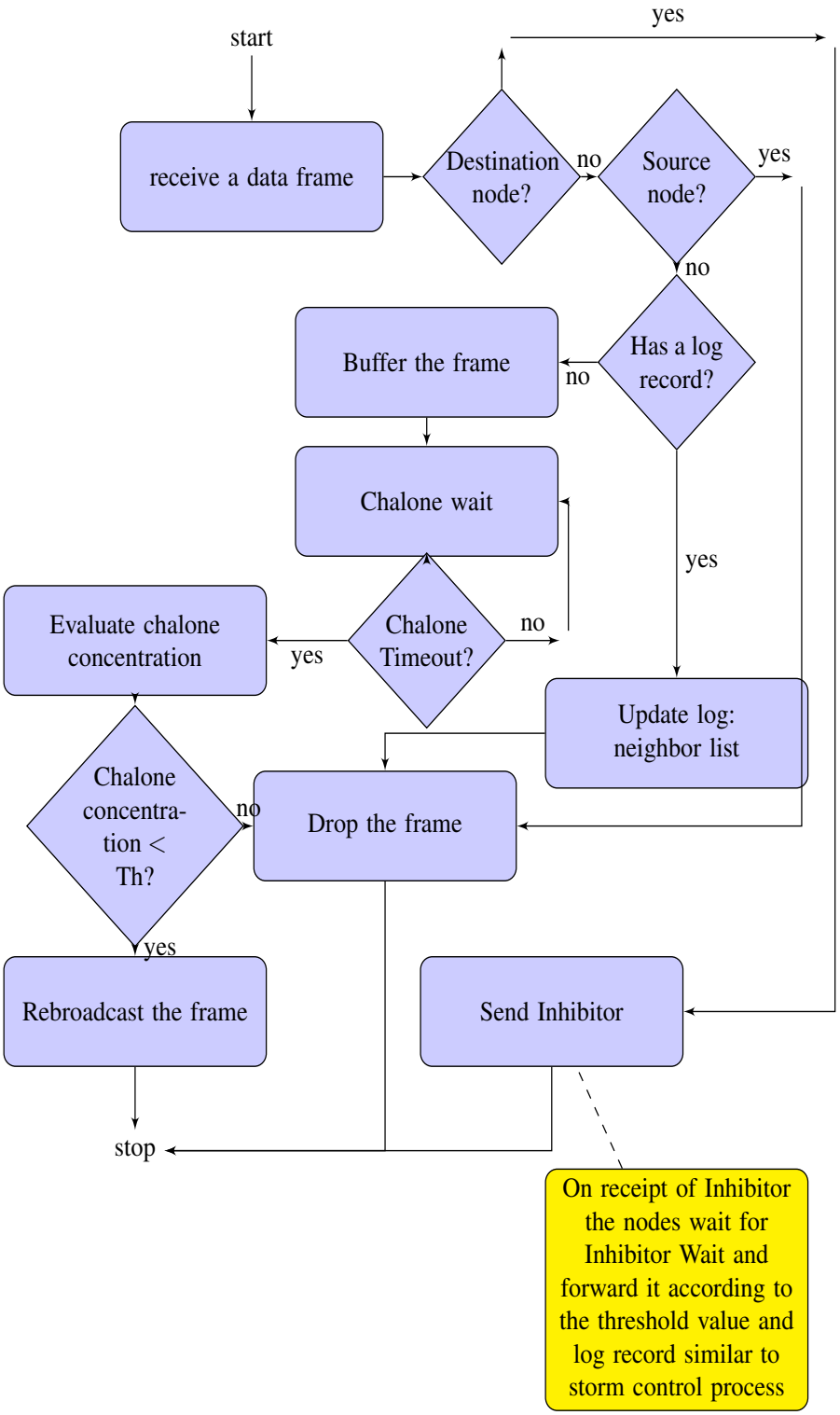

Figure 5.3: Event flow at a receipt of a data frame by a node

time stamp	source MAC	destination MAC	seq number	data state	inhibitor state	inhibitor count	neighbor list

Figure 5.4: Log format

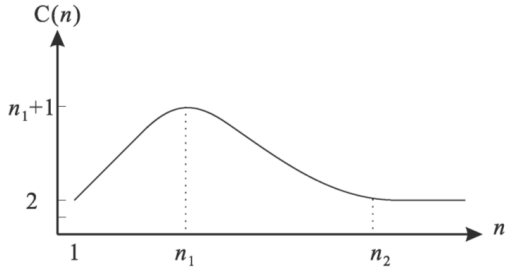

Figure 5.5: Abstract shape of threshold function proposed in [69]

Chalone threshold

Chalone threshold should be an optimal value for not to cause too many redundant rebroadcasts and for the frame to be able to reach the destination. Threshold depends on the node density [69] and an adaptive counter-based flooding mechanism is proposed where the threshold is a function of the size of neighborhood. According to [69] the lowest possible threshold is 2 and the highest possible is n+1. An abstract shape for threshold function $C(n)$ is suggested as in Figure 5.5. When n is small the threshold should be larger and for larger n threshold should be smaller. Exact shape of $C(n)$ is derived using an experiment in [69].

The threshold can also be attached to a probability of rebroadcasting a received data frame. A dynamic probabilistic flooding scheme is proposed in [135]. According to [104] and [136] there exists a threshold probability $P_c < 1$ such that all nodes in an unpartitioned MANET can be reached and there will not be a considerable improvement in reachability with $P > P_c$. P_c should be higher for sparse networks and lower for dense networks. Zhang and Agrawal [135] analyze time complexity of their dynamic probabilistic flooding mechanism using a set of recursive equations that involve the total number of nodes that receive a data frame, the number of nodes that receive the frame at the i_{th} time slot and ready to rebroadcast and the number of nodes that actually rebroadcast the frame at the i_{th} time slot. They start with a simple example network

and generalize the results.

The threshold should set to an initial value and then should adapt to the frame count according to a suitable function. They should also have an upper limit. According to [69] only a few rebroadcasts can be saved by setting the threshold >6 in sparse networks.

Inhibitor wait

Inhibitor wait should be less than the *chalone wait* to make sure that the inhibitor is adequately fast to catch the flooding wave that propagates beyond the destination. It is also advisable to predict and initiate the inhibition process earlier rather than waiting until the destination is reached.

Data buffer

According to Figure 5.3 data frames should be buffered until a decision is made whether to rebroadcast or discard it. Time duration for buffering the frame and how the buffer should be maintained depends on a number of factors. For example, a frame should be kept in the buffer at least for chalone wait time added with some processing overhead time.

Frame log

A log record of a frame should reside in a log of a node for a maximum period of time equals to the lifetime of the frame. Lifetime of a frame in the case of unicast is only until it is delivered to the destination. Therefore, the longest lifetime of a log record is the time taken by a frame to travel from one end to the other end of a network with all the delays included. Hence the lifetime of a log record depends both on the diameter of the network in terms of the number of hops and waiting times at each hop. Details of the fields of a log record shown in Figure 5.4 are as follows:

Frame ID is the combination of source MAC, destination MAC and the sequence number. A unicast data frame is uniquely identified by a Frame ID and its correspond-

ing inhibitor also carries Frame ID.

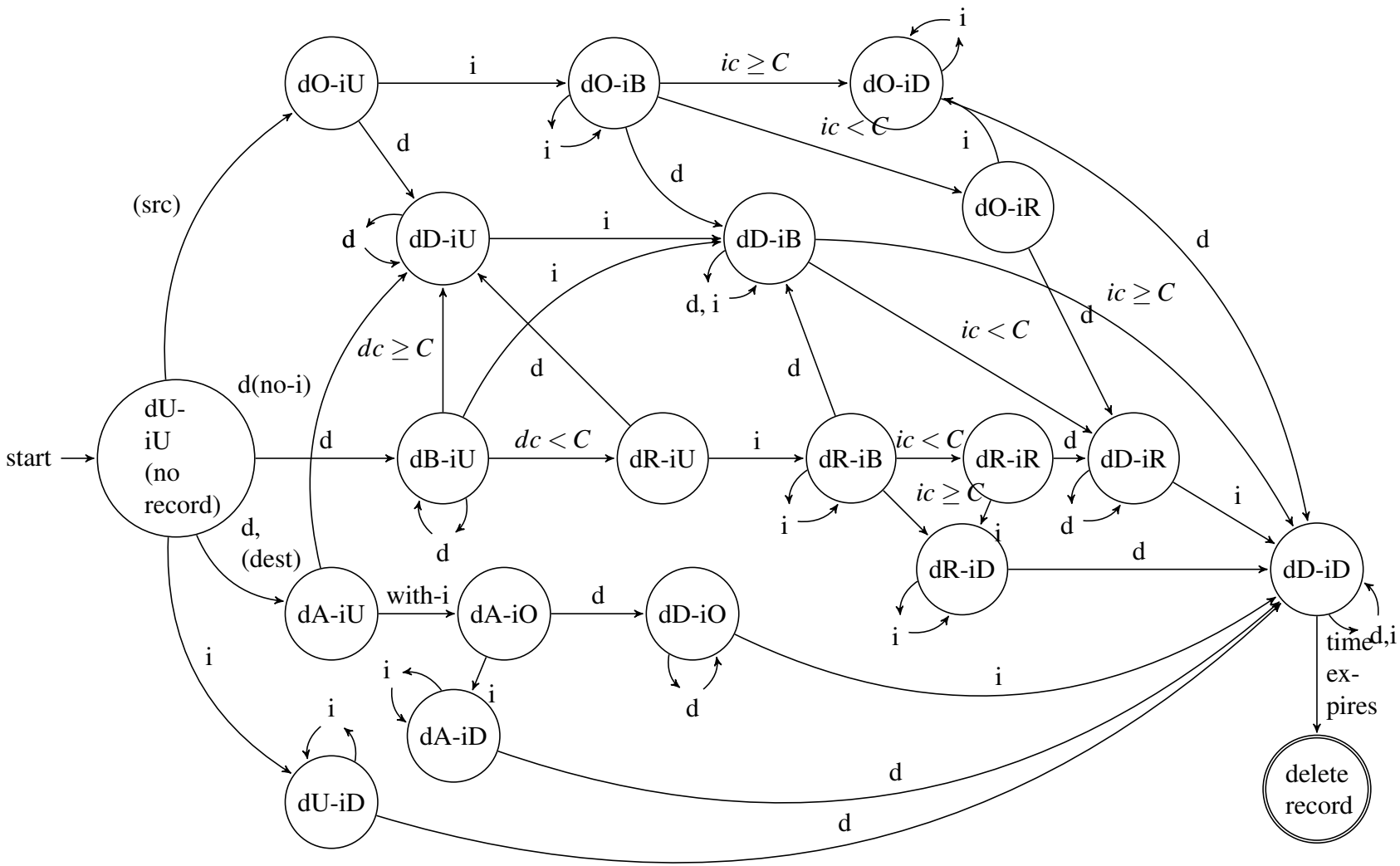

Figure 5.6: State diagram for the protocol (d-data, i-inhibitor, U-unknown, O-originated, B-buffered, R-rebroadcast, D-discarded, A-accepted, c-concentration, C-threshold)

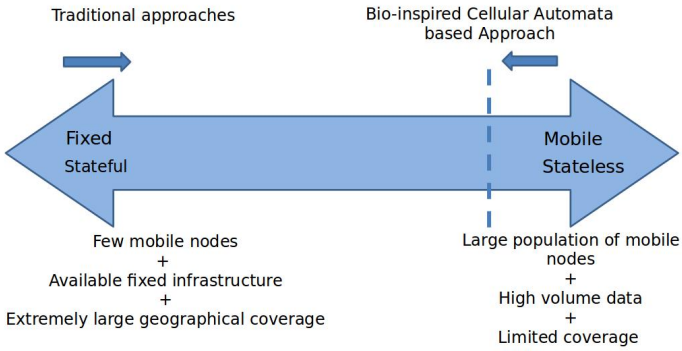

Figure 5.7: Summary of comparison of our routing approach with reference to fixed stateful and mobile-stateless routing paradigms

Data state carries one of the states shown in state transition diagram in Figure 5.6. An incoming data frame from the physical layer will be buffered when it is received for the first time and will be discarded when it is received subsequently. When redundant frames are received while the frame is in data buffer the neighbor list in the log record will be updated before discarding the frame. When the frame is no longer in the buffer so that it is finished with processing the redundant frames will be silently discarded.

Inhibitor state carries one of the states shown in state transition diagram in Figure 5.6. Similar to the data frames, the inhibitors incoming from the physical layer are either buffered or discarded. While an inhibitor is already in the buffer subsequently received inhibitors result in an increment in the inhibitor count before getting discarded. If an inhibitor is completely processed according to the log and no longer resides in the buffer, redundant inhibitors are silently discarded.

The cost of maintaining a frame log is comparable to cost of performing simple flooding apart from the addition of few more bits into the record. In simple flooding a node has to record the source address and the sequence number in a log for checking whether subsequently received frames are duplicates.

5.4 Summary

We proposed a unicast protocol for MANETs based on simple flooding but reduces redundant rebroadcasts by a counter based mechanism inspired by the chalone mechanism in biological organ growth. The nodes simply maintains a message log which is totally local to the node and does not perform any beaconing or neighbor information gathering. Hence our protocol is based on the mobile-stateless extreme of the routing paradigms. However, it should be placed slightly towards the stateful side due to the maintenance of local states in the form of a message log as shown in Figure 5.7.

CHAPTER VI

ANALYTICAL MODEL FOR THE PROTOCOL

6.1 Introduction

In this chapter, we develop an analytical model to analyze endcast schemes based on Viswanath-Obraczka [2] model. According to Viswanath-Obraczka model, probabilistic flooding can be modeled by the tree-structured graph in Figure 6.1 as previously discussed in Section 3.2.1

The total number of nodes reached by probabilistic flooding is estimated using Equation 6.1 in Viswanath-Obraczka model. Here, N_T is the total number of nodes that receive the transmission of S in Figure 6.1, l is the transmission level, N is the

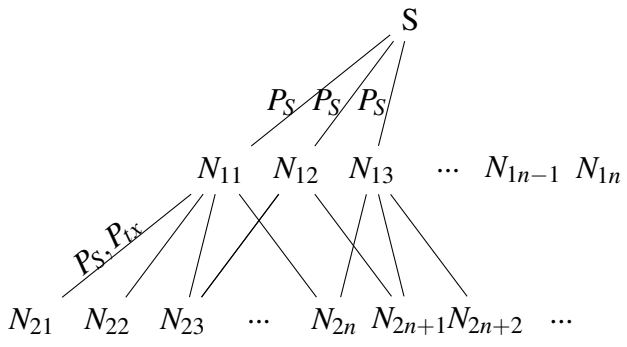

Figure 6.1: Data propagation in probabilistic flooding

number of nodes within a transmission region, β is the expected increase in the coverage area achieved by the second level retransmission, P_S is the probability of successful transmission, P_b is the probability of successful reception and P_{tx} is the probability of rebroadcasting in probabilistic flooding. The process of deriving Equation 6.1 is presented in detail in Section 6.2.

$$N_T = P_S N + P_S N \sum_{i=1}^{l-1} (\beta P_{tx} P_b N)^i \tag{6.1}$$

The parameter P_{tx} in Equation 6.1 can be modified according to the flooding scheme used in endcast. The probability P_S can represent the node to node transmission characteristics including the impact of mobility on wireless links apart from CSMA hidden terminal problem modeled in Viswanath-Obraczka model. In this chapter, we illustrate how the parameter P_{tx} is modified according to the parameters of the proposed endcast scheme. Further, we improve the method of estimating parameter β.

The proposed endcast scheme consists of counter based threshold driven flooding. The aspects that should be modeled include the followings:

- Propagation of flooding messages as a *flooding wave* as previously explained in Section 4.2 (Figure 4.2)
- Counter value and the threshold value
- Effect of mobility on the propagation of flooding wave
- Effect of realistic wireless conditions such as hidden terminal problem

6.2 Modeling of probabilistic flooding with Viswanath-Obraczka model

As previously explained in Section 3.7.2 we selected Viswanath-Obraczka model because of its ability to model hidden terminal problem of CSMA, reachability of multihop flooding and probabilistic flooding (Table 3.9). As explained in Section 3.5 we have selected IEEE 802.11 DCF as the underlying MAC protocol and it is a Carrier

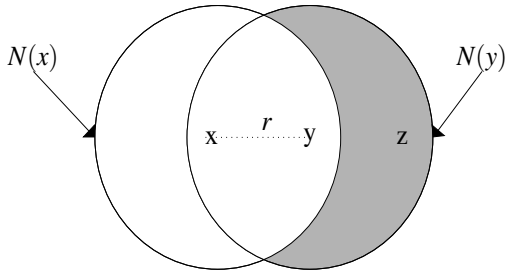

Figure 6.2: Illustration of hidden node problem [4]

Sense Multiple Access (CSMA) protocol. Flooding happens in terms of node level broadcasts at the MAC layer, thus there is no RTS-CTS mechanism used for collision avoidance in IEEE 802.11 MAC. Therefore, MAC protocol is basically the non-persistent CSMA.

6.2.1 Modeling node-to-node transmission on CSMA MAC

The critical problem in multihop communication using CSMA is the hidden terminal problem [2, 92, 87, 89, 90, 91]. Viswanath-Obraczka captures the effect of hidden terminal problem by the parameter P_S that denotes the probability of successful transmission and the properties of CSMA are incorporated in deriving P_S as explained in this section.

Consider the scenario in Figure 6.2 for illustrating the hidden terminal problem. Node y is in the hearing region of x denoted by $N(x)$. Node z is in the hearing region of y denoted by $N(y)$ but not in $N(x)$. Therefore, x is unable to detect any communication from z to y. Therefore, node z is a hidden terminal for a transmission from x to y.

Modeling hidden terminal problem in CSMA Viswanath-Obraczka model captures the hidden terminal problem in its node-to-node transmission model as proposed by Wu and Varshney [92], which is a Markov chain model. A. A. Markov in trying to statistically investigate text in Pushkin's poetry came up with a complex chain scheme which was later known as Markov chain [137]. Basic results of Markov processes are as follows [92] for the convenience of referring to CSMA MAC model:

Definition 1: If a stochastic process $\{X(t), t \in (0,\infty\}$ with state space $E = \{0,1,2,...\}$ has some points in time at which the process restarts itself then it is called a regenerative process. For such a regenerative process there exists a time T after which the process is a probabilistic replica of the whole process. There exists a limiting probability that expresses the long run probability that the process is in a specific state, j.

$$P_j = \lim_{t\to\infty} P\{X(t) = j\}, j \in E \tag{6.2}$$

Theorem 1: for all $j \geq 0$;

$$P_j = \frac{E[\text{Amount of time in state j during a cycle}]}{E[\text{time of one cycle}]} \tag{6.3}$$

Definition 2: If the state transitions of a stochastic process happens according to a Markov chain and it is a regenerative process then the process is a Markov regenerative process.

Theorem 2: For a Markov regenerative process limiting probability P_j can be calculated as follows:

$$P_j = \frac{P(j)D_j}{\sum_i P(i)D_i} \tag{6.4}$$

where P_j is the long run proportion of transitions which are in to state j, D_j is the mean time spent in state j per cycle ($j-j$ transition) and the Markov chain is positive recurrent (i.e. if a state is revisited then the process is recurrent; if the time duration from first visit to the second visit is finite then it is a positive recurrent state) and irreducible (i.e. all states are in one class or communicate with each other) [138].

Markov chain model of node to node transmission Wu and Varshney [92] model the node to node transmission in the presence of hidden terminal problem as a Markov chain with three states. The three states are *idle state* (I), *successful transmission state* (S) and *collision transmission state* (C) as shown in Figure 6.3.

According to Figure 6.3 a node x leaves the state I with probability p' or remains in state I with probability $(1-p')$. Therefore:

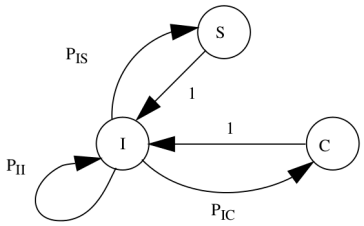

Figure 6.3: Three state Markov chain model of a node

$$P_{II} = 1 - p'$$

The following expression holds for steady state probabilities:

$$P(I) = P(I)P_{II} + P(C) + P(S)$$

The following equation also holds:

$$P(I) + P(C) + P(S) = 1$$

Therefore:

$$P(I) = P(I)P_{II} + 1 - P(I)$$

$$P(I) = \frac{1}{1+p'}$$

There are four conditions to be fulfilled for a successful transmission to happen from x to y in Figure 6.2. For describing these conditions following notations are used: When r is the distance between x and y, $C(r)$ is the area of the region $N(x) \cap N(y)$, $B(r)$ is the area of the region $N(y) - N(x)$ it is found in [89] that Equations 6.5, 6.6 and 6.7 can be used to estimate the areas $C(r)$ and $B(r)$.

Referring to [89];

$$C(r) = 2R^2 q\left(\frac{r}{2R}\right) \tag{6.5}$$

$$B(r) = \pi R^2 - 2R^2 q\left(\frac{r}{2R}\right) \tag{6.6}$$

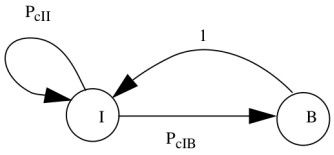

Figure 6.4: Two state Markov chain model of a channel

where

$$q(t) = arccos(t) - t\sqrt{1-t^2} \tag{6.7}$$

Further, it is required to refer to the operational details of CSMA to understand the conditions for a successful node-to-node transmission in CSMA.

Operational model of CSMA CSMA transmission is modeled as a Bernoulli process in [89]. A Bernoulli process is simply a sequence of coin flips with a consistently unfair coin which gives the outcome 1 with a probability p all the time. CSMA transmission is assumed to happen at discrete time slots of duration a and it takes τ number of such slots to complete a packet transmission. Nodes listen to the channel with a probability p and does not listen with a probability $(1-p)$. Therefore, the channel sensing behavior in a sequence of slots that can be modeled as a Bernoulli process [89].

Takagi and Kleinrock [89] also estimate the probability p' of actual transmission in a slot in terms of the channel sensing probability p as in Equation 6.8. Here P_{cI} is the probability that the channel is sensed to be idle.

$$p' = pP_{cI} \tag{6.8}$$

Wu and Varshney [92] determine P_{cI} using two state Markov chain model of the channel. The states are *busy* (denoted B) and *idle* (denoted I) as shown in Figure 6.4.

The channel of the node x, $CH(x)$ will transit from *idle* state to itself in the next time slot only if all its neighbors do not actually transmit during that slot. Hence the transition probability P_{cII} depends on the number of neighbors in the node's transmis-

sion range as in Equation 6.9. Here $\acute{p}$ is the probability of actual transmission during a time slot and the $p(i)$ is the probability of having i nodes in the neighborhood.

$$P_{cII} = \sum_{0}^{\infty} (1-\acute{p})^i p(i) \tag{6.9}$$

Steady state probability of state I is computed as follows because the only two ways that the process goes to state I is either from I to I with the probability P_{cII} or from B to I with the probability 1:

$$P_c(I) = P_c(I)P_{cII} + P_c(B)$$

Further, the following equation also holds for this two state Markov chain:

$$P_c(I) + P_c(B) = 1$$

Therefore;

$$P_c(I) = P_c(I)P_{cII} + (1 - P_c(I))$$

$$P_c(I) = \frac{1}{2 - P_{cII}}$$

According to the definition of limiting probability in Equation 6.4 the limiting probability that $CH(x)$ stays in state I is:

$$P_{cI} = \frac{D_I P_c(I)}{D_B P_c(B) + D_I P_c(I)} \tag{6.10}$$

Thereby $\acute{p}$ can be calculated using Equation 6.8.

Conditions for a successful node-to-node transmission in CSMA A transmission from node x to y that are r distance apart will be successful when x transmits in a slot, y does not transmit during that slot, nodes in $C(r)$ do not transmit during that slot and nodes in $B(r)$ do not transmit for $2\tau + 1$ slots. Therefore, the probability of node x having a transition from state I to S during a transmission from x to y (denoted by $P_{IS}(r)$) depends on all these conditions and it is a function of distance r between x and y. Each probability has to be calculated according to the node distribution.

$$P_{IS}(r) = \begin{cases} \text{Prob}(x \text{ transmits in a slot}). \\ \text{Prob}(y \text{ does not transmit in the same slor}|r). \\ \text{Prob(nodes in } C(r) \text{ region do not transmit in the same slot}|r). \\ \text{Prob(nodes in B(r)do not transmit in } 2\tau + 1\text{slots}|r) \end{cases} \tag{6.11}$$

The transition probability P_{IS} for node x is if the probability density function of the distance between x and y is given by $f(r)$:

$$P_{IS} = \int_0^R f(r) P_{IS}(r) dr \tag{6.12}$$

Also,

$$P(S) = P(I) P_{IS}$$

Limiting probability of successful transmission:

$$P_S = \frac{D_S P(S)}{D_S P(S) + D_I P(I) + D_C P(C)} \tag{6.13}$$

It is required to substitute the value of p' to obtain the solution for P_S in Equation 6.13 of Wu and Varshney [92]. The parameter p', in turn is obtained by solving Equation 6.10 for a given network scenario particularly for a specific node distribution.

An alternative definition for P_S is proposed by Shah-Mansouri et al. [139]. According to their reasoning, total time a channel is engaged in any state can be divided into three terms; time during which the channel is engaged in successful transmission (T_S), time in which channel is experiencing collisions (T_C) and the time during which the channel is idle. Accordingly, Shah-Mansouri et al. [139] define P_S as in Equation 6.14.

$$P_S = \frac{T_S}{T_S + T_C}$$

$$P_S = \frac{D_S P(S)}{D_S P(S) + D_C P(C)} \tag{6.14}$$

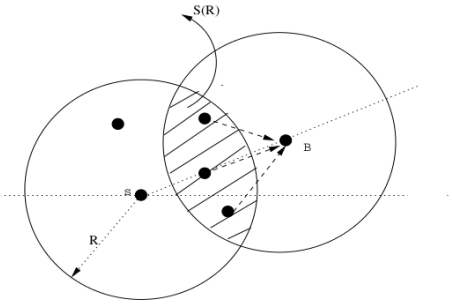

Figure 6.5: Second level retransmission

6.2.2 Modeling multihop transmission in flooding schemes

Viswanath and Obraczka [2] expand the work of Wu and Varshney [92] to determine the probability of CSMA's successful transmission in multihop flooding. They estimate the probability of successful reception of data by nodes in a MANET when the flooding wave passes through the network. The model assumes that the flooding wave terminates after each packet is retransmitted a maximum of l hops and l is determined by the diameter of the network. The *reachability* is given by the sum of nodes reached by each transmission.

According to Figure 6.5, S is the source. N is the average number of nodes in the S's transmission region. Probability of successful transmission by S to any one of its neighbors is P_S given by Equation 6.13.

The event of exactly N_S number of neighbors successfully receive the transmission from S, is modeled by Binomial probability distribution as given by Equation 6.15.

$$P(N_S) = \binom{N}{N_S} P_S^{N_S}(1-P_S)^{N-N_S} \tag{6.15}$$

$$\bar{N_S} = E[N_S] = P_S N$$

$\bar{N_S}$ is the number of neighboring nodes that will retransmit the received data. Out of these $\bar{N_S}$ nodes only the retransmissions of those nodes in the region $S(R)$ will reach node B. Number of nodes in the region $S(R)$ is denoted by N_b.

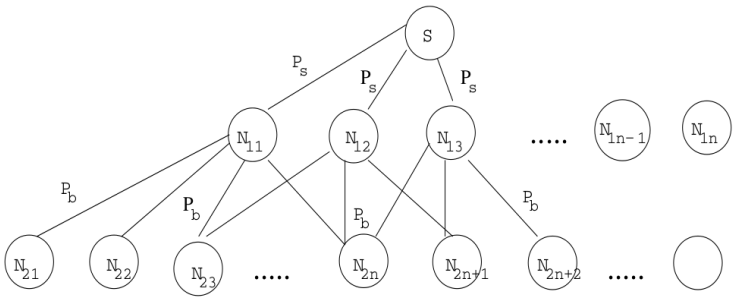

Figure 6.6: First two retransmissions of flooding

$$N_b = \frac{S(R)}{\pi R^2}\bar{N_S}$$

$$\bar{N_b} = E[N_b]$$

$$P_b = P(\text{B receives at least one copy of data}/\bar{N_b}\text{ nodes transmit})$$

The probability of successful reception at any retransmission level is P_b.

Reachability of Flooding: The above analysis is then extended to l levels of retransmissions. The number of nodes reached by the transmission of the source is N_1 given by:

$$N_1 = P_S N$$

N_2 is the number of nodes newly reached by the second transmission and it is given by:

$$N_2 = \beta P_b N N_1$$

$$N_2 = \beta P_b N P_S N$$

Here β is the expected percentage increase in the coverage of nodes as the second transmission will have a significant overlap with nodes covered by the first transmission.

$$N_3 = (\beta P_b N)^2 P_S N$$

Similarly,

$$N_l = (\beta P_b N)^{l-1} P_S N$$

Therefore, the reachability of flooding is:

$$N_T = \sum_{i=1}^{l} N_i$$

$$N_T = P_S N + P_S N \sum_{i=1}^{l-1} (\beta P_b N)^i$$

Modeling probabilistic flooding Viswanath-Obraczka model also captures probabilistic flooding where a node receiving a frame for the first time is assumed to retransmit it with a probability P_{tx}. The probability of successful reception at any retransmission level is P_b.

$$P_b = P(\text{B receives at least one copy of data}/\bar{N_b} P_{tx} \text{ nodes transmit})$$

$$P_b = 1 - P(\text{B receives no copy}/\bar{N_b} P_{tx})$$

$$P_b = 1 - (1 - P_S)^{\bar{N_b} P_{tx}}$$

The number of nodes reached by the transmission of the source is N_1 given by:

$$N_1 = P_S N$$

N_2 is the number of nodes newly reached by the second transmission and it is given by:

$$N_2 = \beta P_{tx} P_b N N_1$$

Number of nodes newly reached by the l^{th} retransmission:

$$N_l = (\beta P_{tx} P_b N)^{l-1} P_S N$$

Therefore, the reachability is given by:

$$N_T = P_S N + P_S N \sum_{i=1}^{l-1} (\beta P_{tx} P_b N)^i$$

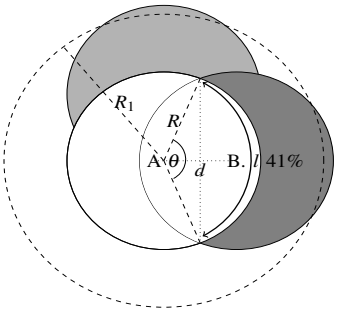

Figure 6.7: Estimating the average area covered by rebroadcasts

6.3 Proposed modifications to Viswanath-Obraczka model

Viswanath-Obraczka model uses $\beta = 41\%$, which is the average additional coverage when two transmission ranges overlap as found by Tseng et al. [4]. We modify the equation to capture the varying additional coverage areas at different rebroadcast levels in probabilistic flooding by replacing β by β_i as previously shown in Section 4.4 where i is the rebroadcast level. Further, we convert P_{tx} into a parameter that depends on *chalone concentration* (C) and *chalone threshold* (K) in such a way that $P_{tx} = P\{C < K\}$. Note that chalone concentration refers to the count of redundant frames and chalone threshold refers to the threshold in counter based flooding as described in Section 5.2 and these terms resemble the cell biological inspiration.

$$N_T = P_S N + P_S N \sum_{i=1}^{l-1} \beta_i (P\{C < K\} P_b N)^i \tag{6.16}$$

Additional coverage at each level of rebroadcast The parameter β_i is estimated using Equation 6.17. The additional area covered by each rebroadcast level b_i is given by Equation 6.18 as previously derived in Section 4.4. Equation 6.18 is based on the average additional area covered by rebroadcast of a single neighbor, which is $0.41\pi R^2$ [4]. For example, the average additional area b covered by all neighbors of A will be given by $0.41k\pi R^2$ if the maximum number of neighbors (highest node degree)

$deg_{max} \geq k$. Here k is the number of arc lengths that cover the circumference of A's radio range circle (Figure 6.7).

$$\beta_i = \frac{b_i}{\pi R^2}\% \tag{6.17}$$

$$b_i = \begin{cases} 0.41 k_i \pi R^2 & deg_{max} \geq k_i \\ 0.41 deg_{max} \pi R^2 & deg_{max} < k_i \end{cases} \tag{6.18}$$

As shown in Figure 6.7 the arc length l can be found by Equation 6.19.

$$l = 2R\cos^{-1}\frac{d}{2R} \tag{6.19}$$

$$k_1 = \frac{\pi}{\cos^{-1}\frac{d}{2R}} \tag{6.20}$$

$$k_i = \frac{\pi R_{i-1}}{R\cos^{-1}\frac{d}{2R}} \qquad i > 1 \tag{6.21}$$

Let A_{level1} be the area inside the dashed circle in Figure 6.7 and R_1 is the radius of the circle.

$$A_{level1} = \pi R^2 + b_1 \tag{6.22}$$

$$R_1 = \sqrt{\frac{A_{level1}}{\pi}} \tag{6.23}$$

$$C_{level1} = 2\pi R_{level1} \tag{6.24}$$

$$k_{level2} = \frac{\pi R_{level1}}{R\cos^{-1}\frac{d}{2R}} \tag{6.25}$$

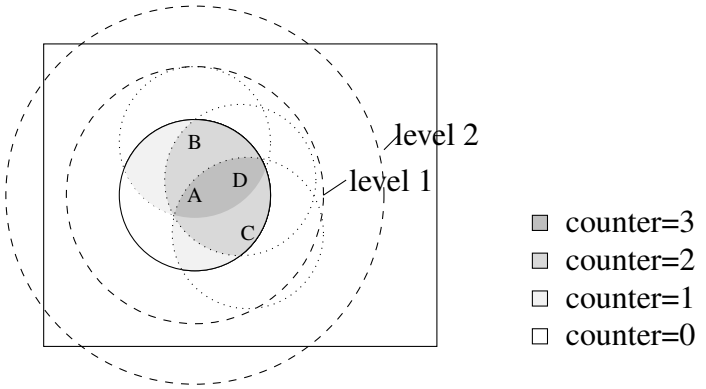

Figure 6.8: Geometric interpretation of counter based flooding

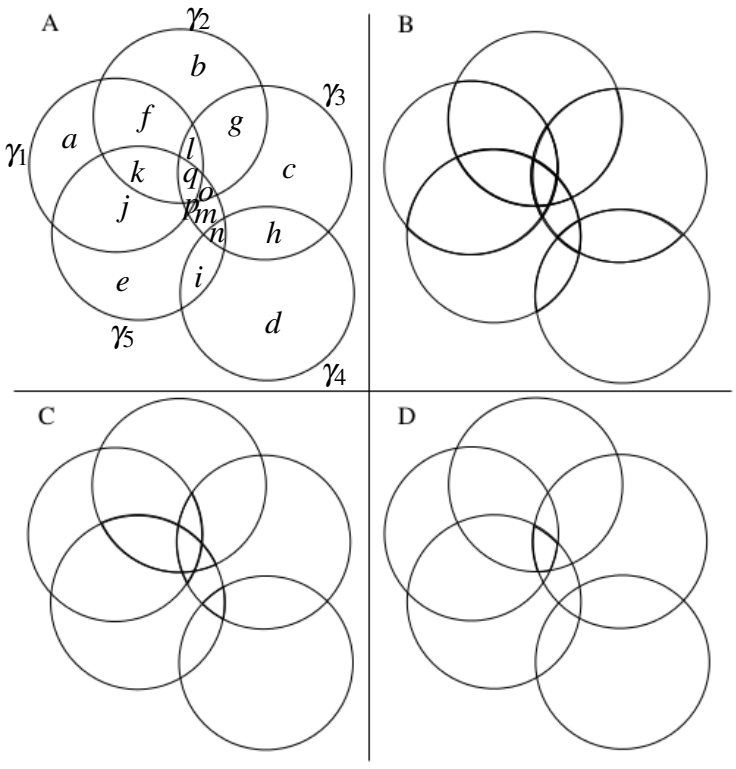

Figure 6.9: Illustration of first four steps in Librino algorithm for calculating area of five intersecting circles

6.3.1 Modeling the counter based flooding parameters

Mohammed et al. [140] derive rebroadcast probability as a function of neighborhood and counter values. We also identified that counter based flooding parameters can be interpreted as a probability of rebroadcasting. In the proposed counter based threshold driven endcast mechanism, a node will rebroadcast a received data frame when the number of copies of the same frame received during Chalone Wait (Chalone concentration) is less than a threshold (Chalone threshold). Therefore, we map the probability that the Chalone concentration is less than the Chalone threshold (K) to P_{tx} in Viswanath-Obraczka's probabilistic flooding model.

Chalone concentration C is a discrete random variable, which can be described by a probability mass function $f(c)$. Hence $P = P\{C < K\}$ is the cumulative distribution function $F(C)$. By the definition:

$$F(C) = \sum_{i=0}^{K} f(c)$$

In order to construct the probability mass function $f(c)$, it is required to find the probabilities that a node receive c number of copies of the same frame where $0 \leq c < N$ and N is the number of tentative rebroadcasting nodes. According to the analysis in Section 4.5, the probability that a node will record a particular counter value at a given time depends on the relative positions of the tentative rebroadcasters at that time. Consider the original broadcast of a frame by node A in Figure 6.8. The neighbors of A, namely, B, C, and D will receive this frame. Let all of them rebroadcast the frame then any node in the dark gray area will record a counter value of three as it receives from B, C, and D after receiving originally from A. Similarly, the white area in A's range receives only from A and records a counter value of zero, light gray area records a counter value of one and gray area records a counter value of two.

Probability $P\{C = c\}$ that a node records a particular counter value c is the set of points in the region that will be covered by c number of circles divided by all possible points in the region. This implies that the probability should be expressed in terms of areas as in Equation 6.26 where A_c denotes the intersection area of c circles and A_{reg} is the total area of the region in which the circles are deployed. The centers of the circles

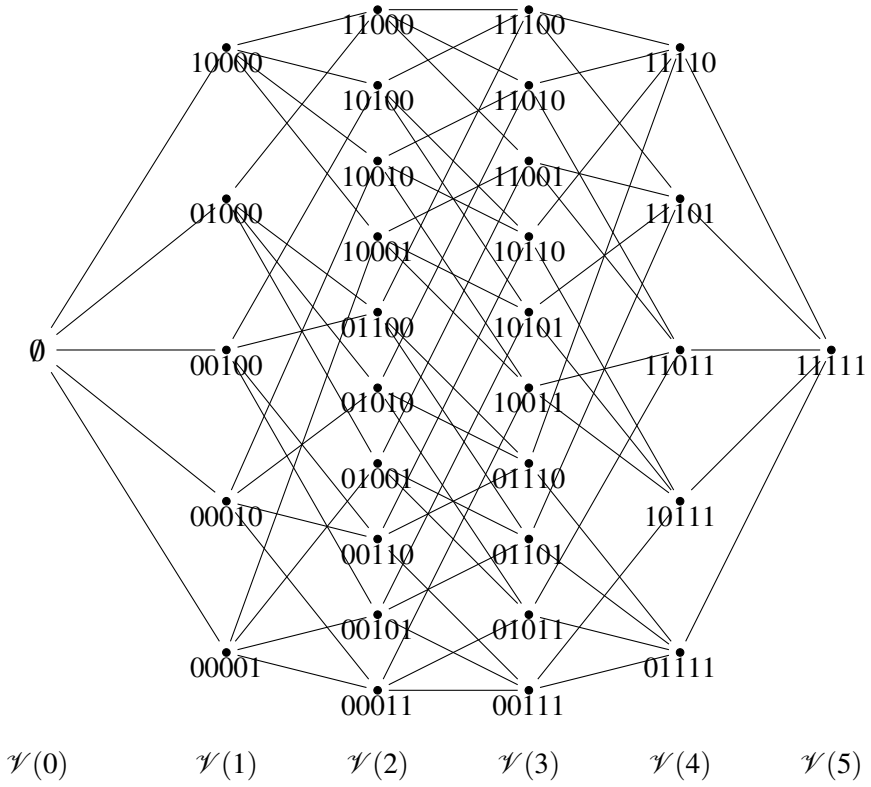

Figure 6.10: Trellis structure for sample five circles

are the potential rebroadcasters.

$$P\{C = c\} = \frac{A_c}{A_{reg}} \tag{6.26}$$

Calculating the area of intersection for more than three circles is considered practically unsolvable as a closed form expression because there are a huge number of possible configurations for how the circles can intersect [112] when the number of circles increases. Librino et al. [112] proposed an algorithm that iteratively computes the intersection area of an arbitrary number of circles.

We will follow the algorithm that we name *Librino algorithm* on the sample set of five circles in Figure 6.9. The aim is to find the areas of *exclusive intersection* that Librino et al. [112] define as the intersection of a certain subset of circles excluding the regions covered by the other circles in a set Z of circles. Set $\mathscr{E}$ of the exclusive intersections are a disjoint set and the elements of $\mathscr{E}$ for the sample set are denoted by

the letters a through q in Figure 6.9. Librino et al. define the set $\mathscr{I}$ that denotes all possible intersections including non exclusive intersections.

Librino algorithm

Step 1: Calculate the area of each circle (in our MANET scenario, the area of a circle is πR^2 as all the nodes have the same transmission range)

Step 2: Calculate the intersection area of any two circles (which can be calculated by the expression for area of intersection of two circles derived by Tseng et al. [4] or by Equation 4.16)

Step 3: Calculate the intersection area of triplet of circles (which can be found using the method proposed by Fewell [141], in which the intersection is perceived as a *circular triangle* defined as a triangle with circular arcs for its sides)

Step 4: Calculate the area of intersection of n number of circles where $3 < n \leq N_c$ by algebraic manipulation of the areas calculated in above steps. Here, N_c is the number of circles. The existence and the area of intersections are recorded as a tree for tracking.

The tree built in Step 4 above is a *Trellis structure* given by set $\mathscr{V}$ of vertices with each vertex representing an intersection of circles. Vertices are divided into subsets $\mathscr{V}(n)$ with $n = 1,2,...,N_c$ where $\mathscr{V}(n)$ represents a set of all the intersections among n circles out of N_c. The subsets are ordered from $\mathscr{V}(1)$ through $\mathscr{V}(N_c)$ and an edge can connect only vertices of two consecutive subsets $\mathscr{V}(n)$ and $\mathscr{V}(n+1)$ iff $\mathscr{S}(j) \subset \mathscr{S}(i)$. A vertex i is also uniquely labelled using a sequence of N_c bits ($b_i = b_1^i b_2^i ... b_{N_c}^i$) with each bit representing a circle in the set of N_c circles. The Trellis structure corresponding to the example in Figure 6.9 is given in Figure 6.10.

The edges are drawn according to $N_c - 1$ binary transition matrices $M_{n,n+1}^{(N_c)}$ and the properties of the matrices are as follows:

1. $M_{0,1}^{(N_c)}$ is an $N_c \times 1$ matrix with all the elements are 1's

2. $M^{(N_c)}_{n,n+1}$ is a $p \times q$ matrix is For $1 \leq n < N_c$, where

$$p = \binom{N_c}{n+1}, q = \binom{N_c}{n}$$

3. Following recursion should be followed with $N_c = N_c - 1$ at each iteration.The recursion ends when we get a zero sized matrix after some number of iteration.

$$M^{(N_c)}_{n,n+1} = \begin{pmatrix} M^{(N_c-1)}_{n-1,n} & I \\ 0 & M^{(N_c-1)}_{n,n+1} \end{pmatrix} \tag{6.27}$$

4. There exists an edge between element i in set $\mathscr{V}(n+1)$ and element j in set $\mathscr{V}(n)$ if $M^{(N_c)}_{n,n+1}(i,j) = 1$ when the elements are ordered according to the decreasing values of their binary label

5. If $n \geq \lceil \frac{N_c}{2} \rceil$ then $M^{(N_c)}_{n,n+1} = (M^{(N_c)}_{N_c-n-1,N_c-n})^c$ where ^{c} indicates the transposition along the secondary diagonal given by transposing element (i,j) by element $(q-j+1, p-i+1)$. Therefore, transition matrices should be calculated using Equation 6.27 only until $N_c - 1 = n+1$.

6. To obtain which set of vertices in $\mathscr{V}(n)$ are connected to vertices in $\mathscr{V}(n+k)$ with $k > 1$ the transition matrix between $\mathscr{V}(n)$ and $\mathscr{V}(n+k)$ is defined as

$$M^{(N_c)}_{n,n+k} = \frac{1}{k!} \prod_{i=0}^{k-1} M^{(N_c)}_{n+k-i-1,n+k-i} \tag{6.28}$$

Accordingly, for the sample set of five circles in Figure 6.9, $M^{(5)}_{(0,1)}$ is a column matrix with all the five elements are 1s. $M^{(5)}_{(1,2)}$ is a 10×5 matrix ($\binom{5}{2} \times \binom{5}{1}$) and calculated according to property 3 above.

$$M^{(5)}_{(0,1)} = \begin{pmatrix} 1 \\ 1 \\ 1 \\ 1 \\ 1 \end{pmatrix}$$

$$M^{(5)}_{(1,2)} = \begin{pmatrix} M^{(4)}_{0,1} & I \\ 0 & M^{(4)}_{1,2} \end{pmatrix} \quad M^{(4)}_{(1,2)} = \begin{pmatrix} M^{(3)}_{0,1} & I \\ 0 & M^{(3)}_{1,2} \end{pmatrix} \quad M^{(3)}_{(1,2)} = \begin{pmatrix} M^{(2)}_{0,1} & I \\ 0 & M^{(2)}_{1,2} \end{pmatrix}$$

Size of $M_{1,2}^{(2)}$ is $\binom{2}{2} \times \binom{2}{1}$ which is a 1×1 matrix so that the iteration ends after calculating $M_{1,2}^{(2)}$. From Equation 6.27 $\binom{3}{2} \times \binom{3}{1}$ matrix $M_{1,2}^{(3)}$, $\binom{4}{2} \times \binom{4}{1}$ matrix $M_{1,2}^{(4)}$, and $\binom{5}{2} \times \binom{5}{1}$ matrix $M_{1,2}^{(5)}$ are obtained:

$$M_{1,2}^{(2)} = \begin{pmatrix} 1 \end{pmatrix} M_{1,2}^{(3)} = \begin{pmatrix} 1 & 1 & 0 \\ 1 & 0 & 1 \\ 0 & 1 & 1 \end{pmatrix} M_{1,2}^{(4)} = \begin{pmatrix} 1 & 1 & 0 & 0 \\ 1 & 0 & 1 & 0 \\ 1 & 0 & 0 & 1 \\ 0 & 1 & 1 & 0 \\ 0 & 1 & 0 & 1 \\ 0 & 0 & 1 & 1 \end{pmatrix}$$

$$M_{1,2}^{(5)} = \begin{pmatrix} 1 & 1 & 0 & 0 & 0 \\ 1 & 0 & 1 & 0 & 0 \\ 1 & 0 & 0 & 1 & 0 \\ 1 & 0 & 0 & 0 & 1 \\ 0 & 1 & 1 & 0 & 0 \\ 0 & 1 & 0 & 1 & 0 \\ 0 & 1 & 0 & 0 & 1 \\ 0 & 0 & 1 & 1 & 0 \\ 0 & 0 & 1 & 0 & 1 \\ 0 & 0 & 0 & 1 & 1 \end{pmatrix}$$

The edges from set $\mathscr{V}(1)$ to $\mathscr{V}(2)$ in the Trellis in Figure 6.10 are drawn by referring to $M_{1,2}^{(5)}$ in such a way that there exists an edge between element i in set $\mathscr{V}(2)$ and element j in set $\mathscr{V}(1)$ if $M_{1,2}^{(5)}(i,j) = 1$. For example there is an edge between last element in $\mathscr{V}(2)$ and the last element in $\mathscr{V}(1)$ because the last element in $M_{1,2}^{(5)}$ is 1.

For the given example of five circles, $\lceil \frac{N_c}{2} \rceil = 3$. Therefore from property 5 above, $M_{3,4}^{(5)} = (M_{1,2}^{(5)})^c$. Since $p = 10, q = 5$ elements (i,j) should be exchanged with $(6 -$

$j, 11-i$). Accordingly:

$$M_{3,4}^{(5)} = \begin{pmatrix} 1 & 1 & 0 & 1 & 0 & 0 & 1 & 0 & 0 & 0 \\ 1 & 0 & 1 & 0 & 1 & 0 & 0 & 1 & 0 & 0 \\ 0 & 1 & 1 & 0 & 0 & 1 & 0 & 0 & 1 & 0 \\ 0 & 0 & 0 & 1 & 1 & 1 & 0 & 0 & 0 & 1 \\ 0 & 0 & 0 & 0 & 0 & 0 & 1 & 1 & 1 & 1 \end{pmatrix}$$

Computation of the intersection areas - Librino algorithm continued

(Steps 1 to 4 perform the tasks of calculating area of intersection up to three circles and then building the Trellis structure for the intersection areas among many circles as described above)

Step 5: Initialize the auxiliary variable L_n, which is the vector containing the decimal labels of all the elements in set $\mathscr{V}(n)$, E_n which is the vector containing existence of an intersection, vectors r containing radii, x_c and y_c containing co-ordinates of the centers of the circles, and matrix D containing distances among the centers.

$$L_n = \frac{1}{n-1} M_{n-1,n} L_{n-1} \tag{6.29}$$

For the sample five circles we first initialize vectors L_n as follows.$L_1 = \{16, 8, 4, 2, 1\}$ and using Equation 6.29 $L2$ is obtained by:

$$L_2 = M_{1,2}^{(5)} L1 = \begin{pmatrix} 1 & 1 & 0 & 0 & 0 \\ 1 & 0 & 1 & 0 & 0 \\ 1 & 0 & 0 & 1 & 0 \\ 1 & 0 & 0 & 0 & 1 \\ 0 & 1 & 1 & 0 & 0 \\ 0 & 1 & 0 & 1 & 0 \\ 0 & 1 & 0 & 0 & 1 \\ 0 & 0 & 1 & 1 & 0 \\ 0 & 0 & 1 & 0 & 1 \\ 0 & 0 & 0 & 1 & 1 \end{pmatrix} \begin{pmatrix} 16 \\ 8 \\ 4 \\ 2 \\ 1 \end{pmatrix} = \begin{pmatrix} 24 \\ 20 \\ 18 \\ 17 \\ 12 \\ 10 \\ 9 \\ 6 \\ 5 \\ 3 \end{pmatrix}$$

Similarly, $L_3 = \{28,26,25,22,21,19,14,13,11,7\}$, $L_4 = \{30,29,27,23,15\}$, $L_5 = \{31\}$.

E_n vectors are also initialized as follows: E_1 has 5 elements each of which will be 1 as none of the vertices in $\mathscr{V}(1)$ is empty. According to Librino et al. we have to do an additional check for up to two circles and modify the existence matrix in such a way that the elements are 1 only when there exists an intersection. For instance, in the example there is no intersection between circles γ_1 and γ_4 therefore the vertex labelled 10010 in $\mathscr{V}(2)$ should not have edges coming from 10000 and 00010 in $\mathscr{V}(1)$. Similarly, there is no intersection between circles γ_2 and γ_4 also that result in 0 in the 6^{th} element in E_2.

$$E_1 = \begin{pmatrix} 1 \\ 1 \\ 1 \\ 1 \\ 1 \end{pmatrix}$$

$$E_{n+1} = max[M_{n,n+1}E_n - n, 0]$$

$$E_2 = M_{1,2}^{(5)}E_1 = \begin{pmatrix} 1 & 1 & 0 & 0 & 0 \\ 1 & 0 & 1 & 0 & 0 \\ 1 & 0 & 0 & 1 & 0 \\ 1 & 0 & 0 & 0 & 1 \\ 0 & 1 & 1 & 0 & 0 \\ 0 & 1 & 0 & 1 & 0 \\ 0 & 1 & 0 & 0 & 1 \\ 0 & 0 & 1 & 1 & 0 \\ 0 & 0 & 1 & 0 & 1 \\ 0 & 0 & 0 & 1 & 1 \end{pmatrix} \begin{pmatrix} 1 \\ 1 \\ 1 \\ 1 \\ 1 \end{pmatrix} = \begin{pmatrix} 1 \\ 1 \\ 1 \\ 1 \\ 1 \\ 1 \\ 1 \\ 1 \\ 1 \\ 1 \end{pmatrix} => \begin{pmatrix} 1 \\ 1 \\ 0 \\ 1 \\ 1 \\ 0 \\ 1 \\ 1 \\ 1 \\ 1 \end{pmatrix}$$

$$E_3 = max[M_{2,3}E_2 - 2, 0] = \begin{pmatrix} 1 & 1 & 0 & 0 & 1 & 0 & 0 & 0 & 0 & 0 \\ 1 & 0 & 1 & 0 & 0 & 1 & 0 & 0 & 0 & 0 \\ 1 & 0 & 0 & 1 & 0 & 0 & 1 & 0 & 0 & 0 \\ 0 & 1 & 1 & 0 & 0 & 0 & 0 & 1 & 0 & 0 \\ 0 & 1 & 0 & 1 & 0 & 0 & 0 & 0 & 1 & 0 \\ 0 & 0 & 1 & 1 & 0 & 0 & 0 & 0 & 0 & 1 \\ 0 & 0 & 0 & 0 & 1 & 1 & 0 & 1 & 0 & 0 \\ 0 & 0 & 0 & 0 & 1 & 0 & 1 & 0 & 1 & 0 \\ 0 & 0 & 0 & 0 & 0 & 1 & 1 & 0 & 0 & 1 \\ 0 & 0 & 0 & 0 & 0 & 0 & 0 & 1 & 1 & 1 \end{pmatrix} \begin{pmatrix} 1 \\ 1 \\ 0 \\ 1 \\ 1 \\ 0 \\ 1 \\ 1 \\ 1 \\ 1 \end{pmatrix} = \begin{pmatrix} 1 \\ 0 \\ 1 \\ 0 \\ 1 \\ 0 \\ 0 \\ 1 \\ 0 \\ 1 \end{pmatrix}$$

$$E_4 = max[M_{3,4}E_3 - 3, 0] = \begin{pmatrix} 1 & 1 & 0 & 1 & 0 & 0 & 1 & 0 & 0 & 0 \\ 1 & 0 & 1 & 0 & 1 & 0 & 0 & 1 & 0 & 0 \\ 0 & 1 & 1 & 0 & 0 & 1 & 0 & 0 & 1 & 0 \\ 0 & 0 & 0 & 1 & 1 & 1 & 0 & 0 & 0 & 1 \\ 0 & 0 & 0 & 0 & 0 & 0 & 1 & 1 & 1 & 1 \end{pmatrix} \begin{pmatrix} 1 \\ 0 \\ 1 \\ 0 \\ 1 \\ 0 \\ 0 \\ 1 \\ 0 \\ 1 \end{pmatrix} = \begin{pmatrix} 0 \\ 1 \\ 0 \\ 0 \\ 0 \end{pmatrix}$$

Area vector A_n contains the values of all the intersection areas and it is a column vector with $\binom{N_c}{n}$ elements. The elements corresponding to non existing areas are set to 0. Referring to Figure 6.9 we get area vectors as:

Table 6.1: Recursive calculation of intersection areas

i	$\hat{A}_i$	$N_c - 1$	**expression**	**expanded expression**
1	$\hat{A}_1$	4	$A_1 - \sum_j^4 (-1)^j M_{1,j}^T A_j$	$A_1 - M_{1,2}^T A_2 + M_{1,3}^T A_3 - M_{1,4}^T A_4$
2	$\hat{A}_2$	4	$A_2 - \sum_j^4 (-1)^{j-1} M_{2,j}^T A_j$	$A_2 - M_{2,3}^T A_3 + M_{2,4}^T A_4$
3	$\hat{A}_3$	4	$A_3 - \sum_j^4 (-1)^{j-2} M_{3,j}^T A_j$	$A_3 - M_{3,4}^T A_4$
4	$\hat{A}_4$	4	A_4	-

$$A_1 = \begin{pmatrix} \pi R^2 \\ \pi R^2 \\ \pi R^2 \\ \pi R^2 \\ \pi R^2 \end{pmatrix} \quad A_2 = \begin{pmatrix} l+q+k+f \\ l+p+q \\ 0 \\ p+q+k+j \\ o+q+l+g \\ 0 \\ k+o+q \\ n+h \\ m+n+o+p+q \\ n+i \end{pmatrix} \quad A_3 = \begin{pmatrix} l+q \\ 0 \\ k+q \\ 0 \\ p+q \\ 0 \\ 0 \\ o+q \\ 0 \\ n \end{pmatrix} \quad A_4 = \begin{pmatrix} 0 \\ q \\ 0 \\ 0 \\ 0 \end{pmatrix}$$

$$\hat{A}_i = \begin{cases} A_i - \sum_{j=i+1}^{N_c-1} (-1)^{j-i+1} M_{i,j}^T A_j & i < N_c - 1 \\ A_i & i = N_c - 1 \end{cases} \tag{6.30}$$

For the sample five circles the calculation of $\hat{A}_n$ is given in Table 6.1.

Using the Equation 6.28 we get $M_{i,j}$ matrices:

$$M_{1,3} = \frac{1}{2!}(M_{2,3} \times M_{1,2}) = \begin{pmatrix} 1 & 1 & 1 & 0 & 0 \\ 1 & 1 & 0 & 1 & 0 \\ 1 & 1 & 0 & 0 & 1 \\ 1 & 0 & 1 & 1 & 0 \\ 1 & 0 & 1 & 0 & 1 \\ 1 & 0 & 0 & 1 & 1 \\ 0 & 1 & 1 & 1 & 0 \\ 0 & 1 & 1 & 0 & 1 \\ 0 & 1 & 0 & 1 & 1 \\ 0 & 0 & 1 & 1 & 1 \end{pmatrix}$$

$$M_{1,4} = \frac{2!}{3!}(M_{3,4} \times M_{1,3}) = \begin{pmatrix} 1 & 1 & 1 & 1 & 0 \\ 1 & 1 & 1 & 0 & 1 \\ 1 & 1 & 0 & 1 & 1 \\ 1 & 0 & 1 & 1 & 1 \\ 0 & 1 & 1 & 1 & 1 \end{pmatrix}$$

Similarly, $\hat{A}_n$ were:

$$\hat{A}_1 = \begin{pmatrix} \pi R^2 - f - j - k - l - p - q \\ \pi R^2 - f - g - k - l - o - q \\ \pi R^2 - g - h - l - m - n - o - p - q \\ \pi R^2 - h - i - n \\ \pi R^2 - i - j - k - m - n - o - p - q \end{pmatrix} \quad \hat{A}_2 = \begin{pmatrix} f \\ 0 \\ 0 \\ j \\ g \\ 0 \\ 0 \\ h \\ m \\ i \end{pmatrix} \quad \hat{A}_3 = \begin{pmatrix} l \\ 0 \\ k \\ 0 \\ p \\ 0 \\ 0 \\ o \\ 0 \\ n \end{pmatrix} \quad \hat{A}_4 = \begin{pmatrix} 0 \\ q \\ 0 \\ 0 \\ 0 \end{pmatrix}$$

It is observed that $\hat{A}_1$ gives the area where each circle has no overlap with any other circle, $\hat{A}_2$ gives the area where two circles overlap and so on. The calculations correctly match with the observation in Figure 6.9.

Implication of Librino algorithm on counter based flooding in MANET When the source node broadcasts the frame, the neighbors in the circular region of the source receive and become tentative rebroadcasters at level 1. We can use the Librino algorithm above on the neighborhood of the source to find out the maximum counter value that will be experienced by nodes at different areas. For example, if the circles in Figure 6.9 are the communication regions of five rebroadcasting nodes in the first level of rebroadcast in a MANET, then there are four transmission regions that overlap in the area of size q. If a node that already has received the original transmission of the source resides in the area of size q then it receives four more frames from level 1 rebroadcast, thus the counter becomes four. The probability that a node resides in the region of size q resulting in counter $c = 4$ is $q/\pi R^2$. Similarly, the probability of recording counter values three is $(l+k+n+o+p)/\pi R^2$. This way we can estimate the probability of having each counter value in a given node placement which in turn depends on the application scenario.

6.3.2 Modeling node mobility

Section 6.3.1 presents how we modeled the counter based threshold driven flooding by modifying the parameter P_{tx} in Viswanath-Obraczka probabilistic flooding model. We replaced P_{tx} with $P\{C < K\}$ where C is the chalone concentration and K is the chalone threshold. In order to estimate $P\{C < K\}$ we constructed the probability mass function (pmf) of counter values c expected for a given node placement in a network and we denoted this pmf by $f(c)$. The intersection areas of transmission range circles of the nodes were estimated using Librino algorithm because the maximum counter value a node can record is equal to the number of circles that overlap on the location of the node.

In the presence of mobility, $f(c)$ will change over time as the overlapping circles have relative motion. For example, in Figure 6.11 we have illustrated the change of overlapping areas due to mobility by referring to two snap shots of a network at $t = t_0$ and $t = t_1$. Consider node B in Figure 6.11 at time $t = t_0$ and $t = t_1$ (node B is denoted by $\acute{B}$ at t_1). The counter is two for B at $t = t_0$ and it remains the same by $t = t_1$.

However, node C that has a counter of two at $t = t_0$ changes to three by $t = t_1$.

Another impact of mobility is that the wireless links exist as far as the transmitter and the receiver do not move away from the communication ranges of each other. The probability of completing a transmission of a data frame was previously analyzed in Section 4.4.5. This probability should be incorporated in Viswanath-Obraczka model in calculating P_S.

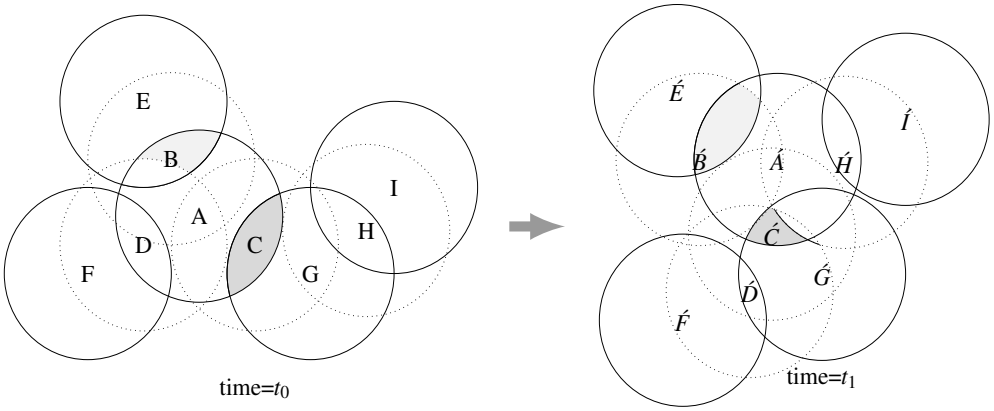

Figure 6.11: Illustration of change in counter values of nodes in the presence of mobility

6.4 Modeling the proposed protocol in a sample CSMA based network

A set of nodes that runs non persistent CSMA is assumed to be placed on a plane in a Poisson distributed manner with $\lambda = \frac{N}{\pi}$ where N is the average neighborhood of nodes (node density). CSMA is assumed to be slotted with slot time a. The frame transmission time is T and $T = \tau a$. Transmission range of a node is R. It is assumed $T = R = 1$ for mathematical purposes and other parameters will be normalized accordingly. Nodes are assumed to listen to a channel as a Bernoulli process with parameter p.

The example network scenarios are (i) $N = 8$ and (ii) $N = 100$.

Deriving transmission probability The probability p' of an actual transmission happening during a time slot is $p' = pP_{cI}$. P_{cI} is the limiting probability that the channel is sensed Idle. According to Equation 6.9:

$$P_{cII} = \sum_{0}^{\infty} (1-p')^i p(i)$$

Probability $p(i)$ that there are i neighbors for a node is given for Poisson distributed node placement by:

$$p(i) = \frac{(\lambda \pi R^2)^i}{i!} e^{-\lambda \pi R^2}$$

Therefore:

$$P_{cII} = \sum_{i=0}^{\infty} (1-p')^i \frac{(\lambda \pi R^2)^i}{i!} e^{-\lambda \pi R^2} = e^{p'N}$$

However:

$$P_{cI} = \frac{D_I P_c(I)}{D_B P_c(B) + D_I P_c(I)}$$

Here $D_I = a$ and $D_B = T = 1$. Therefore:

$$p' = \frac{ap}{(1-e^{p'N}) + a} \tag{6.31}$$

Channel characteristics were analyzed by solving the recursive equation 6.31 using Mathematica. The solutions resulted in the plot in Figure 6.12.

Deriving node to node successful transmission probability Transition probability, $P_{IS}(r)$ from Idle to Successful Transmission in the three state Markov chain given by Equation 6.11:

$$P_{IS}(r) = p'(1-p')e^{-p'\lambda 2q\left(\frac{r}{2}\right)} e^{-p'\lambda(\pi - 2q\left(\frac{r}{2}\right))(2\tau+1)}$$

where $q(t)$ is given by Equation 6.7. An example hidden terminal scenario is illustrated in Figure 6.13. Accordingly, for a transmission from X to Y, the nodes in region $B(r)$ act as hidden terminals. It is because X cannot sense any on going communication between Z and Y, thus X will continue to transmit to Y. This results in a collision at Y. The probability density function of the distance between x and y in Figure 6.13

$$f(r) = 2r, 0 < r < 1$$

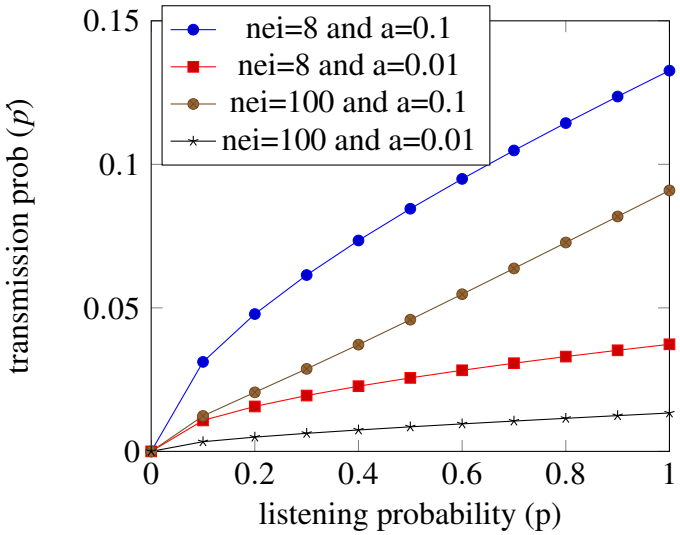

Figure 6.12: Variation of transmission probability, p' with listening probability, p with the intention to transmit

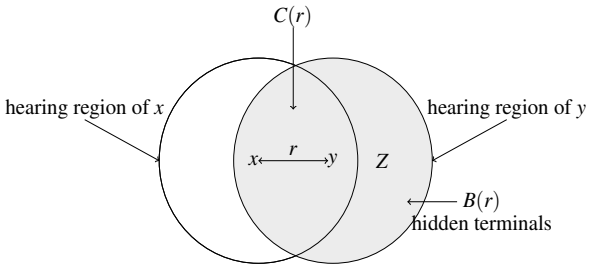

Figure 6.13: Illustration of hidden terminal problem for transmission from X to Y

From Equation 6.12

$$P_{IS} = \int_0^1 2rp'(1-p')e^{-p'\lambda 2q\left(\frac{r}{2}\right)}e^{-p'\lambda(\pi-2q\left(\frac{r}{2}\right))(2\tau+1)}dr$$

$$P(S) = \frac{2p'(1-p')e^{-(2\tau+1)pN}\int_0^1 e^{\frac{4pN\tau}{\pi}q\left(\frac{r}{2}\right)}rdr}{1+p'}$$

$$P_S = \frac{2p'(1-p')e^{-(2\tau+1)pN}\int_0^1 e^{\frac{4pN\tau}{\pi}q\left(\frac{r}{2}\right)}rdr}{p'+a}$$

According to Figure 6.14 P_S is a negligible value when the node density is high. Therefore, P_S was redefined based on the work by Shah-Mansouri et al. [139]. By

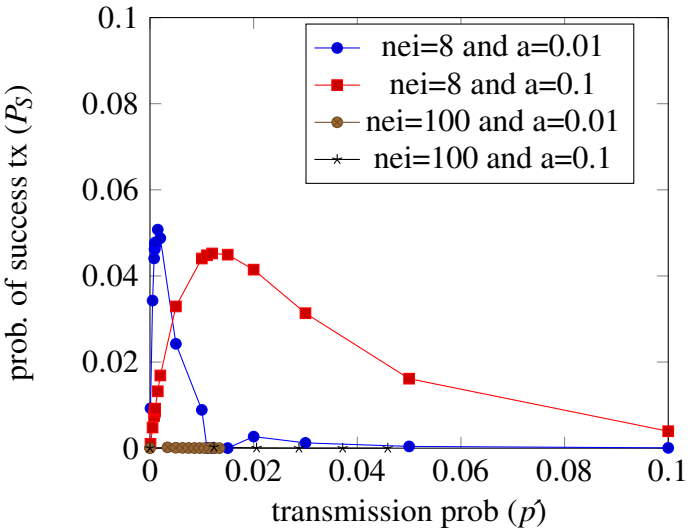

Figure 6.14: Behavior of successful transmission probability, P_S from a node to node with transmission probability, p' of the source node

Table 6.2: Comparison of theoretical results with original Viswanath-Obraczka model P_S [2] and P_S in [139]

Parameter	**Value for original P_S in [2]**	**Value for P_S in [139]**
p'	0.0002	0.0002
P_S	0.0045	0.2561
$\bar{N_b}$	0.27	15.02

replacing Equation 6.13 with the following:

$$P_S = \frac{D_S P(S)}{D_S P(S) + D_C P(C)} \tag{6.32}$$

We obtain the revised expression for P_S for the considered MANET scenario as:

$$P_S = 2(1-p')e^{-(2\tau+1)p'N} \int_0^1 e^{\frac{4p'N\tau}{\pi} q(\frac{r}{2})} r dr$$

For $p' = 0.0002$ the successful transmission probability P_S was calculated for MANET with $N = 100$ and the values are given in Table 6.2.

Calculating second level retransmitting neighbors

$$N_b = \frac{S(R)}{\pi R^2}\bar{N_S} = \frac{P_S N}{\pi}(2acos(\frac{r}{2}) - r\sqrt{1-\frac{r^2}{4}})$$

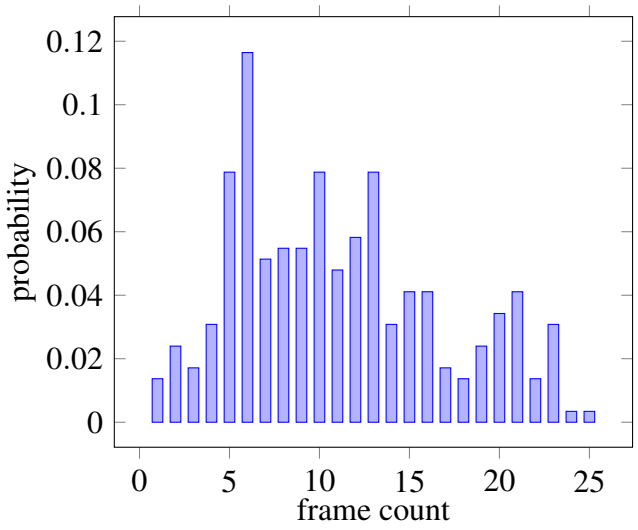

Figure 6.15: Probability mass function of frame count from simulation data

$$E[N_b] = \bar{N_b} = \int_0^{2\pi} \int_0^1 \frac{P_S N}{\pi} \frac{r dr d\theta}{\pi} (2acos(\frac{r}{2}) - r\sqrt{1 - \frac{r^2}{4}})$$

$$\bar{N_b} = P_S N \frac{2}{\pi} \int_0^1 (2acos(\frac{r}{2}) - r\sqrt{1 - \frac{r^2}{4}}) r dr$$

Calculating the probability of rebroadcasting This is the probability that chalone concentration is less than chalone threshold. In order to calculate this probability, following steps will be followed:

Step 1: Construct the probability mass function of C, $f(c)$

We obtained simulation data for a $100m \times 100m$ playground with 300 nodes which gives the plot of C as in Figure 6.15 for simplicity.

Step 2: Calculate the cumulative distribution function to obtain $P\{C < K\}$ using the equation:

$$F(C) = \sum_{i=0}^{K} f(c)$$

According to Figure 6.15 for different chalone thresholds the probabilities that chalone concentration is less than the threshold are as in Table 6.3.

Reachability analysis The reachability was calculated according to Equation 6.33 using the parameter set in Table 6.4. In Equation 6.33 we do not consider variable cov-

Table 6.3: Probabilities that the frame count is less than different threshold values

Chalone threshold	**P**$\{C < K\}$
1	0.04
2	0.06
3	0.08
4	0.11

Table 6.4: Parameter set for the reachability analysis of an example MANET

Parameter	**Value**
Playground	100m×100m
Total nodes	300
Transmission radius	40m
Average neighborhood	100
Listening probability, p	0.0005
Slots per frame Tx time, τ	100
Rebroadcasting probabilities P_{tx}	0.04, 0.06, 0.08 and 0.11
Mobility	No

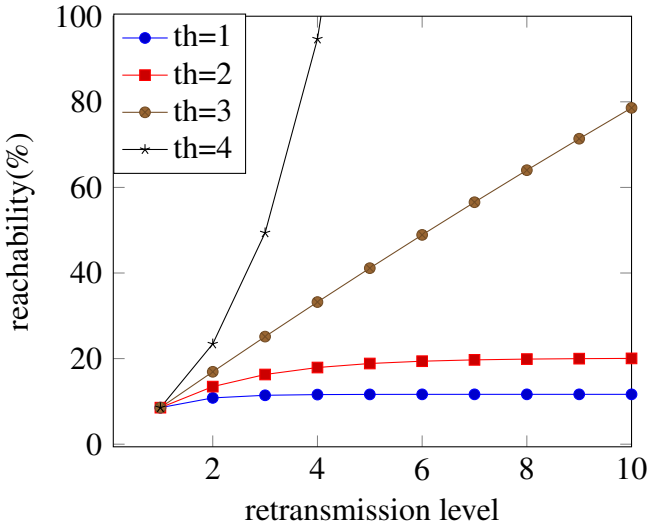

Figure 6.16: Reachability with retransmission level in a MANET having density 100

erage areas by different rebroadcast levels, thus we use β instead of β_i for simplifying the analysis.

$$N_T = P_S N + P_S N \sum_{i=1}^{l-1} (\beta P\{C < K\} P_b N)^i \tag{6.33}$$

The resulting plot of reachability against different retransmission levels is as in Figure 6.16. According to Figure 6.16 low threshold such as one and two result in reachability that asymptotically reach small percentage of around 20%, which implies that the threshold values of two and below fail to reach more than 20% of the nodes. Threshold value 3 and above is capable of delivering the messages to all the nodes in the network. When the threshold increased from three, reachability curve becomes steeper so that the nodes are reached by few rebroadcast levels.

6.5 Summary

In this chapter, we developed a model to analyze endcast schemes based on Viswanath-Obraczka model. Viswanath-Obraczka model consists of a graph based representation of a flooding MANET in which the vertices denote the nodes and an edge denotes a transmission of a data frame from one node to another. The graph is organized into levels that represent the level of actual rebroadcast in simple flooding and potential level of rebroadcast in efficient flooding schemes. The number of newly reached nodes at each level of rebroadcast is estimated using a geometric method in which the area of additional coverage is calculated. Viswanath-Obraczka model is capable of representing only simple flooding and probabilistic flooding in static network with preliminary method of estimating number of newly reached nodes by each level of rebroadcast. However, Viswanath-Obraczka model captures link layer characteristics such as slot time in CSMA MAC and hidden terminal problem in terms of the probability of node to node transmission.

We extend Viswanath-Obraczka model in such a way that efficient flooding schemes can be analyzed. Our modifications to the original model are (i) estimation of number of newly reached nodes with a comprehensive geometric analysis of the propagation of flooding wave, (ii) inclusion of the parameters such as counter and threshold in

counter based flooding into the probability of rebroadcasting and (iii) incorperating node mobility into the model.

We illustrate how the model is applied to the proposed endcast mechanism that is based on counter-based flooding. In modeling counter based flooding with this analytical model, the counter is estimated by considering the overlap of radio range circles of the nodes. We use Librino algorithm to calculate intersection areas of these overlapping circles. The probability of rebroadcasting is interpreted by the probability of counter being than the threshold. This probability is calculated by constructing a probability mass function (pmf) of the counter value. We showed how this pmf can be constructed analytically. We used simulation results to construct the pmf for the purpose of illustrating the application of model in a sample network scenario. The node mobility is modeled using the change of this pmf over time as the overlapping areas of the radio range circles vary with time in the presence of node mobility. The link breakage and reconnection due to mobility are included in the probability of node to node transmission.

We apply the model into a sample network scenario with static nodes and CSMA MAC layer. We evaluated how counter based threshold driven flooding performs in terms of reachability. The results showed that the reachability changes drastically with the slight change in threshold, for example threshold value of two fails to reach more than 20% of the nodes whereas threshold three is capable of reaching all the nodes.

CHAPTER VII

SIMULATION RESULTS FOR THE PROPOSED PROTOCOL

7.1 Introduction

We proposed a cellular automata based flooding scheme for unicast in MANETs in Chapter 5, which we refer to here as CA protocol. This chapter presents the simulative study of the CA protocol. The experiments were conducted on OMNET++ (version 4.4.1) using INET (version 2.1) and MiXiM (version 2.3) frameworks. OMNET++ is an event-driven and modular simulation framework, which supports object oriented programming with C++. INET is an open source model suit for wired and wireless networks developed for OMNET++. MiXiM is a model suit specifically created for mobile and fixed wireless network simulation based on INET.

The simulations are designed for evaluating the performance of CA protocol in comparison with Sequence Number Controlled Flooding (SNCF) or simple flooding. We selected following metrics after a broad survey of available performance metrics in Section 3.3 (Table 3.3):

Redundancy overhead (ROH_{uf}): We refer to redundant copies of the same data frame accumulated in the network as *redundancy overhead for endcast*. In analogy to biological cells that accumulate due to cell division, data frames also get accumu-

lated in the network due to rebroadcasting. Efficient flooding schemes are aimed at reducing the number of redundant rebroadcasts. Therefore, we considered ROH_{uf} as an important metric to evaluate performance of the CA protocol and SNCF.

Saved ReBroadcasts (SRB): SRB is defined as the ratio between the number of nodes that refrain from rebroadcasting and the number of nodes that receive a frame. Accordingly, SRB also measures the redundant rebroadcasts but in terms of number of nodes. $SRB = \frac{r-t}{r}$, where r is the number of receiving nodes and t is the number of transmitting nodes as explained in Section 3.3.

REachability (RE and RE_{uf}): Efficient flooding schemes impose a risk of not reaching the destination in the process of suppressing the rebroadcasts as previously explained in Section 3.3. Therefore, it is essential to evaluate flooding schemes in terms of reachability. Reachability is defined for network wide broadcasts as the ratio between the number nodes reached (r) by the flooding scheme and the number of reachable nodes (e) by topology. Thus, $RE = \frac{r}{e}$. However, we achieve unicast via efficient flooding by purposely curtailing the redundant rebroadcasts. The aim of the CA protocol is to reach the destination as opposed to reaching all nodes in the network in traditional use of flooding schemes. Therefore, we defined *Reachability for endcast* as the ratio between the number of reached node pairs (r_{uf}) by the flooding scheme and the number of all reachable pairs e_{uf}. Thus $RE_{uf} = \frac{r_{uf}}{e_{uf}}$. We use both of these definitions in our simulative study.

Flooding completion time (FCT): Flooding schemes involve a random assessment delay (RAD) as explained in Section 3.2, for example a node that runs simple flooding waits a random period of time to avoid collisions. CA protocol waits both for collision avoidance and to receive redundant frames to extract neighbor information. These waiting periods directly impact the end to end delay for a frame to travel from source to the destination. Therefore, latency is an important metric to compare performance of flooding schemes especially when used for unicast. *Flooding completion time (FCT)* is the interval between the time at which the flooding is initiated and the time at which

the final rebroadcast occurs or the final decision is made not to rebroadcast as defined in Section 3.3.

7.2 Experimental design

We conducted two sets of experiments: initial experiments were based on ideal wireless conditions and the latter set was designed to capture realistic network conditions.

Ideal wireless conditions imply that there are no collisions, no interferences and even no propagation delays. The protocols are tested in such a scenario in order to isolate protocol specific issues such as impact of the protocol logic on performance such as reachability. Further, in ideal wireless condition the frames are instantaneously delivered to all the neighbors. It results in maximum frame counts whereas in realistic wireless conditions some frames may not be delivered for instance due to collisions. Therefore, ideal wireless scenario results in the maximum reception of frames as well as maximum number of rebroadcasts so that it will give worst performance in terms of redundant frames for any flooding scheme. As a first step of evaluating the protocols, we collected only the number of frames with varying network parameters such as number of nodes and neighborhood size.

Realistic wireless network conditions include collisions, interferences and propagation delays of wireless links. In multihop networks there are additional problems such as hidden terminal problem and exposed source problem. Furthermore, CA protocol is targeted at application scenarios such as disaster situation explained in Chapter 1. Therefore, the protocol must be tested in the presence of mobility. Moreover, the network density should be properly defined for the tests. Hence this set of experiments was designed to capture realistic wireless conditions and protocol performance in the presence of node mobility. We also carefully identified network densities for the experiments. The performance metrics are those selected in Table 3.3 that are explained at the beginning of this chapter.

Table 7.1: Simulation parameters for experiments in ideal wireless conditions

Parameter	**Value**
Playground size	600 m $\times$ 400 m
Transmitter range	200 m
Chalone timeout	0.1 μs
Chalone threshold	1 to 3

7.2.1 Experiments based on ideal wireless conditions

This set of experiments was designed to study the performance of CA protocol in comparison with blind rebroadcasting and SNCF in the presence of ideal wireless conditions. Blind rebroadcasting causes a node to rebroadcast every time a message is received. This shows the closest analogy to uncontrolled biological cell proliferation and we based the CA protocol on blind rebroadcasting. However, in general, SNCF is the implemented version of blind rebroadcasting with an improvement such that the frame is rebroadcast only once by any node. Therefore, we compare CA protocol with both blind rebroadcasting and SNCF in these experiments.

These experiments correspond to the simulation parameters given in Table 7.1. We randomly place nodes on the same playground of size $600m \times 400m$ with each node having transmission radius of $200m$. This playground size and transmission range are in comparable sizes as in a number of similar simulative studies [104, 25, 60] and within the ranges in Table 3.4. Chalone timeout is set at a small value as 0.1 μs since the frames are delivered instantaneously in ideal wireless conditions.

7.2.2 Experiments based on realistic wireless conditions

Physical layer settings

Commodity wireless devices in general are in accordance with IEEE 802.11 wireless standards and we selected IEEE 802.11 MAC as the MAC layer after the survey given in Section 3.5. Therefore, we selected IEEE 802.11g implementation of MIXIM-INET for the following experiments.

IEEE 802.11's medium access control (MAC) is called Distributed Coordinate Function (DCF) which is a CSMA/CA scheme [142]. It provides asynchronous, time-

bounded and contention free access control over variety of physical layers [143]. We consider only the basic DCF in standard IEEE 802.11 MAC because broadcasts are handled using basic DCF and flooding schemes are broadcast based.

In basic DCF, before initiating a transmission a node senses the channel to determine whether any other node is transmitting. If the channel is sensed to be idle for a time period that exceeds the Distributed InterFrame Space (DIFS) then the node continues with its transmission. The time after an idle DIFS is slotted and the nodes are allowed to transmit only at the beginning of a slot. Slot duration is equal to the time needed for a node to detect a transmission from any other node, or one way propagation delay.

According to the notation used in IEEE 802.11 standard, Short Interframe Space (SIFS) time is denoted by $aSIFSTime$. It is defined as the nominal time in microseconds taken by the MAC and PHY layers to receive the last symbol of the frame, process it and respond with the first symbol of the earliest possible response frame. The period denoted by $aSlotTime$ is the slot time in microseconds. $DIFS$ is calculated using Equation 7.1 [144].

If an ongoing transmission is sensed, the node defers its own transmission until the end of the current transmission. After that, a backoff interval is selected to initialize the backoff timer. Backoff time is uniformly chosen in the interval (0, CW-1) where CW is defined as the contention window. At the first transmission attempt, CW is set to CWmin and it doubles at each consecutive attempt. Hence the standard IEEE 802.11 MAC is considered to have a slotted binary exponential backoff mechanism [145]. Timer is decreased as long as the channel is sensed to be idle and stopped when the channel is busy. Timer is reactivated when the channel is sensed to be idle for a period longer than DIFS. When the timer reaches zero then the node starts its transmission as shown in Figure 7.1 [144].

$$DIFS = aSIFSTime + 2aSlotTime \tag{7.1}$$

A receiving node sends the ACK after waiting for a SIFS time. Transmitting node waits for an ACK after a transmission and schedules a retransmission after an ACK

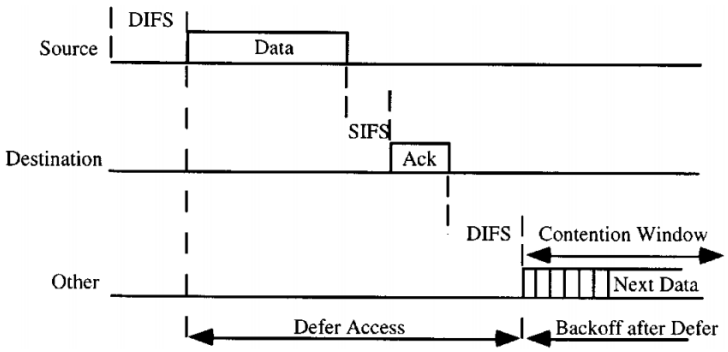

Figure 7.1: Basic IEEE 802.11 DCF protocol [143]

Table 7.2: IEEE 802.11 parameters

Parameter	**Value**	
	2.4GHz band	**5.0GHz band**
Slot time	short = 9 μs, long = 20 μs	9 μs
SIFS	10 μs	16 μs
DIFS (Eq.7.1)	short = 28 μs, long = 50 μs	34 μs
Bitrate	2 Mbps	2 Mbps
CWmin	15	15
CWmax	1023	1023
Retry limit	7 (short) 4 (long)	

timeout. CTS/RTS does not apply for broadcasts. The important parameters are as in Table 7.2 according to IEEE 802.11 standards as at year 2012, which includes IEEE 802.11a, b and g amendments [144].

It was noted that SNCF protocol programmed for ideal wireless physical layer could not deliver the message to the destination due to collisions when the simulations were run on IEEE 802.11g implementation. This was because the random delay in SNCF was originally set to zero resulting in collisions as nodes try to rebroadcast simultaneously as soon as a frame is received. Therefore, we assigned a value for the RAD, in comparable scale as the chalone wait time in CA protocol explained in Chapter 5. This enables the comparison of latencies of the two protocols that is explained in Section 7.3.3.

Table 7.3: Network densities of simulated topologies

Playgrond size	**Average node degree**	**Median node degree**
20m×20m	299.0	299
50m×50m	256.5	260
100m×100m	105.0	104
150m×150m	52.8	53
200m×200m	31.7	31
250m×250m	21.0	20
300m×300m	15.1	14
350m×350m	11.4	11
400m×400m	8.9	9

Network topology

Since this research is on *dense MANETs*, network density is an important factor in simulation studies. We use the definition of density in terms of the number of neighbors per node explained in Section 3.4.

We configured the simulation setup as a 300-node MANET with each node having a power-saving transmission range of around 40m. In order to obtain varying node densities we vary the playground size of the MANET from $20m \times 20m$ to $\frac{1}{2}km \times \frac{1}{2}km$ area. We consider that 300 nodes placed on a $20m \times 20m$ playground mimic a meeting room whereas the same number of nodes dispersed in a $\frac{1}{2}km \times \frac{1}{2}km$ area mimics a disaster site. The resulting network topologies can be characterized in terms of network density as shown in Table 7.3. For example, the network density is around 100 neighbors per node when 300 nodes are dispersed randomly in a $100m \times 100m$ playground with each node having 40m of transmission radius.

It was also required to test the protocols by varying the network size while maintaining the average network density at constant. We selected network density to be 10 and this value was selected to be within the range 4 to 20 (Section 3.4).

Table 7.4: Topologies with constant network density

playground	nodes	density
20mX20m	11	10.00
85mX85m	20	9.61
150mX150m	50	10.70
220mX220m	100	10.55

Table 7.5: Simulation parameters for experiments in realistic wireless conditions

Parameter	Value	
number of nodes	300	
transmission range	40 m	
playground sizes	meeting room	disaster site
	20m×20m	450m×450m
chalone wait	0 to 6 sec	
flooding wait	0 to 6 sec	
threshold	1	

7.3 Simulation based experiments and results

The simulations were run to study the redundancy, reachability and latency aspects of the CA protocol against SNCF as described in this Section by configuring the simulation with ideal wireless conditions (Table 7.1) as well as realistic wireless conditions (Table 7.2) and with network topologies described in Tables 7.3, 7.5 and7.4.

7.3.1 Redundancy overhead

Experiment 1 We placed 20 to 1000 nodes on a playground of size $600m \times 400m$ with each node having $200m$ of transmission range in ideal wireless conditions (Table 7.1). We counted the total number of frames (ROH_{uf}) received by all the nodes in the network by the time the destination is reached, for the same source destination pair when the simulation was run for 10 different node placements under the ideal wireless conditions. We averaged the results over these 10 simulation runs and plot the results with 99% confidence interval as shown in Figure 7.2. Note that the CA protocol was configured without an inhibition scheme to stop the propagation of flooding wave after the destination is reached and also the threshold is set to be one.

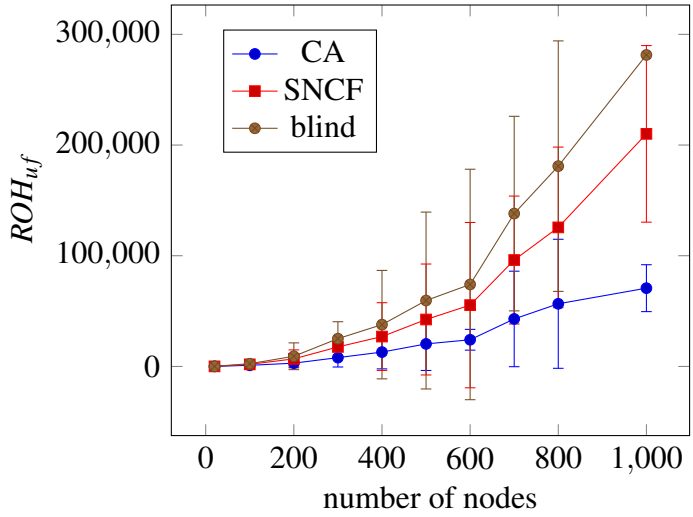

Figure 7.2: Total number of redundant frames received in the network (ROH_{uf}) until the destination is reached for blind, SNCF and CA protocols in ideal wireless conditions

According to Figure 7.2, the CA protocol outperforms both blind and SNCF protocols for all numbers of nodes shown. For example, in a MANET with 100 nodes, blind rebroadcast caused the network to receive the same frame around 2440 times on average, while SNCF and CA protocol caused 1870 and 1000 frames respectively. Thus the CA protocol saves nearly 60% of redundant rebroadcasts compared to blind rebroadcasting whereas the saving is nearly 45% compared to SNCF. Also for 1000-node network the frame count was more than 280,000 for blind rebroadcasting, around 210,000 for SNCF and only around 70,000 frames for CA protocol. CA protocol in small MANETs of 20 nodes also shows a saving of redundant rebroadcasts around 40% and 10% compared to blind and SNCF protocols respectively.

Blind rebroadcasts are unacceptable for dense MANETs in terms of redundant rebroadcasts as the growth of the curve is steeply exponential. Though SNCF is slightly better compared to blind rebroadcasting, it also shows an exponential growth. CA on the other hand shows a slow growing curve thus making it a better protocol for all network sizes shown. The results show satisfactory performance and usability of the proposed protocol in dense MANETs as the number of redundant rebroadcasts has

almost linear and slow growth against network size. This shows that CA protocol reduces storm situation mentioned in Section 2.3 better than SNCF.

Experiment 2 CA protocol is a counter-based threshold driven flooding mechanism which suppresses redundant rebroadcasts depending on the threshold as explained in Chapter 5. In suppressing the rebroadcasts, the protocol imposes a risk of not reaching the intended destination as mentioned in Section 3.3. The 15-node network shown in Figure 7.3 was analyzed in ideal wireless conditions to study how far a frame could travel when running the CA protocol as the threshold varies. In ideal wireless conditions the physical distance that the frame travels is governed only by the protocol operation. For example, nodes within the transmission radius of the source definitely receive the frame. The rebroadcast of these nodes will reach nodes beyond the range of the source definitely for SNCF as all nodes are connected in multihop manner. CA protocol with threshold 1 allows only a few of these nodes to rebroadcast so that nodes on some regions of the playground may not receive the frame compared to SNCF.

We plot the redundant frames against the Euclidean distance between source-destination pairs as shown in Figure 7.4 reusing already available simulation data. According to Figure 7.4 near-complete reachability is achievable at a threshold value of 3 by the proposed protocol similar to SNCF with lower numbers of frames than in SNCF. Figure 7.4 also highlights the impact of threshold on reachability achievable by CA protocol.

In above analyzes we found out that in ideal wireless conditions CA protocol outperforms SNCF in terms of redundant frames accumulated in the network but the physical distance the frames could reach is low compared to SNCF. However, by increasing the threshold, CA protocol could reach farther nodes with still having lower frame counts compared to SNCF. It is essential to test CA protocol in realistic network conditions to further evaluate its performance.

Experiment 3 This experiment aimed at analyzing the redundancy overhead of CA protocol compared to SNCF in the presence of realistic wireless conditions in Table 7.2 with network densities in Table 7.3. We placed 300 nodes in playgrounds of sizes

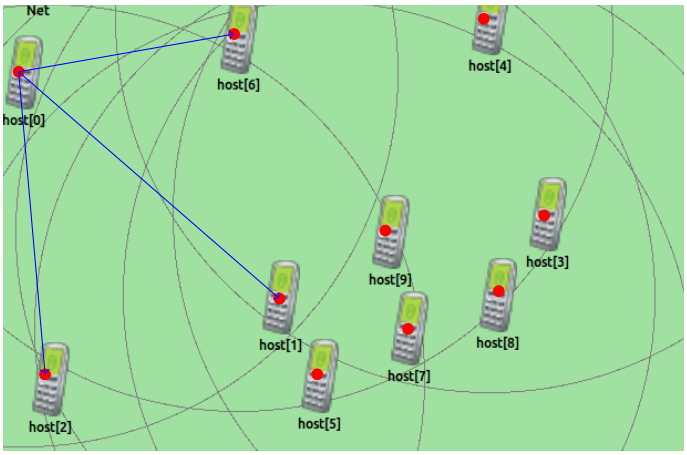

Figure 7.3: Example 15-node network

ranging from $20m \times 20m$ to $400m \times 400m$ so that the network density in terms of average neighbors per node varies from 10 to 300.

Figure 7.5 shows variation of the redundancy overhead in terms of total number of frames accumulate in the network (ROH_{uf}) of CA and SNCF protocols until the end of all the protocol events. Results are interpreted in two ways; redundant frames with the playground size and the same with node densities.

According to Figure 7.5 the total number of accumulated redundant frames at the end of the simulation is low as about 1000 frames for CA protocol for all the network densities and playground sizes and it is a significantly better performance compared to SNCF, which records over 2000 to 50000 frames for the same network configurations. The growth of redundant frames is unacceptably high as it grows from around 2500 frames to 50000 when the network density increases from 10 to 300 neighbors per node. However, CA protocol shows almost constant number of redundant frames for all node densities shown. This should be because the destination is reached by the time around 1000 redundant frames are recorded in the network in all network configurations in CA protocol and thereafter, the inhibition scheme of the CA protocol effectively stops the propagation of frames throughout the network.

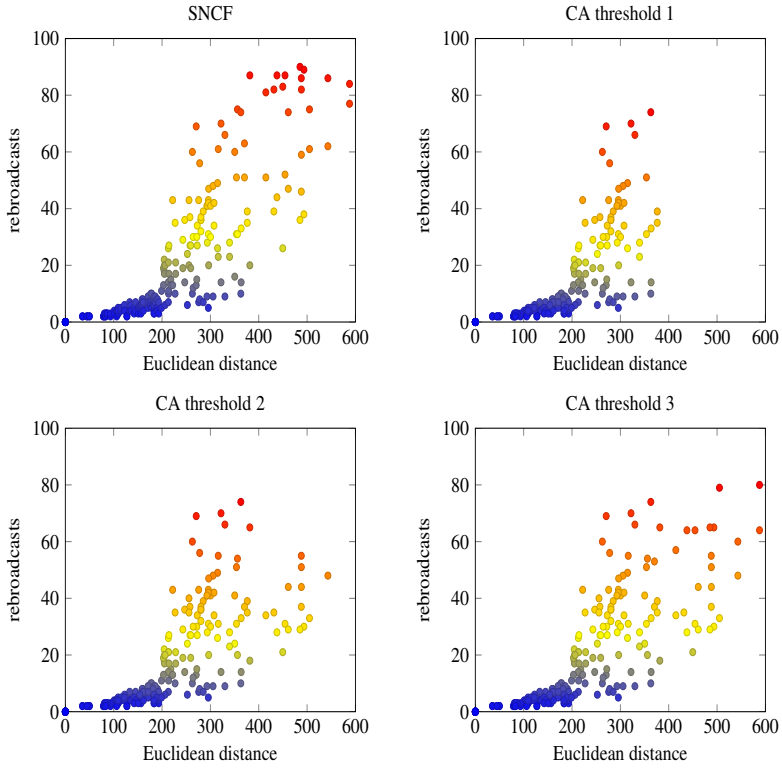

Figure 7.4: Number of rebroadcasts Vs distance between node pairs

Experiment 4 We used the same test configuration in Experiment 3 and obtained the number of nodes that received the frame and the number of nodes that rebroadcast the frame in the networks. We calculated *SRB* as a percentage, as per the definition given at the beginning of this chapter (Section 7.1). The plot of SRB against both the playground size and the network density is in Figure 7.6.

It was observed that all nodes that received a frame, rebroadcast it in SNCF, thus giving no saving of rebroadcasts. CA protocol performs better for all node densities and all playground sizes considered as over 60% saving is recorded for all these network configurations. Interestingly, SRB increases when the network density increases in CA protocol. The saving in rebroadcasts sharply increases by about 30% when the node density increases from 10 to 50.

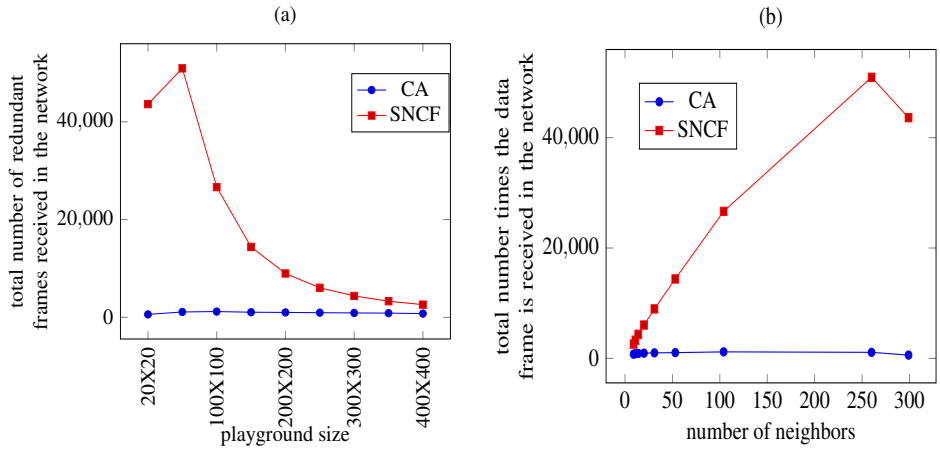

Figure 7.5: Redundant frames until the end of events in SNCF and CA protocols

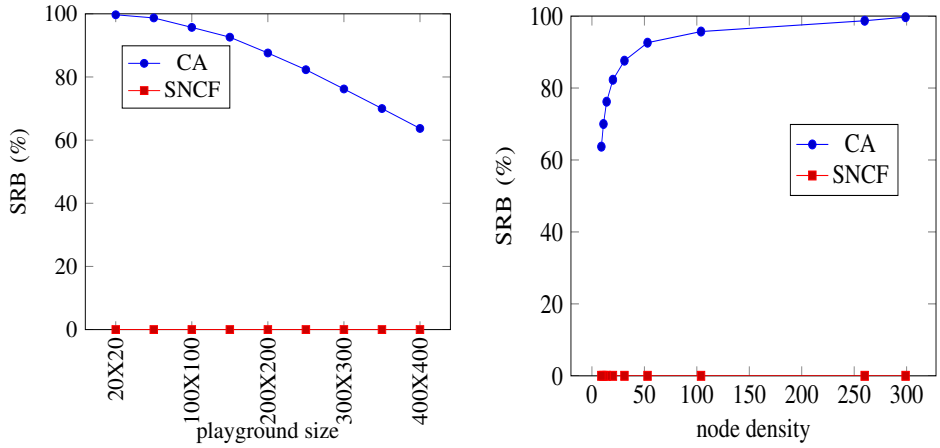

Figure 7.6: Saved rebroadcasts (SRB) for CA and SNCF protocols for a 300-node network

7.3.2 Reachability

In Section 7.3.1 it was observed that CA protocol saves the redundant rebroadcasts both in terms of number of accumulated frames (Figures 7.2 and 7.5) and the number of rebroadcasting nodes (Figure 7.6). This performance gain is due to suppression of rebroadcasts using the threshold driven counter based mechanism. However, suppression of rebroadcasts in turn, imposes a risk of not reaching the destination as already explained in Section 3.3. Therefore, reachability was analyzed according to the original definition, $RE = \frac{r}{e}$ where r is the number of reached nodes and e is the number of

reachable nodes as mentioned in Section 7.1. We find r using simulations whereas e is found using graph theoretic approach as follows:

We model the MANET as a graph in which vertices are the mobile nodes and the edges denote the availability of a direct wireless link between nodes at a given point in time. We first take the Euclidean distance between every node pair and then determine the immediate neighborhood by considering the transmission ranges. It is analogous to super imposing the communication ranges of nodes on the physical location map of the network. The resulting graph can be identified as a *transmission graph* according to the definition in Section 3.7. In order to evaluate the reachability of the resulting graph, we use Floyd-Warshall algorithm for its simplicity, parallel computation for all node pairs, and less pre-processing needs apart from the less complexity as explained in Section 3.7 (Table 3.8). If a path can be found by the algorithm then we can conclude that a node can reach any other node by simple flooding.

Experiment 5 We configured the simulation as in Experiment 3 and obtained number of reachable nodes using Floyd-Warshall all pair shortest path algorithm. Then we executed CA and SNCF protocols to obtain the number of reached nodes. After that we calculated *RE* and plotted the results against both the network densities and playground sizes. Figure 7.7 shows reachability as a percentage, achieved by CA protocol when the playground size and the node density varies. SNCF gave 100% reachability for all node densities and playground sizes considered and this data is not shown in the graph for the clarity of the data points. According to Figure 7.7 the reachability of CA protocol decreases when the node density decreases or the playground size increases and this is for the smallest possible threshold value which is 1.

However, this reduction in RE should not be interpreted as a weakness of the CA protocol because it purposely curtails the rebroadcasts and aimed at delivering unicast data. Therefore, we run experiment 6 to measure RE_{uf} to analyze the performance of CA protocol in unicast.

Experiment 6 In this experiment we maintained the average network density at around 10 neighbors per node by varying the number of nodes from 11 to 100 and

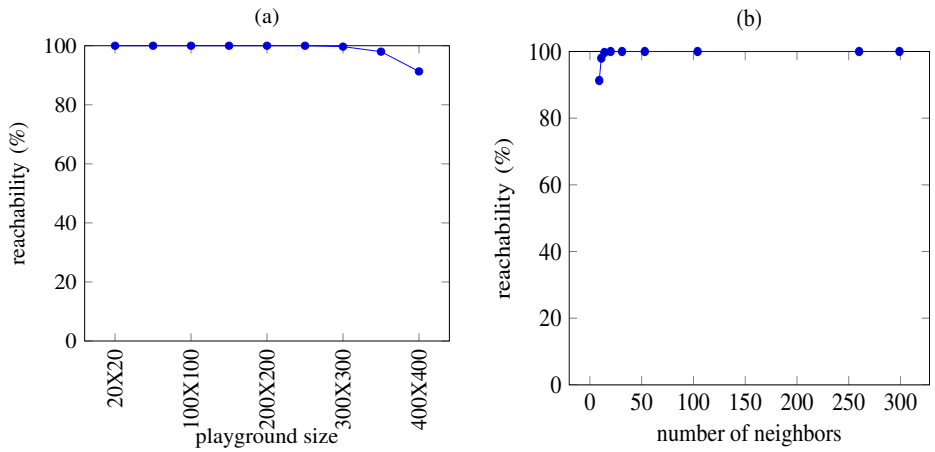

Figure 7.7: Reachability of SNCF and CA protocols. Reachability is 100% for SNCF for all the considered network configurations.

varying the playground size from $20m \times 20m$ to $220m \times 220m$ as shown in Table 7.4. The experiment was on realistic wireless conditions (Table 7.2). When all node pairs are considered, 100-node network requires to be simulated with unicasts for 9900 $(100 \times 100 - 100)$ node pairs. These tests required heavy computational costs, therefore we had to semi automate and repeat the tests manually in batches. Therefore, only 3 data points were obtained as in Figure 7.8.

It was observed according to Figure 7.8(a) that the reachability was 100% for smaller networks of size 10 nodes for SNCF and CA protocol even with threshold of one. We get this complete reachability with CA when threshold is one, while saving about 80% of redundant frames compared to SNCF as in Figure 7.8(b). However, when the network is large as nodes are dispersed in a larger area, the frame should propagate in a multihop manner to reach some node pairs. Depending on which nodes decide to rebroadcast in CA protocol, the destination may not be reached in some cases. This is visible in the 50-node network that reachability of CA is only about 75% when the threshold is one whereas SNCF shows around 90% reachability.

As already found out in Experiment 2 that runs on ideal wireless conditions, threshold of the CA protocol can be increased to improve the reach. According to Figure 7.8(a) reachability increases when the threshold increases in realistic network conditions also, for example, reachability improves from 75% to 90% in the 50-node

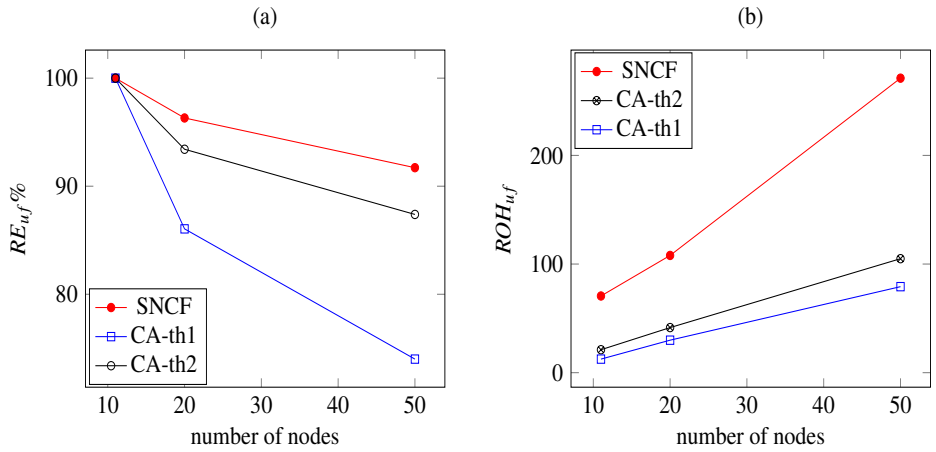

Figure 7.8: Reachability (RE_{uf}) and redundancy overhead (ROH_{uf}) of endcast with SNCF and CA protocols when the network size varies with network density kept constant at 10

network by increasing threshold from one to two. This significant reachability improvement is gained while still saving around 80% of redundancy overhead compared to SNCF.

7.3.3 Latency

Experiment 7 We configured the simulation as in Experiment 3, where CA and SNCF protocols are simulated on realistic network conditions with 300 nodes placed on playgrounds of sizes $20m \times 20m$ to $400m \times 400m$. We obtained flooding completion time (FCT) by taking the difference between the timestamp at which the frame gets originated and the timestamp at the end of the simulation. Accordingly, FCT consists of chalone wait periods in CA protocols and random wait in SNCF, backoff periods and propagation delays of IEEE 802.11 MAC and physical layer. The ACK timeouts do not apply in IEEE 802.11 MAC specifications as broadcasts are not acknowledged. Only single stage backoff at the transmitting node applies in detecting an idle channel. However, the MAC level delays are at microseconds scale whereas RAD times such as chalone wait in CA protocol and random delay in SNCF are set to 0.6 s. Therefore, the latency metrics are governed by RAD time (Section 3.2).

The plot of FCT resulting from CA protocol is comparable with that resulting from

SNCF according to Figure 7.9 as the two curves are almost superimposed on one another. However, there is slightly higher FCT recorded by SNCF compared to CA protocol for highly dense networks according to Figure 7.9 (b), for example, in networks of around densities of 250 and 300 neighbors per node, SNCF takes about 5 more seconds to finish its frame propagation than CA protocol. On the other hand for low density networks such as 10 neighbors per node, the latency is higher in CA protocol with a gap of about 25s.

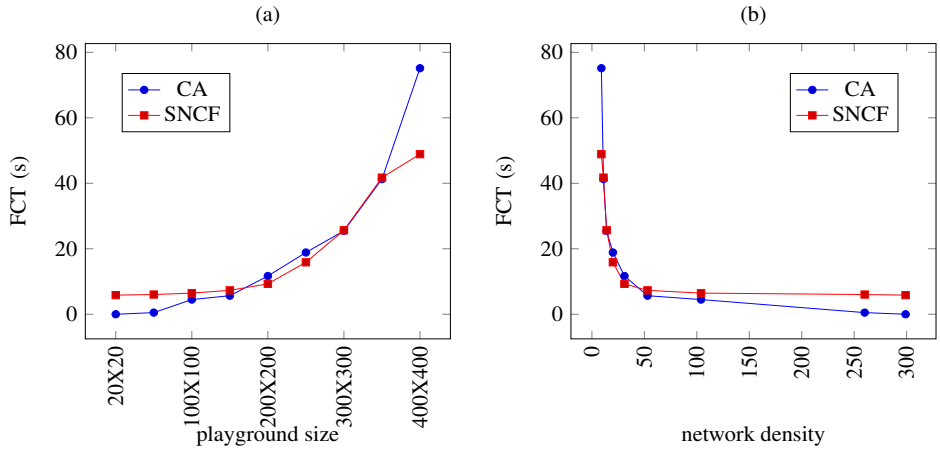

Figure 7.9: Latency of CA protocol in terms of flooding completion time (FCT) in comparison with simple flooding

7.4 Discussion

7.4.1 Effect of storm control

CA protocol controls the redundant rebroadcasting of frames using a counter based mechanism and this was termed storm control in Chapter 5 (Section 5.3).

According to the results obtained in Section 7.3, it was observed that CA protocol saves over 45% of redundant frames compared to SNCF even when it runs without inhibition scheme for flood controlling (Figure 7.2). This saving is recorded when the threshold for storm control was one and the number of nodes were over 100. The nodes were placed on a playground of size $400m \times 600m$ with each node having $200m$

transmission range. Further, when the number of nodes were increased to 1000, the saving of redundant frames increases to 65%.

With the inhibition scheme in operation the saving in redundant frames is over 50% (Figure 7.5) for networks of densities 10 through 300 of average number of neighbors per node. These network densities were obtained by placing 300 nodes in playgrounds of sizes $20m \times 20m$ to $400m \times 400m$ and configuring each node to have power-saving radio range of $40m$. It was observed that the number of frames remain almost constant at around 1000 throughout the total range of network densities in CA protocol whereas the number increased from 2000 to 50000 in SNCF. This implies the saving in redundant frames in CA protocol increases from 50% at network density of 10 to about 98% at network density of 300 with respect to the redundant frames caused by SNCF. These statistics for variety of network configurations can be interpreted as evidence for the effectiveness in saving redundant frames in the network by the storm control using counter based flooding and the flood control using negative acknowledgement.

7.4.2 Effect of inhibition scheme

CA protocol includes an inhibition scheme to stop propagating the frame after the destination is reached, as explained in Chapter 5. The effectiveness of this scheme is evaluated by comparing the total number of redundant rebroadcasts with and without inhibition until all the protocol events are over. Figure 7.2 shows variation of number of redundant frames with varying number of nodes, when the CA protocol operates with and without inhibition scheme in ideal wireless conditions with simulation parameters configured according to Table 7.1.

Figure 7.2 shows almost constant growth rate of about 8 frames per node in the plot corresponding to the case of no inhibition. This growth is due to the continuous propagation of the frame throughout the network after reaching the destination. When the inhibition scheme is in place there is almost no growth in the number of frames when the number of nodes increases as the frame stops propagating soon after the destination is reached. The destination is reached in all networks considered within the total frame count of 100. For example in a 200-node network, the given destination was

reached by the time the total number of frames was counted as 84 when the inhibition scheme was in operation. The frame count was 1405 when the inhibition was not used. This is around fifteen times the recorded number of frames when the inhibition scheme is used. This shows that the inhibition scheme significantly saves redundant frames accumulated after reaching the destination. Therefore, inhibition scheme satisfactorily controls flood situation explained in Section 2.3.

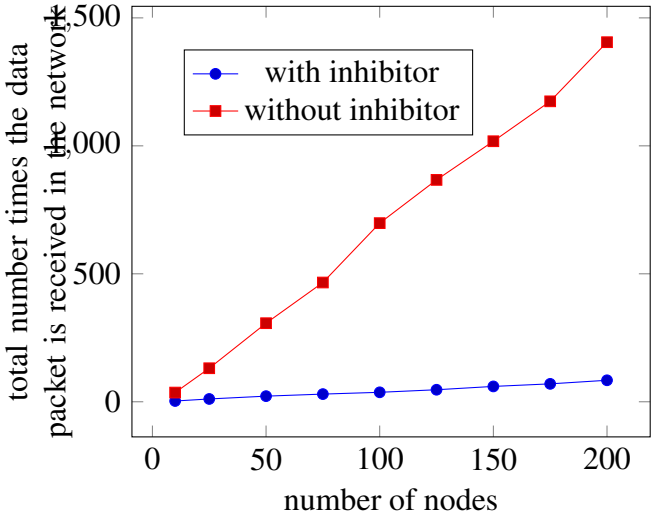

Figure 7.10: Number of redundant rebroadcasts until the end of all events in CA protocol with and without inihibition scheme

7.4.3 Effect of mobility

It is essential to evaluate MANET protocols in the presence of mobility. Random Way Point (RWP) mobility is extensively applied in wireless network simulations [72, 73, 96, 97]. In this mobility model a node selects a random starting position and a random point in the area as the next waypoint. Then it moves towards the selected waypoint at a randomly picked speed between a minimum and a maximum speed. After reaching the determined waypoint it waits for a time duration, normally distributed between a minimum and a maximum, and repeats the process with next selected waypoint [73]. Since the target application scenario is for human mobility as in the case of managing a disaster relief camp as explained in Chapter 1, minimum and maximum speeds are

selected as 1 to 2 m/s and the pause time is between 0 and 0.5s. These values are in line with similar studies that capture human mobility scenarios [72, 73, 96, 97].

Figures 7.11 corresponds to network density of 10 as defined in terms of average neighborhood per node in Section 7.2.2. The simulation was run by increasing the number of nodes and the playground size while maintaining this network density. Transmission radius was also kept fixed at power saving range of 40m. Therefore, the network diameter increases in terms of hop count when the number of nodes increases.

The simulations were run by configuring the network to be static and also by allowing the nodes to move according to RWP mobility with speed from 1 to 2 m/s and pause time from 0 to 0.5 s. We tested SNCF protocol and CA protocol with both static and mobile network configurations for varying network sizes. CA protocol was tested for threshold value one and two, which are denoted as *th1* and *th2* in Figures 7.11.

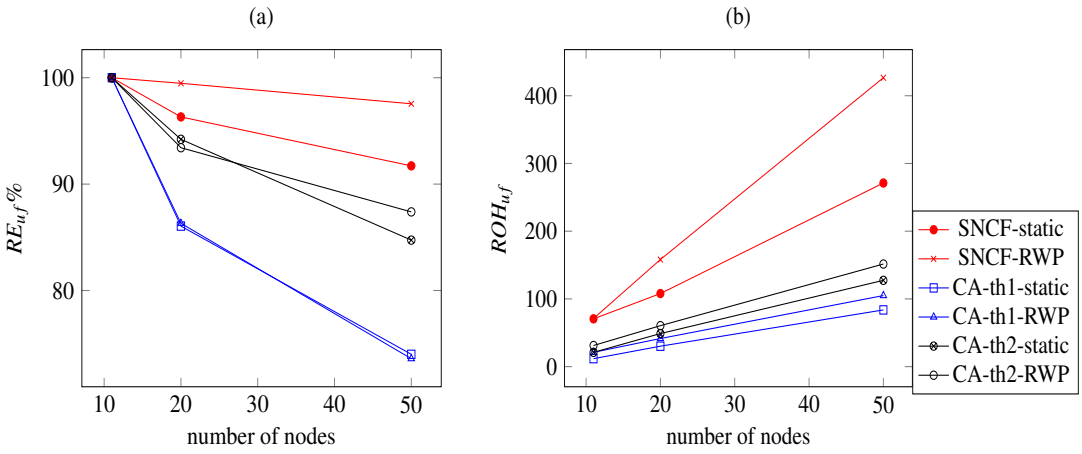

Figure 7.11: Redundancy overhead and reachability of endcast until the destination is reached for SNCF and CA protocols with mobility when the threshold of CA protocol is set at 1 and 2 (*th1* and *th2*)

Figure 7.11(a) shows the number of redundant frames accumulated in the network until the destination is reached when the network size is increased while keeping the average network density constant at 10. Accordingly, SNCF shows the highest frame counts and it grows faster than for CA protocol, for example in a 50 node network SNCF caused accumulation of around 250 frames while CA protocol resulted in a number less than half of that. Furthermore, frame count increases from around 75 to

250 by SNCF in static network when the network size increases from around 10 to 50 nodes. The growth of frame count is even steeper for SNCF when the nodes are mobile as it increases from about 75 to 400. In contrast CA protocol shows only an increase from about 20 to 150 when the network size increases from 10 to 50 nodes.

In the presence of mobility there is a higher frame count than in static networks for all protocol settings. However, the redundant frames caused by SNCF with mobility shows a considerable increase compared to the case of SNCF in static networks, for example, in a 50 node network, the mobility of nodes caused about 60% of increase in redundant frames. In contrast, mobility of nodes does not cause considerable increase in redundant frames compared to static networks when CA protocol is in operation.

Figure 7.11(b)shows how the reachability varies with network size with static nodes and mobile nodes for SNCF, CA protocol with threshold 1 and CA protocol with threshold two. Here, the reachability is according to the definition of RE, redefined for unicast by considering source-destination pairs given in Section 7.1.

As per Figure 7.11(b), mobility seems to assist frame propagation rather than disturbing it because the reachability of SNCF is significantly higher in mobile network rather than in static network. Reachability is almost constant at around 100% for all the network sizes with mobile nodes for SNCF except for a slight decrease in higher network sizes. In contrast, in static networks reachability of SNCF drops from 100 to around 95% when network size increases from 10 to 50. A general perception is that mobility of nodes are destructive in data communication in wireless networks and makes it challenging to device routing mechanisms. That may be true for routing schemes that set up virtual backbones and assign key nodes to act as routers. However, the flooding schemes considered here, can be considered to leverage mobility to enhance data delivery. This is in line with the argument supporting the branch of MANET study known as *opportunistic networks* in which mobility is considered an opportunity for delivering data using *store and carry* behavior of nodes. CA protocol with threshold of two, also shows a slightly higher reachability in mobile networks compared to static networks at least for higher network sizes. CA protocol with threshold of one does not show any difference in reachability when operating on static and

mobile networks.

7.4.4 Effect of chalone threshold

In Experiment 2 it was observed that the chalone threshold is a decisive parameter that governs the reachability (Figure 7.4). In this experiment we measured the physical distances that the frames are able to propagate in ideal wireless conditions using the parameters in Table 7.1. As shown in Figure 7.4, when the threshold was one the CA protocol was able to reach nodes at most 400m apart where as SNCF was able to reach nodes that are up to 600m apart. However, when the threshold was increased to three near complete reach as in SNCF was recorded by CA protocol. This result at the initial stages of the research alarmed the importance of chalone threshold as a tunable parameter in CA protocol in achieving the expected redundancy-reachability tradeoff described in Section 3.3.

Further investigation into the impact of chalone threshold on redundancy and reachability in Experiment 6 verified the above preliminary results. In experiment 6 we evaluated RE_{uf} and ROH_{uf} in networks of different sizes but with constant network density of around 10 neighbors per node. When the two metrics are compared side by side in Figure 7.8 by slightly increasing the threshold reachability could be improved considerably, for example, in a 50 node network the reachability could be increased by about 15% when the threshold was increased simply from one to two. Moreover, this slight increment in threshold does not increase the redundancy overhead in a considerable amount, for example, in the same 50 node network the number of frames increased only by about 6% when the threshold increased from one to two.

7.5 Summary

In this chapter, we evaluated the redundancy, reachability and latency of the proposed counter based threshold driven endcast scheme that we termed CA protocol in comparison with sequence number controlled flooding (SNCF) or simple flooding. The total number of redundant frames caused by flooding schemes is given by the redun-

dancy overhead metric (ROH_{uf}). Reachability was evaluated in two different ways, namely the ratio between reached nodes and reachable nodes (RE), and the ratio between reachable source-destination pairs and reachable pairs (RE_{uf}). Latency metric was the flooding completion time (FCT) which gives the duration between the time at which the frame originated and the time at which all the protocol activities finish.

The simulations were configured in two major settings, namely, ideal wireless conditions and in realistic wireless conditions. In ideal wireless network conditions the collisions, contention, and propagation delays are neglected whereas realistic wireless conditions are simulated using the IEEE 802.11g implementation of the OMNET++, INET and MiXiM simulation framework. IEEE 802.11g simulation modules altogether include the realistic networking conditions modeled at the MAC and physical layer such as propagation delays, collisions, carrier sensing and backoff mechanism.

According to the ROH_{uf} in both realistic and ideal wireless conditions, CA protocol outperforms SNCF in such a way that over 45% of redundant frames are saved by the CA protocol compared to SNCF in all the network configurations starting from 100-node network in ideal wireless conditions (Figure 7.2) and in 300 node network for all node densities ranging from 10 to 300 (Figure 7.5). This saving increases rapidly as networks grow by size in ideal wireless condition and by density in realistic network conditions.

The flooding schemes that suppress rebroadcasts (efficient flooding schemes) there is always redundancy-reachability tradeoff. The lowest threshold of one was able to give a reachability below 85% for networks of size 20 nodes to 50 nodes in realistic network conditions. However by increasing the threshold to two the reachability could be increased to above 90% in these networks. Further, the increase in redundancy overhead is less than 6% by this increment of threshold (Figure 7.8).

The mobility was found to assist the delivery of frames in flooding schemes rather than destructing end to end message delivery as experienced in fixed routing approaches where key nodes are appointed to perform routing and control while maintaining end to end routes. The fact that flooding schemes leverage mobility for message delivery is evident from the reachability plot in Figure 7.11 where all the flooding schemes show

increased reachability in the presence of mobility compared to static configuration, for example, reachability of SNCF in static 50-node network is only about 93% which becomes about 98% when the nodes are mobile.

The inhibition scheme in CA protocol was also found to be effective in reducing the redundancy overhead (Figure 7.10) as the protocol with inhibition shows almost constant count of redundant frames where the count grows rapidly when the network size increases by number of nodes. For example in CA protocol with inhibition, the frame count grows only by about 8 frames per every 25 nodes added to the network. In contrast, the protocol without the inhibition scheme shows a growth of redundant frame count by about 170 frames per every 25 nodes.

CHAPTER VIII

DISCUSSION AND CONCLUSIONS

A key objective of this research is to build a theoretical basis to analyze the problem of routing in MANETs approached from a different paradigm that we term as *mobile-stateless paradigm*, which is completely different from traditional MANET routing. Nodes do not have to keep any state information or they can become *stateless* if they are allowed to blindly rebroadcast every data frame that they receive thus allowing for unrestricted node *mobility*. However, *blind rebroadcasting* is unacceptably inefficient. Instead, we can use *simple flooding*, in which a node rebroadcasts a frame only when it is received for the first time. There are flooding schemes proposed in the literature that allow only a sub set of the nodes to rebroadcast and these schemes are referred to as *efficient flooding*. Conventional use of any kind of network flooding is to disseminate a message to all the nodes in a network. In contrast, we propose to use flooding for unicast. We did not come across any other work that attempts unicast via flooding, although flooding schemes are suggested for multicast as mentioned in Chapter 3.

Endcast We leveraged efficient flooding as a unicast mechanism conforming to mobile-stateless routing paradigm and we term it *endcast*. We also developed a model to analyze endcast schemes in terms of evolution of a graph $G(V,E)$, where the set of vertices V represent the nodes and an edge $(u,v) \in E$ is added when a frame is received by a node v due to rebroadcasting of another node u during the propagation of a frame via flooding. In our model, the number of edges are estimated using geometric analysis of

the network.

Our model captures the major problems in flooding, namely, the *broadcast storm problem* and the situation that we call *broadcast flood problem* that is particularly observed in endcast. Broadcast storm problem refers to the situation where excessive number of redundant frames are transmitted all over the network causing heavy contention and collisions. This situation is already researched in the literature aiming at improving conventional use of flooding for network wide broadcast. When flooding is used for unicast, it is wasteful to leave the frames to propagate beyond the destination and we refer to this situation as broadcast flood problem.

The theoretical model that we built for analyzing endcast is capable of:

- Modeling the propagation of data via flooding schemes including simple flooding, probabilistic flooding and counter based flooding
- Analyzing flooding in networks with static nodes as well as mobile nodes
- Estimating the level of broadcast storm problem and broadcast flood problem
- Modeling the physical and MAC layer impacts such as hidden terminal problem

According to the graph theoretic model proposed by Viswanath and Obraczka [2] for analyzing multihop flooding in static networks, the propagation of a frame results in a tree-structured graph rooted at the source node as in Figure 8.1. We refer to this model as *Viswanath-Obraczka model* for brevity. The propagation happens as levels of rebroadcast where the level represents the number of hops a frame has propagated from the source due to rebroadcast. However, Viswanath-Obraczka model estimates the number of newly reached nodes at each level of rebroadcast using a single parameter β that is fixed for all the levels of rebroadcast. They consider $\beta = 41\%$ based on the additional area covered by a rebroadcast of an immediate neighbor derived by Wu and Varshney [92]. Viswanath-obraczka model also analyzes probabilistic flooding using an arbitrary rebroadcasting probability P_{tx}.

Our model extends the Viswanath-Obraczka model as follows:

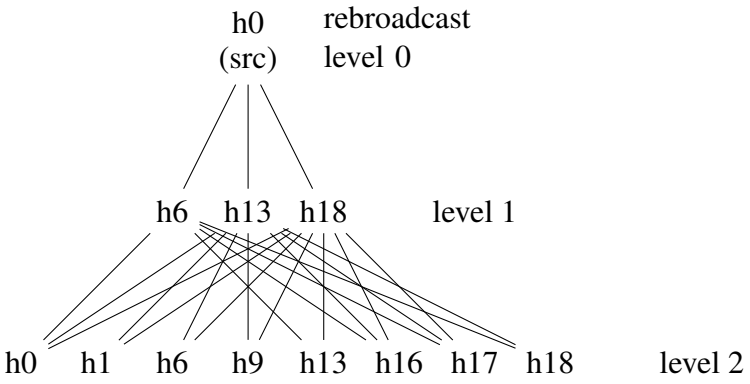

Figure 8.1: Redundant rebroadcasting in simple flooding modeled as graph evolution

- We calculate the additional area covered by each level of rebroadcast geometrically so that β varies from level to level.
- We incorporate time domain in the graph to model flooding schemes that involve an assessment time before making a rebroadcast decision.
- We model node mobility using the time domain representation of the graph as well as the mobility-dependent variation of coverage areas.
- Instead of using a random P_{tx} we interpret P_{tx} in terms of different parameters in flooding schemes, for example we derive a P_{tx} for counter based flooding.

Modeling simple flooding in static networks An example graph is shown in Figure 8.1 and this is a part extracted from Figure 4.7. Unicast is achieved when at least one edge is incident at the destination node in the graph. According to Figure 8.1 node h0 is able to unicast to any of the nodes in the graph because this is a connected graph.

We perceive the propagation of the data frame via flooding as a *flooding wave* as shown in Figure 8.2. When node A in Figure 8.2 initiates a flooding operation, A's neighbors rebroadcast in such a way that new nodes, for example the nodes residing in the dotted area in Figure 8.2 receive the frame. These newly reached nodes will rebroadcast at the next level to reach another set of new nodes. This process can be visualized similar to how a drop of water fallen on a static pool of water causes a circular water wave that propagates outwards as in Figure 8.2.

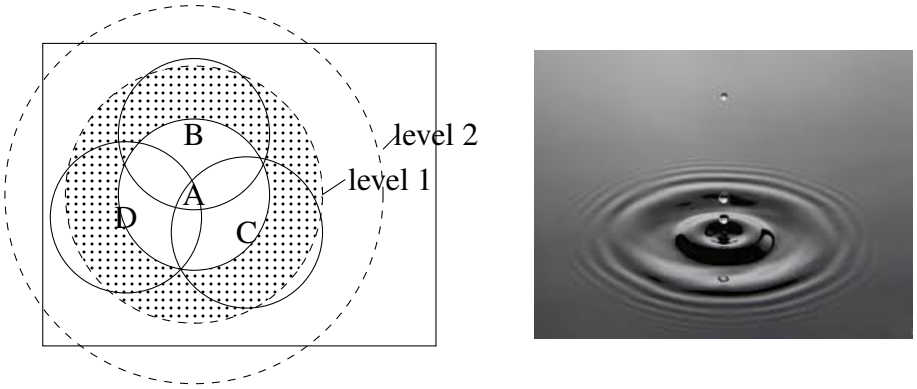

Figure 8.2: Geometric estimation of reached nodes at each rebroadcast level

According to Figure 8.2, the propagation of flooding wave takes several steps represented by levels in the tree as in Figure 8.1. These levels that we term as *rebroadcast levels* can be interpreted as the number of hops that the flooding wave has propagated from the source node.

Total number of edges quantify the number of redundant frames in the network and can be used to evaluate the broadcast storm problem of a given network scenario. For example, consider a unicast communication between h0 and h9 in Figure 8.1. If the frame could be directed to a single node using a directional antenna as opposed to broadcast links, h0 can reach h9 via h13 such that the total number of frames in the network is 2. However, in simple flooding, the frame count given by the total number of edges is 22. Therefore, there are 20 redundant frames caused by simple flooding.

Geometric estimation of redundant rebroadcasts The above graph based representation of endcast gave the insight that the neighborhood is a prominent parameter, on which the redundancy, broadcast storms and flood situation depend on. Given a network topology in terms of an adjacency matrix, one is able to develop the endcast graph but it is not feasible to develop graph for dense networks and count the edges. Therefore, we estimate the numbers of newly reached nodes by each rebroadcast using geometric analysis of coverage areas of the nodes in the network as explained in Section 4.2. We model the node distribution as a Poisson point process. However, it is flexible to use any other node distribution to estimate number of nodes covered by a

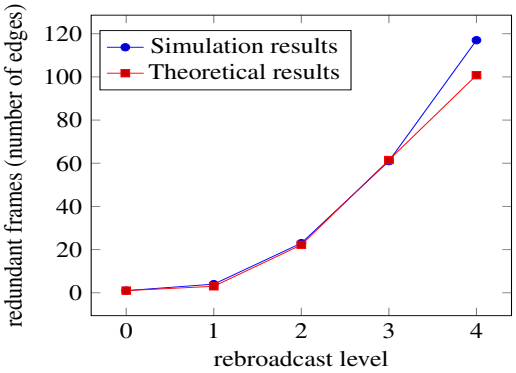

Figure 8.3: Redundant rebroadcast frames with rebroadcast levels in simple flooding for a sample 20-node network

given area and the region of the network.

We simulated simple flooding in the sample 20-node network given in Section 4.4 and also we analytically estimated the number of edges that should be in endcast graph by following the process of geometric analysis of areas covered by flooding in Section 4.4. The simulation results are plotted in Figure 8.3 in comparison with analytical results. Figure 8.3 verifies that the proposed analytical model correctly interprets the sample scenario.

Modeling storm situation The variation of total number of redundant frames with increasing rebroadcast levels interprets the propagation of simple flooding and this interpretation helps visualizing the intensity of broadcast storm problem. For example, simple flooding causes exponential growth in the number of redundant frames in MANETs and the growth becomes steeper when the network density increases according to Figure 8.4 extracted from the analysis of redundant frames against rebroadcast level in Section 4.2.

Modeling flood situation In simple flooding, a frame will propagate throughout the network passing through the destination. The number of edges spanning beyond the rebroadcast level that reaches the destination is a quantifier of broadcast flood situation. For example, if the destination is h18 in Figure 8.1 it records only 3 frames in the network by the time h18 receives the frame that is at rebroadcast level 1. However,

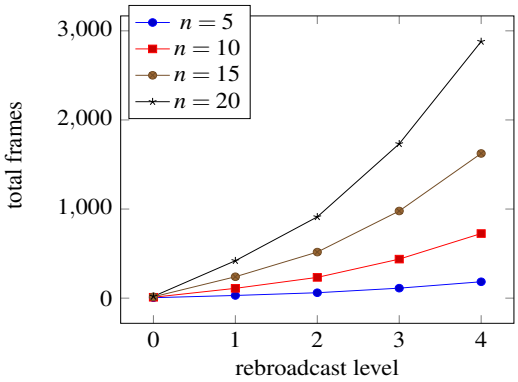

Figure 8.4: Total number of frames received in the network by propagation of simple flooding for networks having different average neighborhood, n

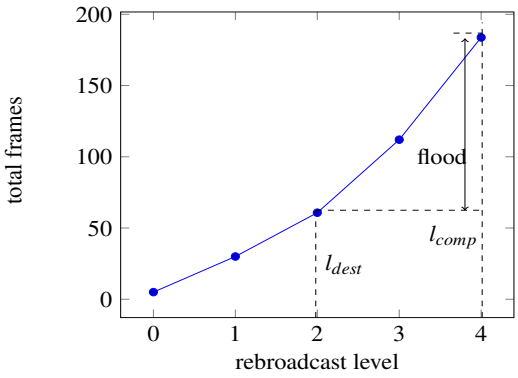

Figure 8.5: Total number of frames received in the network by propagation of simple flooding for networks having average neighborhood, $n = 5$

the flooding wave continues to propagate beyond h18, which results in 19 more frames wastefully. In geometric analysis, the location of the destination relative to the source determines at which rebroadcast level l_{dest}, the frame will be delivered to the destination. In redundant frames Vs rebroadcast level graph, the number of frames beyond l_{dest} quantifies the broadcast flood problem. Assuming that the destination is reached at rebroadcast level 2 in the graph in Figure 8.5 the flood problem can be quantified by the difference between the accumulated number of frames at l_{dest} and number at completion of flooding wave (l_{comp}).

Representing the time domain in flooding schemes The graph that models a flooding scheme such as counter based flooding or distance based flooding requires time do-

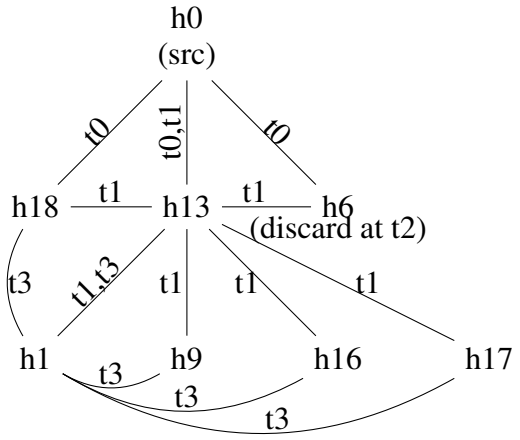

Figure 8.6: Redundant rebroadcasting in flooding modeled as graph evolution with time

main to be included because of the random assessment delay (RAD) in these schemes. The existence of an edge in the graph or the rebroadcasting of a received frame by a node depends on the difference of RADs of nodes. Time domain representation is also required to model the effect of mobility on the propagation of flooding wave as the wireless links between nodes will change with time when the nodes move. We model these time dependencies by indexing the edges with time as in Figure 8.6 and this concept comes from *time evolving graphs*.

For example, if h0 sends the frame at t0, edges (h0,h6), (h0,h13) and (h0,h18) exist at t0 thus they are indexed with t0 in Figure 8.6. If h13 has the least RAD h13 will rebroadcast first at t1. Meanwhile, h6 and h18 wait with the frame received from h0 in their buffers. If at t2, RAD of h6 elapses, the frame counter is 1 due to the rebroadcast of h13 received at t1. If we model counter based flooding with threshold 1, h6 refrain from rebroadcasting at t2. Similarly, h18 also decides not to rebroadcast at a time $t > t2$. At t3, h1 rebroadcasts and the frame is received by the neighbors of h1. By a time $t > t3$, when the RADs of neighbors of h1 elapse, no one will rebroadcast as all the neighbors receive the frame from h1 as a redundant frame while the frame is already in buffer from $t = t1$.

According to the evolution of the graph it can be noted that every time a frame is received due to rebroadcasting, there will be a set of time indices added to the existing

edges or new edges are added to the graph. Therefore the count of time indices gives the number of frames accumulated in the network. Number of time indices when plotted against time, we can evaluate the level of broadcast storm and flood conditions in a given MANET scenario that varies with time.

Modeling the effect of node mobility on flooding schemes We can use the same time-evolving-graph model as in Figure 8.6 to evaluate the impact of mobility on broadcast storm and flood situations as the number of redundant frames is given by the number of time indices on these graphs. According to the survey of mobility models in Section 3.6 we selected *Random Waypoint (RWP) mobility model* to analyze flooding schemes. RWP and few other mobility models can be decomposed into epochs of movement that are of constant speed and at fixed direction. Movement of a node along a fixed direction at constant speed is termed *Constant Velocity (CV) mobility model* in [95]. We showed in Section 4.4.5 The number of newly reached nodes at different level of rebroadcast should be adjusted with the probability of completing a communication due to mobility. We showed how to estimate the probability of a complete communication happening between two moving nodes based on the work of Cho and Hayes [95]. According to this method the probability that a complete frame is transmitted between two moving nodes depends on the relative motion of the two nodes, frame size and the date rate.

Biologically inspired storm control There are efficient flooding schemes proposed to mitigate broadcast storm problem in the literature as surveyed in Chapter 3. We identified probabilistic flooding and counter based flooding to base our endcast scheme because these schemes require minimum and totally local state information for the protocol operation as mentioned in Section 3.2.

In parallel, we surveyed biological systems that are similar in characteristics to the broadcast storm problem as mentioned in Section 2.3.1. Consequently, we realized that *cell proliferation* in organ growth closely mimics the broadcast storm problem caused by blind rebroadcasting. Similar to how biological cells keep on dividing in organ growth, data frames keep on being rebroadcast in blind rebroadcasting. However,

organs terminate the growth by regulating cell division using the *chalone mechanism* explained in Section 5.2. Control of cell proliferation by chalone mechanism is similar to broadcast storm control by counter based flooding. Therefore, we selected *counter based flooding* as the basis for our endcast scheme by mapping the cell proliferation control using chalone method to control of rebroadcasting using counter based mechanism as explained in Section 5.2.

Negative acknowledgement based flood control We developed an inhibition scheme to catch and stop a flooding wave beyond the destination. This is achieved by a small sized control frame that we term as an *inhibitor* that is forced to propagate faster than the data frame. Inhibitor also propagates via counter based flooding but the RAD is set considerably smaller than the RAD used for data rebroadcasting. We also limit the propagation of the inhibitor only to the region covered by the data propagation. It is mandatory for a node to have heard about the data frame in order to rebroadcast an inhibitor. Therefore, an important component of the proposed endcast scheme is the frame log that keeps track of data frames and actions taken on the frames as explained in Section 5.3.

Proposed protocol We developed a endcast scheme that consists of a storm control mechanism and a flood control mechanism. Storm control is achieved by counter based flooding. A node that receives a frame for the first time buffers it and waits a time period termed as *chalone wait*. It counts the number of copies of the same frame that may be subsequently received from neighbors, which we termed as *chalone concentration*. The node decides to rebroadcast the frame if the chalone concentration is less than a pre defined threshold termed as *chalone threshold* after the chalone wait elapses. The word *chalone* in these terms resembles the cell biological inspiration.

A frame is uniquely identified by frame ID that consists of source MAC address, destination MAC and sequence number generated by the source. On the receipt of a frame, the nodes insert a record of the frame indexed by frame ID in a log. Each log record includes a *data state* that carries information such as whether the frame was rebroadcast or discarded.

The flood control mechanism is based on negative acknowledgement. When the frame propagates across the network as a flooding wave, the destination is reached at some point. Then the destination sends a control frame termed *inhibitor* that carries the corresponding frame ID to imply that the relevant frame must not be further rebroadcast. The nodes also log this information as *inhibitor state* against the frame ID.

Performance of proposed endcast scheme We evaluated the proposed endcast scheme using both the simulations and analytical models. The evaluation was mainly focused on *redundancy metrics* and *reachability*. The protocol saves redundant rebroadcast of frames when the chalone threshold is maintained at smaller values, for example, with threshold value one it saves over 45% of redundant frames compared to simple flooding even when it runs without inhibition scheme in a 100 node network and the saving increases to 65% when the number of nodes increases to 1000 in Figure 7.2.

However, the low thresholds impose the risk of not delivering the frame to the destination, for example, the analytical results in Figure 6.16 shows that the low threshold values of two and below fail to reach more than 20% of the nodes and the reachability increases rapidly with increase of threshold. This is also verified by simulation results, for instance, reachability is about 75% in a 50-node network with threshold value of one where as simple flooding shows 100% reachability so that it was able to deliver the message between nearly all the node pairs (7.8). The reachability is improved to about 90% when the threshold was set to two but the redundancy overhead increases. It is a tradeoff between redundancy and reachability (Section 3.3). It was found in the simulation study that a balance between redundancy and reachability could be achieved by adjusting the threshold value, for example, threshold value two was found to be the best choice in that particular network configuration because the reachability improved from 75% to 90% while the increase in redundancy overhead is less than 6% compared to threshold value one (Figure 7.8).

The simulation results show that the inhibition mechanism in the proposed protocol is effective as it saves a considerable amount of redundant rebroadcasts, for example, in Figure 7.10 the frame count grows only by about 8 frames per every 25 nodes added

to the network when inhibition scheme is in operation. In contrast, the protocol without the inhibition scheme shows a growth of redundant frame count by about 170 frames per every 25 nodes.

Mobility was found to enhance the communication in flooding schemes as opposed to destructing the routes in fixed-stateful routing mechanisms. It is evident from Figure 7.11 that the reachability of SNCF in static 50-node network is only about 93% which becomes about 98% when the nodes are mobile. Similarly, in the proposed protocol with threshold two, the reachability increases from 87% to 90% in the 50-node network when the nodes become mobile.

The delay characteristics of the proposed protocol was comparable to that of simple flooding.

Modeling a endcast scheme We developed the following procedure to model and evaluate endcast schemes:

- Propagation of messages by flooding schemes is modeled using a graph $G(V,E)$, in which the set of vertices V represents the nodes in the network and an edge $(u,v) \in V$ represents that a frame is received by v from u and we call this graph the *flooding graph*.

- Messages propagate in stages that we term as *rebroadcast levels* and these levels represent the number of hops from the source that the frames have propagated

- The number of nodes reached by each rebroadcast level is estimated using a geometric method in which the physical area covered by each rebroadcast level is approximated by circular regions centered at the source. The number of nodes in the additional area covered by each rebroadcast level (annulus between circular regions) is calculated by assuming a certain node distribution that in turn depends on the MANET scenario.

- The existence of an edge in the flooding graph vary with time when the availability of wireless links vary with time (e.g. due to node mobility) or the nodes wait before making a rebroadcast decision (e.g. RAD - random assessment delay in

counter based flooding). The edges in the flooding graph are indexed with time to represent the time domain of the flooding scheme.

- The parameters used to make the rebroadcast decision in *efficient flooding schemes* are interpreted by the rebroadcast probability. For example, the counter value and the threshold in counter based flooding is interpreted as the probability that the counter is less than the threshold. This probability in counter based flooding that we used in our proposed endcast mechanism is estimated using a probability mass function that we constructed using the areas of overlapping radio range circles. The number of circles that overlap at a location in the network is equal to the maximum counter value that a node at that location will record. The probability that a a point is in such a location is given by the areas of overlap by different numbers of circles. We used *Librino algorithm* to calculate these areas.

- The probability mass function that governs the rebroadcast probability of nodes in different flooding schemes changes with mobility, for example in counter based flooding the areas of overlapping of radio range circles change with time when nodes move.

- The number of accumulated messages due to the flooding scheme can be evaluated with respect to rebroadcast levels and time by varying different parameters of the flooding scheme (e.g. threshold of the counter based flooding) and also the reachability of the protocol can be evaluated using the proposed model

- The data obtained using our model can be used to analyze endcast (uf) schemes in terms of the metrics that we defined particularly for uf such as redundancy overhead (ROH_{uf}), reachability (RE_{uf}), flooding completion time FCT, and end to end delay $E2E_{uf}$

Summary

We broadly explored routing in MANETs in a range of schemes from the fixed-stateful routing in one end to the mobile-stateless routing in other end. It was found that the

fixed-stateful routing is not suitable for MANETs that are highly dynamic and dense. As a solution, we proposed a novel concept termed as endcast that can be placed closer to the mobile stateless end.

Consequently, we carried out a focused study on flooding schemes in MANETs to find out the state of the art of MANET flooding under the topics such as flooding protocols, underlying MAC and physical layer protocols for flooding, performance problems in flooding, evaluation metrics for flooding and theoretical models for flooding.

We investigated the problem of achieving unicast via flooding and modeled the problem using a graph theoretic approach. The model was further developed using geometric analyses and probabilistic analyses of variety of aspects of MANETs such as the area covered by rebroadcasts by different levels of rebroadcast, node mobility and parameters of flooding schemes such as the counter and the threshold in counter based flooding.

A specific problem that we addressed was to develop a endcast scheme to send data from one node to another using multihop broadcast links in such way that the nodes do not keep global states of the network. We developed a scheme that consists of a broadcast storm controlling mechanism inspired by biological cell division in the growth of organs and a broadcast flood controlling mechanism that uses negative acknowledgement messages. The both mechanisms use counter based flooding to carry the messages. The analytical results and the simulation studies show that the proposed scheme outperforms simple flooding in dense MANETs and also it is tunable to the requirement of the MANET by trading off between redundancy and reachability.

APPENDIX: RELATED PUBLICATIONS

Some of the research results achieved within the duration of this thesis study was published in following articles:

Journal papers

- S. J. Sooriyaarachchi, W. A. C. Fernando, C. D. Gamage, "A Cell Biology Inspired Model for Managing Packet Broadcasts in Mobile Ad-hoc Networks", *ICACT-TACT Journal - Transactions on Advanced Communications Technology*, vol. 4, no. 5, pp. 664-672, Sep. 2015.

Conference papers

- S. Sooriyaarachchi, "A Cell Biology Inspired Data Packet Forwarding Scheme in Mobile Ad-hoc Networks", in *IEEE 16th International Symposium on a World of Wireless, Mobile and Multimedia Networks (WoWMoM 2015)*, Boston, MA, USA, 14-17 Jun. 2015.
- S. J. Sooriyaarachchi and C. D. Gamage, "A Cell Biology Inspired Model for Managing Packet Broadcasts in Mobile Ad-hoc Networks", in *The 17th International Conference on Advanced Communications Technology (ICACT 2015)*, Pyeong Chang, Korea, 1-3 Jul. 2015, pp. 693-698.
- S. J. Sooriyaarachchi, W. A. C. Fernando, C. D. Gamage, "Evaluation of Scalability of Hybrid Wireless Mesh Protocol in IEEE 802.11", in *Interna-*

tional Conference on Advances in ICT for Emerging Regions (ICTer 2015), Colombo, Sri Lanka, 24-26 Aug. 2015, pp. 152-159.

– S. J. Sooriyaarachchi, "Poster: A Cell Biology Inspired Model for Controlling Redundant Rebroadcasts in Mobile Ad-hoc Networks", in *ACM 2015 Workshop on Wireless of the Students, by the Students and for the Students (S3'15)*, Paris, France, 11 Sep. 2015, p. 10.

BIBLIOGRAPHY

[1] H. F. Wedde, M. Farooq, T. Pannenbaecker, B. Vogel, C. Mueller, J. Meth, and R. Jeruschkat, "BeeAdHoc: An energy efficient routing algorithm for mobile ad hoc networks inspired by bee behavior," in *Proc. Genetic and Evolutionary Computation Conference*, Washington, DC, USA, Jun. 2005, pp. 153–160.

[2] K. Viswanath and K. Obraczka, "Modeling the performance of flooding in wireless multi-hop ad hoc networks," *Computer Communications*, vol. 29, no. 8, pp. 949–956, 2006.

[3] M. Conti and S. Giordano, "Multihop ad hoc networking: The theory," *IEEE Communications Magazine*, vol. 45, no. 4, pp. 78–86, 2007.

[4] Y. C. Tseng, S. Y. Ni, Y. S. Chen, and J. P. Sheu, "The broadcast storm problem in a mobile ad hoc network," *Wireless networks*, vol. 8, no. 2-3, pp. 153–167, 2002.

[5] B. Williams and T. Camp, "Comparison of broadcasting techniques for mobile ad hoc networks," in *3rd ACM international symposium on Mobile ad hoc networking and computing*, Jun. 2002, pp. 194–205.

[6] N. Abramson, "Development of the ALOHANET," *IEEE Transactions On Information Theory*, vol. IT-31, no. 2, pp. 119–123, Mar. 1985.

[7] V. A. Dubendorf, *Wireless Data Technologies*. John Wiley and Sons Ltd, 2003, ch. 1.

[8] G. R. Hiertz, D. Denteneer, S. Max, R. Taori, J. Cardona, L. Berlemann, and B. Walke, "Ieee 802.11s: The wlan mesh standard," *IEEE Wireless Communications*, vol. 17, no. 1, pp. 104–111, Feb. 2010.

[9] M. Abolhasan, T. Wysocki, and E. Dutkiewicz, "A review of routing protocols for mobile ad hoc networks," *Ad hoc networks*, vol. 2, no. 1, pp. 1–22, 2004.

[10] P. Sholander, A. Yankopolus, P. Coccoli, and S. S. Tabrizi, "Experimental comparison of hybrid and proactive manet routing protocols," in *MILCOM 2002*, vol. 1, 2002, pp. 513–518.

[11] C. Santivanez, "Asymptotic behavior of mobile ad hoc routing protocols with respect to traffic, mobility, and size," Northeastern University, CDSP Technical Report TRCDSP-00-52., 2000.

[12] J. Blum, M. Ding, A. Thaeler, and X. Cheng, "Connected dominating set in sensor networks and MANETs," *Handbook of combinatorial optimization*, pp. 329–369, 2004.

[13] J. Gao, L. Guibas, J. Hershberger, L. Zhang, and A. Zhu, "Discrete mobile centers," in *The seventeenth annual ACM symposium on Computational geometry*, 2001, pp. 188–196.

[14] L. Jia, R. Rajaraman, and T. Suel, "An efficient distributed algorithm for constructing small dominating sets," *Distributed Computing*, vol. 15, no. 4, pp. 193–205, 2002.

[15] F. Kuhn, T. Nieberg, T. Moscibroda, and R. Wattenhofer, "Local approximation schemes for ad hoc and sensor networks," in *The ACM joint workshop on Foundations of mobile computing*, 2005, pp. 97–103.

[16] F. Kuhn and R. Wattenhofer, "Constant-time distributed dominating set approximation," *Distributed Computing*, vol. 17, no. 4, pp. 303–310, 2005.

[17] K. M. Alzoubi, P. J. Wan, and O. Frieder, "Message-optimal connected dominating sets in mobile ad hoc networks," in *The 3rd ACM international symposium on Mobile ad hoc networking and computing*, 2002, pp. 157–164.

[18] R. Sivakumar, B. Das, and V. Bharghavan, "An improved spine-based infrastructure for routing in ad hoc networks," in *IEEE Symposium on Computers and Communications*, 1998.

[19] B. Das, R. Sivakumar, and V. Bharghavan, "Routing in ad hoc networks using a spine," in *The Sixth IEEE International Conference on Computer Communications and Networks*, 1997, pp. 34–39.

[20] B. Das and V. Bharghavan, "Routing in ad-hoc networks using minimum connected dominating sets," in *IEEE International Conference on Communications (ICC'97) Towards the Knowledge Millennium*, 1997, pp. 376–380.

[21] R. Sivakumar, B. Das, and V. Bharghavan, "An improved spine-based infrastructure for routing in ad hoc networks," in *IEEE Symposium on Computers and Communications*, 1998.

[22] I. Stojmenovic, M. Seddigh, and J. Zunic, "Dominating sets and neighbor elimination-based broadcasting algorithms in wireless networks," *IEEE Transactions on Parallel and Distributed Systems*, vol. 13, no. 1, pp. 14–25, 2002.

[23] K. M. Alzoubi, P. J. Wan, and O. Frieder, "Distributed heuristics for connected dominating sets in wireless ad hoc networks," *Journal of Communications and Networks*, vol. 4, no. 1, pp. 22–29, 2002.

[24] P. J. Wan, K. M. Alzoubi, and O. Friede, "Distributed construction of connected dominating set in wireless ad hoc networks," in *IEEE INFOCOM 2002*, vol. 3, 2002, pp. 1597–1604.

[25] C. Ho, K. Obraczka, G. Tsudik, and K. Viswanath, "Flooding for reliable multicast in multi-hop ad hoc networks," in *The 3rd ACM international workshop*

on discrete algorithms and methods for mobile computing and communications, 1999, pp. 64–71.

[26] A. Rahman, W. Olesinski, and P. Gburzynski, "Controlled flooding in wireless ad-hoc networks," in *IEEE International Workshop on in Wireless Ad-Hoc Networks*, 2004, pp. 73–78.

[27] M. Gunes, U. Sorges, and I. Bouazizi, "ARA the ant-colony based routing algorithm for manets," in *Proc. International Workshop on Ad Hoc Networking (IWAHN 2002)*, Vancouver, British Columbia, Canada, Aug. 2002.

[28] R. Schoonderwoerd, J. L. Bruten, O. E. Holland, and L. J. M. Rothkrantz, "Ant-based load balancing in telecommunications networks," *Adapt. Behav.*, vol. 5, no. 2, pp. 169–195, 1996.

[29] G. D. Caro, F. Ducatelle, and L. M. Gambardella, "AntHocNet: an adaptive nature-inspired algorithm for routing in mobile ad hoc networks," *European Transactions on Telecommunications*, vol. 16, no. 5, pp. 443–455, Sep. 2005.

[30] Jean-yves and L. Boudec, "An artificial immune system for misbehavior detection in mobile ad-hoc networks with virtual thymus, clustering, danger signal and memory detectors," in *International Journal of Unconventional Computing*, 2004, p. 2005.

[31] P. Kefalas, G. Eleftherakis, M. Holcombe, and I. Stamatopoulou, *Formal Modelling of the Dynamic Behaviour of Biology-Inspired, Agent-Based Systems*. Idea Group Inc., 2005, pp. 243–244.

[32] J. E. Bell and P. R. McMullen, "Ant colony optimization techniques for the vehicle routing problem," *Advanced Engineering Informatics*, vol. 18, no. 1, pp. 41–48, 2004.

[33] M. Farooq, *Bee-inspired protocol engineering: from nature to networks*. Springer Science and Business Media, 2008.

[34] A. Giagkos and M. S. Wilson, "BeeIP: Bee-inspired protocol for routing in mobile ad-hoc networks," *Springer SAB*, pp. 263–272, 2010.

[35] M. Roth and S. Wicker, "Termite: Ad-hoc networking with stigmergy," in *IEEE Global Telecommunications Conference (GLOBECOM 2003)*, 2003, pp. 2937–2941.

[36] A. M. Zungeru, L. M. Ang, and K. P. Seng, "Termite-hill: Performance optimized swarm intelligence based routing algorithm for wireless sensor networks," *Journal of Network and Computer Applications*, vol. 35, no. 6, pp. 1901–1917, 2012.

[37] S. S. Iyengar, H. C. Wu, N. Balakrishnan, and S. Y. Chang, "Biologically inspired cooperative routing for wireless mobile sensor networks," *IEEE Systems Journal*, vol. 1, no. 1, pp. 29–37, 2007.

[38] S. Marwaha, C. K. Tham, and D. Srinivasan, "Mobile agents based routing protocol for mobile ad hoc networks," in *IEEE Global Telecommunications Conference (GLOBECOM 2002)*, 2002, pp. 163–167.

[39] K. Nishimura and K. Takahashi, "A multi-agent routing protocol with congestion control for manet," in *European Conference on Modelling and Simulation*, 2007, pp. 1–6.

[40] S. S. Manvi and M. S. Kakkasageri, "Multicast routing in mobile ad hoc networks by using a multiagent system," *Information Sciences*, vol. 178, no. 6, pp. 1611–1628, 2008.

[41] R. R. Choudhury, K. Paul, and S. Bandyopadhyay, "MARP: a multi-agent routing protocol for mobile wireless ad hoc networks," *Autonomous Agents and Multi-Agent Systems*, vol. 8, no. 1, pp. 47–68, 2004.

[42] N. Mazhar and M. Farooq, "A hybrid artificial immune system (AIS) model for power aware secure mobile ad hoc networks (MANETs) routing protocols," *Applied Soft Computing*, vol. 11, no. 8, pp. 5695–5714, 2011.

[43] J. Y. L. Boudec and S. Sarafijanovic, "An artificial immune system approach to misbehavior detection in mobile ad hoc networks," *Biologically Inspired Approaches to Advanced Information Technology*, pp. 396–411, 2004.

[44] R. Pradhan, M. R. Kabat, and S. P. Sahoo, "A bacteria foraging-particle swarm optimization algorithm for qos multicast routing," *Swarm, Evolutionary, and Memetic Computing*, pp. 590–600, 2013.

[45] B. Niu, H. Wang, L. J. Tan, L. Li, and J. W. Wang, "Vehicle routing problem with time windows based on adaptive bacterial foraging optimization," *Intelligent Computing Theories and Applications*, pp. 672–679, 2012.

[46] L. Tan, F. Lin, and H. Wang, "Adaptive comprehensive learning bacterial foraging optimization and its application on vehicle routing problem with time windows," *Neurocomputing*, vol. 151, pp. 1208–1215, 2015.

[47] C. Roadknight and I. Marshall, "Communications network," Jan. 13 2009, US Patent 7,478,162. [Online]. Available: https://www.google.com/patents/US7478162

[48] T. Wokoma, L. L. Shum, L. Sacks, and I. Marshall, "A biologically-inspired clustering algorithm dependent on spatial data in sensor networks," in *The Second European Workshop on Wireless Sensor Networks*, 2005, pp. 386–390.

[49] A. Einolghozati, M. Sardari, A. Beirami, and F. Fekri, "Consensus problem under diffusion-based molecular communication," in *45th Annual Conference on Information Sciences and Systems (CISS)*, 2011, pp. 1–6.

[50] M. Pierobon and I. F. Akyildiz, "A physical end-to-end model for molecular communication in nanonetworks," *IEEE Journal on Selected Areas in Communications*, vol. 28, no. 4, pp. 602–611, 2010.

[51] A. Khelil, C. Becker, J. Tian, and K. Rothermel, "An epidemic model for information diffusion in manets," in *5th ACM international workshop on Modeling analysis and simulation of wireless and mobile systems*, 2002, pp. 54–60.

[52] P. De, Y. Liu, and S. K. Das, "An epidemic theoretic framework for evaluating broadcast protocols in wireless sensor networks," in *IEEE International Conference on Mobile Adhoc and Sensor Systems (MASS 2007)*, 2007, pp. 1–9.

[53] J. C. Lui and J.Baron, "Mechanisms limiting body growth in mammals," *Endocrine Reviews*, vol. 32, no. 3, pp. 422–440, Jun. 2011.

[54] N. B. Chang and M. Liu, "Controlled flooding search in a large network," *IEEE/ACM Transactions on Networking*, vol. 15, no. 2, pp. 436–449, 2007.

[55] K. A. Harras, K. C. Almeroth, and E. M. Belding-Royer, "Delay tolerant mobile networks (DTMNS): Controlled flooding in sparse mobile networks," *Networking*, pp. 1180–1192, 2005.

[56] B. Wang, K. I. Pedersen, T. E. Kolding, and P. E. Mogensen, "Performance of voip on hsdpa," in *The 61st IEEE Vehicular Technology Conference (VTC 2005)*, vol. 4, 2005, pp. 2335–2339.

[57] P. Ameigeiras, J. Wigard, and P. Mogensen, "Performance of the M-LWDF scheduling algorithm for streaming services in HSDPA," in *The 60th IEEE Vehicular Technology Conference (VTC 2004)*, vol. 2, 2004, pp. 999–1003.

[58] M. Assaad and D. Zeghlache, *TCP performance over UMTS-HSDPA systems*. CRC Press, 2006.

[59] J. Gao, L. Guibas, N. Milosavljevic, and J. Hershberger, "Sparse data aggregation in sensor networks," in *The 6th ACM international conference on Information processing in sensor networks*, 2007, pp. 430–439.

[60] Y. Yi, M. Gerla, and T. J. Kwon, "Efficient flooding in ad hoc networks: a comparative performance study," in *IEEE International Conference on Communications (ICC 2003)*, vol. 2, 2003, pp. 1059–1063.

[61] M. B. Yassein, S. F. Nimer, and A. Y. Al-Dubai, "A new dynamic counter-based broadcasting scheme for mobile ad hoc networks," *Simulation Modelling Practice and Theory*, vol. 19, no. 1, pp. 553–563, 2011.

[62] D. G. Reina, S. L. Toral, P. Johnson, and F. Barrero, "A survey on probabilistic broadcast schemes for wireless ad hoc networks," *Ad hoc Networks*, vol. 25, pp. 263–292, 2015.

[63] S. Pleisch, M. Balakrishnan, K. Birman, and R. V. Renesse, "MISTRAL: efficient flooding in mobile ad-hoc networks," in *The 7th ACM international symposium on mobile ad hoc networking and computing*, 2006, pp. 1–12.

[64] J. Wu and W. Lou, "Forward node set based broadcast in clustered mobile ad hoc networks," *Wireless Communications and Mobile Computing*, vol. 3, no. 2, pp. 155–173, 2003.

[65] H. Liu, P. J. Wan, X. Jia, X. Liu, and F. F. Yao, "Efficient flooding scheme based on 1-hop information in mobile ad hoc networks," in *IEEE INFOCOM*, 2006.

[66] Y. Cai, K. A. Hua, and A. Phillips, "Leveraging 1-hop neighborhood knowledge for efficient flooding in wireless ad hoc networks," in *IEEE International Performance, Computing, and Communications Conference (IPCCC 2005)*, 2005, pp. 347–354.

[67] S. Butenko, X. Cheng, D. Z. Du, and P. M. Pardalos, "On the construction of virtual backbone for ad hoc wireless network," *Cooperative control: Models, applications and algorithms*, pp. 43–54, 2003.

[68] A. Mohammed, M. Ould-Khaoua, and L. Mackenzie, "An efficient counter-based broadcast scheme for mobile ad hoc networks," *Formal Methods and Stochastic Models for Performance Evaluation*, pp. 275–283, 2007.

[69] Y. C. Tseng, S. Y. Ni, and E. Y. Shih, "Adaptive approaches to relieving broadcast storms in a wireless multihop mobile ad hoc network," *IEEE Transactions on Computers*, vol. 52, no. 5, pp. 545–557, 2003.

[70] A. Keshavarz-Haddad, V. Ribeiro, and R. Riedi, "Color-based broadcasting for ad hoc networks," in *The 4th IEEE International Symposium on Modeling and*

Optimization in Mobile, Ad Hoc and Wireless Networks (WiOpt 2006), 2006, pp. 1–10.

[71] C. Chen, C. K. Hsu, and H. K. Wang, "A distance-aware counter-based broadcast scheme for wireless ad hoc networks," in *IEEE Military Communications Conference (MILCOM 2005)*, 2005, pp. 1052–1058.

[72] M. Cornils, M. Bahr, and T. Gamer, "Simulative analysis of the hybrid wireless mesh protocol (HWMP)," in *European Wireless Conference (EW)*, Apr. 2010, pp. 536–543.

[73] M. Ikeda, T. Honda, T. Oda, S. Sakamoto, and L. Barolli, "Analysis of WMN-GA simulation results: WMN performance considering stationary and mobile scenarios," in *IEEE 28th International Conference on Advanced Information Networking and Applications*, 2014, pp. 337–342.

[74] A. H. Mozumder, T. Acharjee, and S. Roy, "Scalability performance analysis of BATMAN and HWMP protocols in wireless mesh networks using ns-3," in *IEEE Green Computing Communication and Electrical Engineering (ICGCCEE)*, Mar. 2014, pp. 1–5.

[75] I. Ibrahim, N. M. Latiff, S. K. Yusof, N. N. Malik, and S. H. Ariffin, "Performance comparison of AODV and HWMP routing protocols in wireless mesh networks," in *IEEE RF and Microwave Conference (RFM)*, Dec. 2013, pp. 116–120.

[76] F. Maan and N. Mazhar, "MANET routing protocols vs mobility models: A performance evaluation," in *Ubiquitous and Future Networks (ICUFN)*, Jun. 2011, pp. 179–184.

[77] B. Nassereddine, A. Maach, and S. Bennani, "The scalability of the hybrid protocol in wireless mesh network 802.11s," in *Mediterrannean Microwave Symposium (MMS)*, Nov. 2009, pp. 1–7.

[78] S. Bari, F. Anwar, and M. Masud, "Performance study of hybrid wireless mesh protocol (HWMP) for ieee 802.11s wlan mesh networks," in *International Conference on Computer and Communication Engineering (ICCCE)*, Jul. 2012, pp. 712–716.

[79] H. Zhang and Z. P. Jiang, "Performance analysis of broadcasting schemes in mobile ad hoc networks," *IEEE Communications Letters*, vol. 8, no. 12, pp. 718–720, 2004.

[80] J. Cartigny and D. Simplot, "Border node retransmission based probabilistic broadcast protocols in ad-hoc networks," in *36th Annual Hawaii International Conference on System Sciences*, 2003, pp. 10–19.

[81] M. Bani-Yassein, M. Ould-Khaoua, L. M. Mackenzie, and S. Papanastasiou, "Performance analysis of adjusted probabilistic broadcasting in mobile ad hoc networks," *International Journal of Wireless Information Networks*, vol. 13, no. 2, pp. 127–140, 2006.

[82] I. A. Khan, A. Javaid, and H. L. Qian, "Coverage-based dynamically adjusted probabilistic forwarding for wireless mobile ad hoc networks," in *ACM international workshop on Heterogeneous sensor and actor networks*, 2008, pp. 81–88.

[83] S. Busanelli, G. Ferrari, and S. Panichpapiboon, "Efficient broadcasting in IEEE 802.11 networks through irresponsible forwarding," in *IEEE Global Telecommunications Conference (GLOBECOM 2009)*, 2009, pp. 1–6.

[84] O. M. H. Rehman, H. Bourdoucen, and M. Ould-Khaoua, "Forward link quality estimation in vanets for sender-oriented alert messages broadcast," *Journal of Network and Computer Applications*, vol. 58, pp. 23–41, 2015.

[85] G. S. Li, W. L. Wang, and X. W. Yao, "An adaptive and opportunistic broadcast protocol for vehicular ad hoc networks," *International Journal of Automation and Computing*, vol. 9, no. 4, pp. 378–387, 2012.

[86] C. Bettstetter, "On the minimum node degree and connectivity of a wireless multihop network," in *The 3rd ACM international symposium on Mobile ad hoc networking and computing*, 2002, pp. 80–91.

[87] H. Menouar, F. Filali, and M. Lenardi, "A survey and qualitative analysis of MAC protocols for vehicular ad hoc networks," *IEEE Wireless Communications*, vol. 13, no. 5, pp. 30–35, 2006.

[88] S. S. Lara, "An analysis of the reservation-ALOHA protocol for satellite packet switching," 1978.

[89] H. Takagi and L. Kleinrock, "Optimal transmission ranges for randomly distributed packet radio terminals," *IEEE Transactions on Communications*, vol. 32, no. 3, pp. 246–257, 1984.

[90] I. Demirkol, C. Ersoy, and F. Alagoz, "MAC protocols for wireless sensor networks: a survey," *IEEE Communications Magazine*, vol. 44, no. 4, pp. 115–121, 2006.

[91] F. Borgonovo, A. Capone, M. Cesana, and L. Fratta, "ADHOC MAC: new MAC architecture for ad hoc networks providing efficient and reliable point-to-point and broadcast services," *Wireless Networks*, vol. 10, no. 4, pp. 359–366, 2004.

[92] L. Wu and P. K. Varshney, "Performance analysis of csma and btma protocols in multihop networks (i) - single channel case," *Information Sciences*, vol. 120, no. 1, pp. 159–177, 1999.

[93] W. Ye, J. Heidemann, and D. Estrin, "An energy-efficient MAC protocol for wireless sensor networks," in *Twenty-First Annual Joint Conference of the IEEE Computer and Communications Societies INFOCOM 2002*, vol. 3, 2002, pp. 1567–1576.

[94] C. Bettstetter, "Mobility modeling in wireless networks: categorization, smooth movement, and border effects," *ACM SIGMOBILE Mobile Computing and Communications Review*, vol. 5, no. 3, pp. 55–66, 2001.

[95] S. Cho and J. P. Hayes, "Impact of mobility on connection in ad hoc networks," in *IEEE Wireless Communications and Networking Conference*, vol. 3, 2005, pp. 1650–1656.

[96] N. Sabah and A. Hocanin, "Gamma random waypoint mobility model for wireless ad hoc networks," *International Journal of Communication Systems*, vol. 26, no. 11, pp. 1433–1445, 2013.

[97] O. Younes and N. Thomas, "Analysis of the expected number of hops in mobile ad hoc networks with random waypoint mobility," *Electronic notes in theoretical computer science*, vol. 275, pp. 143–158, 2011.

[98] F. Bai, N. Sadagopan, and A. Helmy, "IMPORTANT: a framework to systematically analyze the impact of mobility on performance of routing protocols for adhoc networks," in *Twenty-Second Annual Joint Conference of the IEEE Computer and Communications Societies INFOCOM 2003*, vol. 2, 2003, pp. 825–835.

[99] F. Kuhn, R. Wattenhofer, and A. Zollinger, "Ad hoc networks beyond unit disk graphs," *Wireless Networks*, vol. 14, no. 5, pp. 715–729, 2008.

[100] R. Rajaraman, "Topology control and routing in ad hoc networks: A survey," *ACM SIGACT News*, vol. 33, no. 2, pp. 60–73, 2002.

[101] A. Ferreira, "Building a reference combinatorial model for manets," *IEEE Network*, vol. 18, no. 5, pp. 24–29, 2004.

[102] A. Ferreira, A. Goldman, and J. Monteiro, "Performance evaluation of routing protocols for manets with known connectivity patterns using evolving graphs," *Wireless Networks*, vol. 16, no. 3, pp. 627–640, 2010.

[103] J. S. Baras and T. Jiang, "Cooperative games, phase transitions on graphs and distributed trust in MANET," in *43rd IEEE Conference on Decision and Control*, 2004, pp. 93–98.

[104] Y. Sasson, D. Cavin, and A. Schiper, "Probabilistic broadcast for flooding in wireless mobile ad hoc networks," *IEEE Wireless Communications and Networking*, vol. 2, pp. 1124–1130, 2003.

[105] P. Erdos and A. Renyi, "On random graphs. i," *Publ. Math.*, p. 290297, 1959.

[106] M. Penrose, *Random geometric graphs*. Oxford: Oxford University Press, 2003, vol. 5.

[107] H. Wang, H. He, J. Yang, P. S. Yu, and J. X. Yu, "Dual labeling: Answering graph reachability queries in constant time," in *The 22nd International Conference on Data Engineering (ICDE 06)*, 2006, pp. 75–86.

[108] R. W. Floyd, "Algorithm 97: shortest path," *Communications of the ACM*, vol. 5, no. 6, p. 345, 1962.

[109] D. B. Johnson, "Efficient algorithms for shortest paths in sparse networks," *Journal of the ACM (JACM)*, vol. 24, no. 1, pp. 1–13, 1977.

[110] F. B. Zhan and C. E. Noon, "Shortest path algorithms: an evaluation using real road networks," *Transportation Science*, vol. 32, no. 1, pp. 65–73, 1998.

[111] A. Khelil, "A generalized broadcasting technique for mobile ad hoc networks," PhD thesis, pp. 53–63, Apr. 2007. [Online]. Available: http://elib.uni-stuttgart.de/opus/voll texte/2007/3120/pdf/khelil_diss.pdf

[112] F. Librino, M. Levorato, and M. Zorzi, "An algorithmic solution for computing circle intersection areas and its applications to wireless communications," *Wireless Communications and Mobile Computing*, vol. 14, no. 18, pp. 1672–1690, 2014.

[113] S. Srinivasa and M. Haenggi, "Distance distributions in finite uniformly random networks: Theory and applications," *IEEE Transactions on Vehicular Technology*, vol. 59, no. 2, pp. 940–949, 2010.

[114] Y. Zhuang and J. Pan, *A geometrical probability approach to location-critical network performance metrics*. IEEE, 1817-1825.

[115] G. Finkielstain, P. Forcinito, J. Lui, K. Barnes, R. Marino, S. Makaroun, V. Nguyen, J. Lazarus, O. Nilsson, and J. Baron, "An extensive genetic program occurring during postnatal growth in multiple tissues," *Endocrinology*, vol. 150, no. 4, pp. 1791–1800, Apr. 2009.

[116] P. J. Bryant and P. Simpson, "Intrinsic and extrinsic control of growth in developing organs," *The Quarterly Review of Biology*, vol. 59, no. 4, pp. 387–415, Dec. 1984.

[117] P. Forcinito, A. Andrade, G. Finkielstain, J. Baron, O. Nilsson, and J. Lui, "Growth-inhibiting conditions slow growth plate senescence," *Endocrinol*, vol. 208, no. 1, pp. 59–67, Jan. 2011.

[118] W. S. Bullough, "Mitotic and functional homeostasis:a speculative review," *Cancer Research*, vol. 25, no. 10, pp. 1683–1727, Nov. 1965.

[119] H. Onda, "A new hypothesis on mitotic control mechanism in eukaryotic cells: Cell-specific mitosis-inhibiting protein excretion hypothesis," *Theoretical Biology*, vol. 77, no. 3, pp. 367–377, Apr. 1979.

[120] S. Lee, "Regulation of muscle mass by myostatin," *Annual Review of Cell and Developmental Biology*, vol. 20, pp. 61–86, 2004.

[121] K. Elgjo and K. Reichelt, "Chalones: from aqueous extracts to oligopeptides," *Cell Cycle*, vol. 3, no. 9, pp. 1208–1211, Sep. 2004.

[122] D. Bakthavatsalam, D. Brock, N.N.Nikravan, K. Houston, R. Hatton, and R. Gomer, "Chalones: from aqueous extracts to oligopeptides," *Cell Science*, vol. 121, pp. 2473–2480, Aug. 2008.

[123] A. Kansal, S. Torquato, G. Harsh, E. Chiocca, and T. Deisboeck, "Simulated brain tumor growth dynamics using a three-dimensional cellular automaton," *Journal of Theoretical Biology*, vol. 203, no. 4, pp. 367–382, Apr. 2000.

[124] Y. Lee, S. Kouvroukoglou, L. V. McIntire, and K. Zygourakis, "A cellular automaton model for the proliferation of migrating contact-inhibited cells," *Biophysical Journal*, vol. 69, pp. 1284–1298, Oct. 1995.

[125] T. Alarcna, H. Byrneb, and P. Mainia, "A cellular automaton model for tumour growth in inhomogeneous environment," *Journal of Theoretical Biology*, vol. 225, no. 2, pp. 257–274, Nov. 2003.

[126] O. Mireira and A. Deutsch, "Cellular automaton models of tumor development: A critical review," *Advs. Complex Syst*, vol. 5, no. 2/3, pp. 247–268, 2002.

[127] S. Wolfram, "Statistical mechanics of cellular automata," *Reviews of Modern Physics*, vol. 55, no. 3, pp. 601–644, Jul. 1983.

[128] J. Kari, "Theory of cellular automata: A survey," *Theoretical Computer Science*, vol. 334, pp. 3–33, Nov. 2005.

[129] J. I. Barredo, M. Kasanko, N. McCormick, and C. Lavalle, "Modelling dynamic spatial processes: simulation of urban future scenarios through cellular automata," *Landscape and Urban Planning*, vol. 64, pp. 145–160, 2003.

[130] Q.-X. Liu, Z. Jin, and M.-X. Liu, "Spatial organization and evolutional period of the epidemic model using cellular automata," *Physical Review E*, vol. 74, Nov. 2006.

[131] X.-B. Li, R. Jiang, and Q.-S. Wu, "Cellular automaton model simulating traffic flow at an uncontrolled t-shaped intersection," *International Journal of Modern Physics B*, vol. 18, no. 17-19, pp. 2703–2707, 2004.

[132] R. M. Almeida and E. E. N. Macau, "Stochastic cellular automata model for wildland fire spread dynamics," in *9th Brazilian Conference on Dynamics, Control and their Applications (DINCON'10)*, Serra Negra, SP, Jun. 2010, pp. 249–253.

[133] O. Martin, A. M. Odlyzko, and S. Wolfram, "Algebraic properties of cellular automata," *Communications in Mathematical Physics*, vol. 93, pp. 219–258, 1984.

[134] N. H. Packard and S. Wolfram, "Two-dimensional cellular automata," *Journal of Statistical Physics*, vol. 38, no. 5/6, pp. 901–946, 1985.

[135] Q. Zhang and D. P. Agrawal, "Dynamic probabilistic broadcasting in manets," *Journal of parallel and Distributed Computing*, vol. 65, no. 2, pp. 220–233, 2005.

[136] B. Krishnamachari, S. B. Wicker, and R. Bejar, "Phase transition phenomena in wireless ad hoc networks," in *IEEE Global Telecommunications Conference GLOBECOM'01*, 2001, pp. 2921–2925.

[137] A. A. Markov, "Example of a statistical investigation of the text of Eugene Onegin illustrating the dependence between samples in chain," *publisher not identified*, 1955.

[138] S. M. Ross, *Introduction to probability models*. Academic press, 2014.

[139] H. Shah-Mansouri, S. Bahramian, and L. Pakravan, "Performance analysis of flooding over csma in wireless ad-hoc networks," in *IEEE 19th International Symposium on Personal, Indoor and Mobile Radio Communications (PIMRC)*, 2008, pp. 1–5.

[140] A. Mohammed, M. Ould-Khaoua, and L. Mackenzie, "An improved rebroadcast probability function for an efficient counter-based broadcast scheme in manets," in *Formal Methods and Stochastic Models for Performance Evaluation*, K. Wolter, Ed. Springer Berlin Heidelberg, 2007, pp. 275–283.

[141] M. P. Fewell, "Area of common overlap of three circles," DEFENCE SCIENCE AND TECHNOLOGY ORGANISATION EDINBURGH (AUSTRALIA) MARITIME OPERATIONS DIVISION, DSTO-TN-0722, 2006.

[142] G. Bianchi, "Ieee 802.11-saturation throughput analysis," *IEEE Communications Letters*, vol. 2, no. 12, pp. 318–320, 1998.

[143] F. Cal, M. Conti, and E. Gregori, "IEEE 802.11 protocol: design and performance evaluation of an adaptive backoff mechanism," *IEEE Journal on Selected Areas in Communications*, vol. 18, no. 9, pp. 1774–1786, 2000.

[144] I. C. Society, "Part 11: Wireless lan medium access control (mac) and physical layer (phy) specifications," IEEE Standards Association, Tech. Rep., 2012.

[145] F. Cali, M. Conti, and E. Gregori, "Dynamic tuning of the IEEE 802.11 protocol to achieve a theoretical throughput limit," *IEEE/ACM Transactions on Networking (ToN)*, vol. 8, no. 6, pp. 785–799, 2000.